The Novel Role of Extracellular Cardiolipin in Microglial Activation and Neuroinflammation

by

Caitlin Bennett Pointer

B.Sc., The University of British Columbia, 2015

A THESIS SUBMITTED IN PARTIAL FULFILLMENT OF
THE REQUIREMENTS FOR THE DEGREE OF

MASTER OF SCIENCE

in

THE COLLEGE OF GRADUATE STUDIES

(Biology)

THE UNIVERSITY OF BRITISH COLUMBIA
(Okanagan)

April 2017

Thesis Committee:

Dr. Andis Klegeris (Supervisor)

Dr. Bruce Mathieson

Dr. Mark Rheault

Abstract

Alzheimer's disease (AD) is a fatal neurodegenerative disorder characterized by chronic neuroinflammation. Microglia, the immune cells of the brain, become activated in response to pathological stimuli and cellular debris. Once activated, microglia secrete pro-inflammatory mediators, as well as participate in phagocytosis in aims of eliminating the noxious stimuli. Microglial activation is normally beneficial, as it helps maintain homeostatic conditions and regulate the immune status of the brain; however, in AD, microglia become over-activated, which causes the non-specific release of cytotoxic molecules and results in extensive neuronal death. Cardiolipin, a mitochondrial phospholipid implicated in regulating metabolic processes, is significantly reduced in AD brains. Additionally, it has been shown that cardiolipin can be relocated to the outer mitochondrial membrane, as well as to the plasma membrane during various cellular processes. Although the intracellular role of cardiolipin has been well defined, the effects of extracellular cardiolipin on microglial functions implicated in AD pathogenesis have yet to be investigated. The **central hypothesis** of this thesis proposes that extracellular cardiolipin regulates select microglial functions**.** I focused on three specific research objectives: 1) to determine whether extracellular cardiolipin induces the phagocytic activity of microglia, 2) to determine whether extracellular cardiolipin affects microglial functions that impact neuronal viability and 3) to determine whether extracellular cardiolipin alters the secretory profile of microglia. By utilizing *in vitro* cell culture techniques and biological assays with immortalized CNS model cells, as well as primary murine microglia, I demonstrate that extracellular cardiolipin

induces the phagocytic activity of microglia, decreases microglia-mediated cytotoxicity towards neurons, as well as alters the secretory profile of activated microglia by reducing the secretion of key inflammatory mediators, including reactive nitrogen and oxygen species, as well as the pro-inflammatory cytokines tumor necrosis factor-alpha and monocyte chemoattractant protein-1. The findings of this study demonstrate that extracellular cardiolipin regulates several microglial functions that potentially impact select aspects of neuroinflammation implicated in AD. Therefore, extracellular cardiolipin may represent a novel therapeutic agent that promotes the clearance of pathological structures, inhibits the extensive neuronal death and alters the secretory profile of over-activated microglia present in neurodegenerative diseases, such as AD.

Preface

Figures 1.2, 1.4, 1.5 and 1.6 are modified versions of figures 1, 2, 3a and 3b, respectively, from **Pointer, C.B.**, Klegeris, A. (2017) Cardiolipin in Central Nervous System Physiology and Pathology. *Cellular and Molecular Neurobiology*. [ePub ahead of print]. As lead contributor to this review article, I participated in extensive review of available literature, wrote the manuscript and constructed all figures.

I am responsible for all the experimental data presented in this thesis, except for the primary murine microglia immunofluorescence experiments using the rabbit anti-mouse IBA-1 and GFAP antibodies (Figure 3.16), which were conducted by Dr. Lindsay Spielman.

I also co-authored the following publications during my MSc studies:

1. McKenzie, J.A., Spielman, L.J., **Pointer, C.B.**, Lowry, J.R., Bajwa, E., Lee, C., Klegeris, A. (2017) Modifiable Risk Factors of Alzheimer's Disease and Parkinson's Disease: Attenuation of Neuroinflammation as a Possible Common Mechanism. *Current Aging Science*. (In Press)
2. Bajwa, E., **Pointer, C.B.**, Klegeris, A. (2016) Modifiable Risk Factors of Alzheimer's Disease and Neuroinflammation: What are the Links? *Future Neurology*. 11(4): 237-244.
3. **Pointer, C.B.**, Slattery, W.T., Spielman, L.J., Lowry, J.R., McKenzie, J.A., Lee, C., Klegeris, A. (2016) Neuroimmune Interactions of Astrocytes with Other Central Nervous System Cell Types. In: 'New Developments in Astrocytes Research'. Estrada, L. (Ed.), pp. 33-74, Nova Publishers, New York.
4. Schindler, S.M., Spielman, L.J., **Pointer, C.B.**, Slattery, W.T., Bajwa, E., McKenzie, J.A., Lowry, J.R., Klegeris, A. (2015) An Interplay Between Neuroinflammation and Modifiable Risk Factors of Alzheimer's Disease, Parkinson's Disease and Amyotrophic Lateral Sclerosis. In: 'Neuroinflammation in Disease: Risk Factors, Management and Outcomes'. Dawson, R.K. (Ed.), pp. 1-56, Nova Publishers, New York.

Table of Contents

List of Figures

List of Abbreviations

Aβ = beta-amyloid

AD = Alzheimer's disease

ANOVA = analysis of variance

ATP = adenosine triphosphate

Bak = Bcl-2 homologous antagonist killer

Bax = Bcl-2-associated X

β-NAD = beta-nicotinamide adenine dinucleotide

βAPP = beta amyloid precursor protein

BBB = blood-brain barrier

BDNF = brain-derived neurotrophic factor

Bid = BH3 interacting-domain death agonist

BSA = bovine serum albumin

CBS = calf bovine serum

CDP-DAG = cytidine diphosphate-diacylglycerol

CDS = CDP-DAG synthetase

CHL = chemiluminescence

CLS = cardiolipin synthase

CNS = central nervous system

cOD = corrected optical density

CTCF = corrected total cell fluorescence

CTP = cytidine triphosphate

DAMP = damage-associated molecular pattern

DAPI = 4',6-diamidino-2-phenylindole

DAT = dopamine transporter

DMEM/F12 = Dulbecco's modified Eagle medium: nutrient mixture F12 Ham

DMF = N,N-dimethylformamide

DMSO = dimethyl sulfoxide

DPH = diaphorase

EDTA = ethylenediaminetetraacetic acid

ELISA = enzyme-linked immunosorbent assay

ETC = electron transport chain

EtOH = ethanol

FITC = fluorescein isothiocyanate

fMLP = N-formylmethionine-leucyl-phenylalanine

GDNF = glial cell line-derived neurotrophic factor

GFAP = glial fibrillary acidic protein

HBSS = Hanks' balanced salt solution without calcium/magnesium

HCl = hydrogen chloride

HEPA = high-efficiency particulate air

IBA = ionized calcium-binding adaptor molecule

IFN = interferon

IGF = insulin-like growth factor

IL = interleukin

iNOS = inducible nitric oxide synthase

INT = iodonitrotetrazolium chloride

LDH = lactate dehydrogenase

LPS = lipopolysaccharide

LSD = least significant difference

MCP = monocyte chemoattractant protein

MFI = mean fluorescence intensity

MHC = major histocompatibility complex

MTT = 3-(4,5-dimethylthiazol-2-yl)-2,5-diphenyltetrazolium bromide

MtCK = mitochondrial isoform of creatine kinase

nAChR = nicotinic acetylcholine receptor

NADPH = nicotinamide adenine dinucleotide phosphate

NET = norepinephrine transporter

NFT = neurofibrillary tangle

NGF = nerve growth factor

NO = nitric oxide

NT = neurotrophin

OD = optical density

PA = phosphatidic acid

PBS = phosphate-buffered saline

PG = phosphatidylglycerol

PGP = phosphatidylglycerol phosphate

RNS = reactive nitrogen species

ROS = reactive oxygen species

SDS = sodium dodecyl sulphate

SEM = standard error of the mean

SIP = stock isotonic percoll

Smac/DIABLO = second mitochondria-derived activator of caspase/direct inhibitor of apoptosis-binding protein with low pI

tBid = truncated Bid

TNF = tumor necrosis factor

TREM = triggering receptor expressed on myeloid cells

3x Tg-AD = triple transgenic mouse model of AD

Acknowledgements

First, and foremost, I would like to express my deepest gratitude and appreciation to my supervisor, Dr. Andis Klegeris. Under your guidance, I have been able to develop and refine my skills that apply not only to our field of research, but also to life outside of the scientific community. You have offered continual support and patience over the past two years and have shown me that hard work, perseverance, and a little optimism pays off in the end. I am truly fortunate to have been granted this opportunity to work with you, and for that I am sincerely grateful. I would also like to extend a heartfelt thank you to the members of my supervisory committee: to Dr. Bruce Mathieson, your expertise in the field has contributed invaluable insight throughout this process; and to Dr. Mark Rheault, your assistance with confocal microscopy, as well as your continual support and guidance throughout the duration of my program, have been extremely insightful and are greatly appreciated.

I would also like to acknowledge my fellow graduate students in the Department of Biology at UBCO. A special thank you to Aaron Johnstone of Dr. Phil Barker's laboratory for sharing his expertise on the microscope, as well as for always assisting with troubleshooting. I would also like to extend a sincere thank you to all of the undergraduate and graduate students in Dr. Klegeris' Laboratory for Cellular and Molecular Pharmacology for always keeping our lab running smoothly and for readily offering assistance when needed. To Ekta Bajwa, thank you for your edits (especially the late-night ones), for always offering a listening ear and for continually keeping me grounded through this process. To Jordan McKenzie, thank

you for all you have done for the lab, and for myself. Your support and relentless willingness to help is immensely appreciated. Finally, to Lindsay Spielman, I am extremely grateful for your constant support and guidance throughout my degree. I am forever indebted to you for your insights, kind words and, of course, countless hours of editing. Each of you has made my time in this program so enjoyable and I am very grateful to have had the opportunity to work alongside you.

Lastly, I would like to thank my family. To my parents and grandmother, I would not be who I am today without your love and support. Thank you for always being there for me when I need it the most. You inspire me to be better each and every day. And to Taylor Wilson, thank you for your unwavering support, patience, and faith in my abilities. Thank you for encouraging me when I was down and for celebrating with me during my successes. You are my rock.

For my parents

Chapter 1: Introduction

1.1. The Central Nervous System

The central nervous system (CNS) is an intricate and complicated system, comprised of the brain and spinal cord. This system is composed primarily of two main types of cells: neurons and non-neuronal glial cells. Neurons are excitable brain cells that play a critical role in signal transmission and information processing (Ribrault et al., 2011). Neurons, following sufficient excitation, transmit electrical signals in the form of action potentials, which travel down the neuronal axon and cause the release of chemical messengers, called neurotransmitters, at the axon terminals. These neurotransmitters are responsible for signal and information transmission from one neuron to the next (Breedlove and Watson, 2013; Ribrault et al., 2011; Sincich et al., 2009). Efficient transport and propagation of these electrical and chemical signals is crucial for proper brain function, as these processes control all voluntary and involuntary movements, as well as the formation of all thoughts, emotions and memories produced and stored by the brain (Etkin et al., 2015; Keller and Heckhausen, 1990; Murphy et al., 2003).

Glial cells, including oligodendrocytes, astrocytes and microglia, are involved in the regulation of brain homeostasis, as well as in providing nutritional, structural and chemical support to neurons (Jessen, 2004). Oligodendrocytes are involved in the formation of the myelin sheath, a lipid-rich structure that surrounds neuronal axons and acts as an insulating layer that significantly increases the rate of electrical transmission in neurons (Edgar and Nave, 2009; Keirstead and Blakemore, 1999).

Oligodendrocytes also contribute to neuronal support through the expression of various neurotrophic factors including brain-derived neurotrophic factor (BDNF), nerve growth factor (NGF) and neurotrophin (NT)-3, which promote the growth and survival of multiple CNS cell types (Dai et al., 2003; Elkabes et al., 1996; Huang and Reichardt, 2001).

Astrocytes are star-shaped glial cells, which possess long extensions that protrude from the cell body. These cells assist with maintenance of the extracellular environment within the CNS (Jessen, 2004; Parpura et al., 2012). Astrocytes promote homeostatic conditions in the brain by assisting with the maintenance of blood-brain barrier (BBB) integrity, by regulating extracellular potassium levels and by scavenging reactive oxygen species (ROS) in the CNS (Kettenmann and Verkhratsky, 2008; Osborn et al., 2016). Furthermore, astrocytes participate in neuronal support by regulating synapse formation, synaptic transmission and neuronal repair, as well as by supplying neurons with essential energy substrates (Kettenmann and Verkhratsky, 2008; Meyer and Kaspar, 2016; Nedergaard et al., 2003; Sherwood et al., 2006).

Microglia, the resident macrophages of the CNS, play a critical role in promoting neuronal growth and functioning, as well as in regulating the CNS immune status during various states of health and disease. Microglia express and secrete various neurotrophic factors, including BDNF, NGF, glial cell line-derived neurotrophic factor (GDNF), NT-3 and insulin-like growth factor (IGF)-1, which are detected and recognized by surrounding neurons. These growth and trophic factors contribute to neuronal survival, as well as to synaptic development and plasticity

(Elkabes et al., 1996; Huang and Reichardt, 2001; Nakajima and Kohsaka, 2001). It has been demonstrated that these factors not only affect neuronal growth and development, but also regulate the proliferation and maturation of other surrounding microglia (Elkabes et al., 1996; Heese et al., 1998).

Microglia, however, are best known for their role in regulating the neuroimmune status of the CNS. Under normal physiological conditions, microglia are believed to be in a resting and ramified state. In this state, microglia possess long processes that are constantly surveying their surrounding environment for indicators of damage or danger (Kraft and Harry, 2011; Lull and Block, 2010; Nimmerjahn et al., 2005; Saijo and Glass, 2011). Microglia are able to recognize a variety of noxious stimuli, including pathogens, pro-inflammatory mediators and harmful cellular debris. Following interaction with these stimuli, microglia shift to an activated state, which is characterized by alterations in their physiology and secretory profile (Cherry et al., 2014; Kraft and Harry, 2011; Nimmerjahn et al., 2005; Streit et al., 1999). Activated microglia, which assume an amoeboid-like shape devoid of long processes, migrate to the area of insult and propagate the inflammatory response. Microglial activation induces the release of cytokines, such as tumor necrosis factor (TNF)-α and monocyte chemoattractant protein (MCP)-1, which functions to recruit other immune cells to the affected area, as well as other pro-inflammatory mediators and cytotoxic molecules, including reactive nitrogen species (RNS) and ROS (Akiyama et al., 2000; Colton and Gilbert, 1987; Jessen, 2004; Lull and Block, 2010; Parpura et al., 2012; Saijo and Glass, 2011; Yang et al., 2010). Additionally, activated microglia upregulate their expression of major

histocompatibility complex (MHC) proteins, which present antigen peptides to other microglia, as well as perform phagocytosis in attempts to rid the brain of the noxious stimuli (Brown and Vilalta, 2015; Lull and Block, 2010; Saijo and Glass, 2011; von Bernhardi et al., 2015; Yang et al., 2010).

Microglial activation is an extremely beneficial response, as it aids in eliminating noxious molecules, contributes to the maintenance of homeostatic conditions and regulates immune status of the CNS. However, in many CNS diseases, the pathological formations present in the brain cannot be removed by the efforts of the microglia, which leads to their over-activation (Kraft and Harry, 2011; Streit et al., 1999). This over-activation causes dysregulation of microglial functioning and results in the persistent release of cytotoxic molecules, as well as a decrease in expression of trophic factors BDNF and IGF-1, which can ultimately result in damage or death to surrounding brain cells, including other glia and neurons (Banati et al., 1993; Brown and Vilalta, 2015; Budni et al., 2015; Lull and Block, 2010). Following injury, neurons release a variety of damage-associated molecular pattern (DAMP) molecules, as well as additional ROS and RNS, which are recognized by neighboring microglia and induce further activation of these cells (Cherry et al., 2014). This self-perpetuating cycle of microglia-mediated cytotoxicity facilitates extensive neurodegeneration and ultimately induces a chronic neuroinflammatory state, which has been implicated in the pathogenesis of various brain diseases, including Alzheimer's disease (AD) (Figure 1.1) (Akiyama et al., 2000; Cherry et al., 2014; Mandrekar-Colucci and Landreth, 2010; Solito and Sastre, 2012).

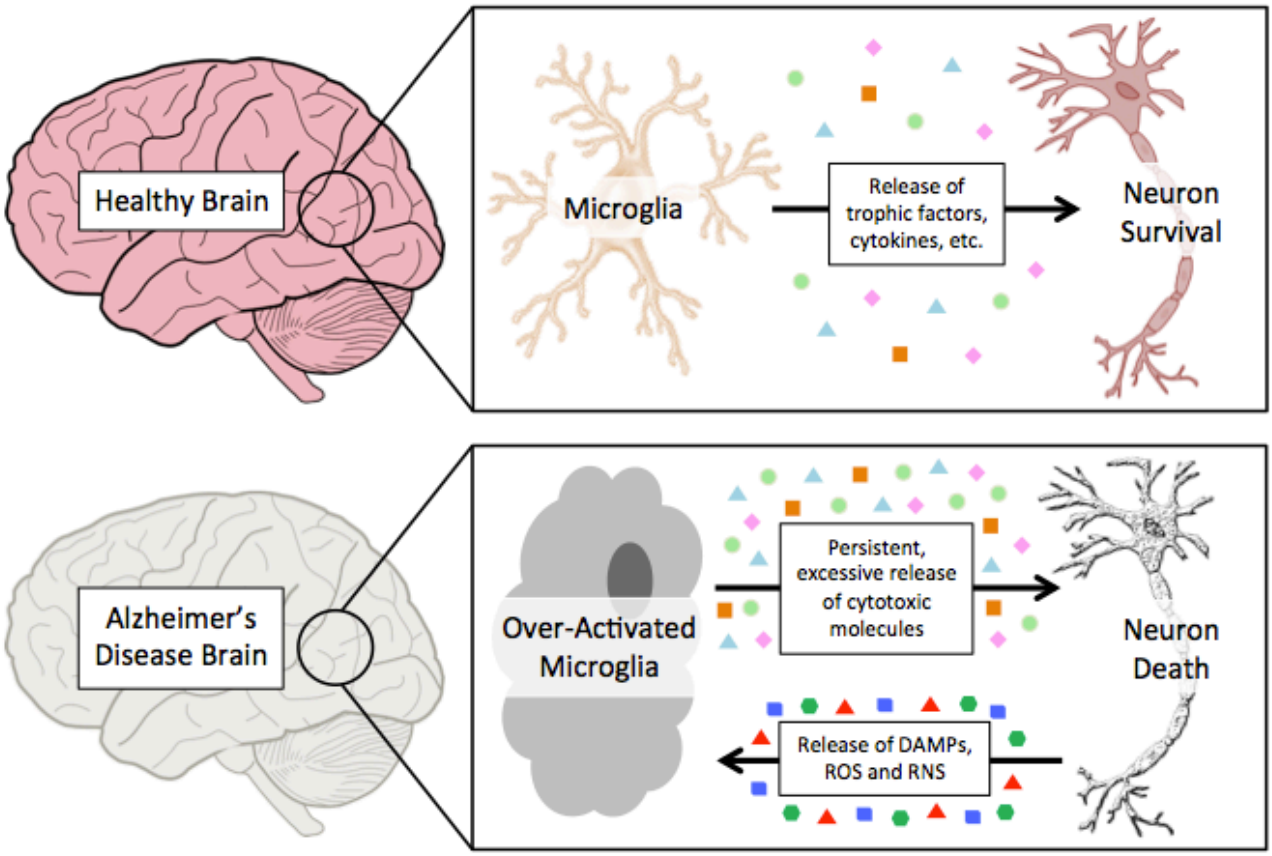

Figure 1.1. Microglial responses in healthy and diseased brains. DAMP = damage-associated molecular pattern, RNS = reactive nitrogen species, ROS = reactive oxygen species.

1.2. Alzheimer's Disease and Neuroinflammation

AD is a chronic and progressive neurodegenerative disorder that currently affects over 35 million people worldwide (Wortmann, 2012). AD is characterized by a decline in cognitive ability, which commonly manifests as significant memory impairment, as well as alterations in behaviour and personality (Breedlove and Watson, 2013; Fernandez et al., 2010; Prince et al., 2015). Although the underlying causes of the disease are still debated, the two molecular hallmarks hypothesized to contribute to AD pathogenesis include the deposition of extracellular beta-amyloid

(Aβ) plaques, as well as the formation of insoluble intracellular fibrillar inclusions called neurofibrillary tangles (NFTs) (Blasko et al., 2004; Wang and Mandelkow, 2016). The Aβ plaques, also known as senile plaques, are formed due to dysregulated processing of beta amyloid precursor protein (βAPP), which leads to the overproduction and reduced clearance of Aβ protein, and thereby promotes Aβ aggregation (Bamberger and Landreth, 2002; Blasko et al., 2004; Monteiro-Cardoso et al., 2015). The formation of NFTs occurs due to the hyperphosphorylation of tau, a protein normally involved in the assembly and stabilization of cytoskeletal microtubules (Mandelkow and Mandelkow, 2012; Sergeant et al., 2008; Terwel et al., 2002). The Aβ plaques and NFTs are implicated in the pathophysiology of AD, as they have been shown to induce microglial activation, as well as produce toxic effects towards surrounding brain cells, thereby propagating the extensive neuron death and chronic neuroinflammation observed in AD brains (Gotz et al., 2010; Monteiro-Cardoso et al., 2015; Wang and Mandelkow, 2016).

Despite over one hundred years of research, there is still limited understanding of the underlying mechanisms that contribute to the onset and progression of AD. This lack of understanding has resulted in a shortage of viable therapeutic strategies available for the treatment of AD (Huang and Mucke, 2012). In attempts to better understand this disease, many hypotheses have been developed with the aim of explaining the pathophysiology of AD. For over two decades, the most widely accepted theory was the Amyloid Cascade Hypothesis of AD, which emphasizes the deposition of Aβ plaques as the initiator of disease pathogenesis. However, this hypothesis fails to thoroughly explain the extensive

neuronal death observed in AD brains, as it has been documented that the extent of Aβ plaque aggregation is not correlated with neuronal loss (Gomez-Isla et al., 1997; Karran et al., 2011; Reitz, 2012). Recently, there has been increasing support for the Inflammation Hypothesis of AD, which proposes neuroinflammation as an integral feature in the progression of the disease, as well as in the development of disease symptoms (Akiyama et al., 2000; Halliday et al., 2000; Wyss-Coray and Rogers, 2012; Zotova et al., 2010). This theory emphasizes the role of microglia, which are able to recognize and respond to the irregular Aβ plaques and NFTs present in AD brains. Following interaction with these stimuli, microglia become activated and participate in the non-specific release of various molecules, including pro-inflammatory cytokines, RNS and ROS, in attempts to rid the brain of the irregular structures (Dheen et al., 2007; Mandrekar-Colucci and Landreth, 2010; McCaulley and Grush, 2015; Rogers and Lue, 2001; Wyss-Coray and Rogers, 2012; Zotova et al., 2010). Despite their efforts, the microglia are unable to clear the brain of the foreign Aβ plaques and NFTs, which results in the over-activation of microglia (Paresce et al., 1997; Rogers and Lue, 2001). As described in section 1.1, the over-activation of microglia leads to the persistent release of cytotoxic molecules and induces a state of chronic neuroinflammation, which can have damaging effects on surrounding cells and result in extensive neuron death (Giulian, 1999; Lull and Block, 2010; Morales et al., 2014; Wyss-Coray and Rogers, 2012). One critical finding, which supports the Inflammation Hypothesis of AD, is the discovery that the over-activation of microglia may precede the formation of the neuritic tangles, and that these cells actually contribute to the hyperphosphorylation of tau, thereby

increasing NFT formation (Gorlovoy et al., 2009). These neurodegenerative changes that occur in response to the over-activation of microglia result in chronic neuroinflammation, which many experts believe contributes to the advancement of AD pathogenesis and resulting cognitive decline (Morales et al., 2014; Venigalla et al., 2015; von Bernhardi et al., 2015).

1.3. Cardiolipin

1.3.1. Biosynthesis and Structure

Cardiolipin is an anionic phospholipid with a distinctive structure consisting of a double glycerophosphate backbone and four fatty acid side chains (Figure 1.2), which differs from the single glycerophosphate backbone and two fatty acid side chains found in most phospholipids (Cheng et al., 2008; Li et al., 2015; Pope et al., 2008). Although most mitochondrial phospholipids are synthesized in the endoplasmic reticulum and subsequently transferred to the mitochondria for utilization, cardiolipin is unique in that it is synthesized exclusively in the mitochondria (Hatch, 2004; Ye et al., 2016). The mature form of cardiolipin resides primarily in the inner mitochondrial membrane, where it constitutes approximately 25% of the total membrane lipids (Chicco and Sparagna, 2007; Mejia et al., 2014; Paradies et al., 2009).

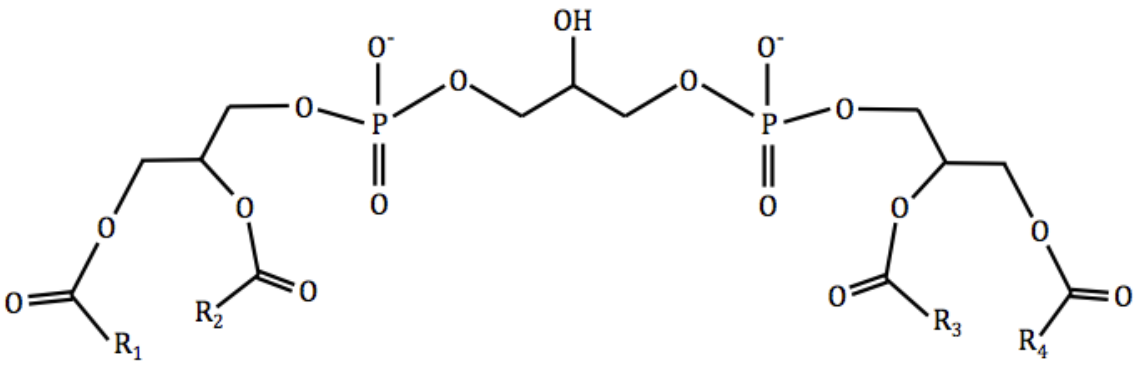

Figure 1.2. Structure of cardiolipin. R = fatty acid side chains.

Mature cardiolipin is synthesized during a two-phase process: *de novo* synthesis and subsequent remodeling (Figure 1.3 and 1.4, respectively). The *de novo* synthesis of immature cardiolipin occurs in the inner mitochondrial membrane, and commences following the formation of cytidine diphosphate-diacylglycerol (CDP-DAG). CDP-DAG is generated after a condensation reaction between phosphatidic acid (PA) and cytidine triphosphate (CTP), which is catalyzed by the activity of CDP-DAG synthetase (CDS). Subsequently, phosphatidylglycerol phosphate (PGP) synthase transfers an activated phosphatidyl group from CDP-DAG to the *sn*-1 position of the *sn*-glycerol-3-phosphate backbone to form PGP. Following its formation, a PGP phosphatase hydrolyzes PGP to form phosphatidylglycerol (PG). The final step of the *de novo* synthesis is catalyzed by cardiolipin synthase (CLS), which transfers a phosphatidyl group from a CDP-DAG molecule to PG, yielding immature cardiolipin (Mejia et al., 2014; Pope et al., 2008; Schlame et al., 2000).

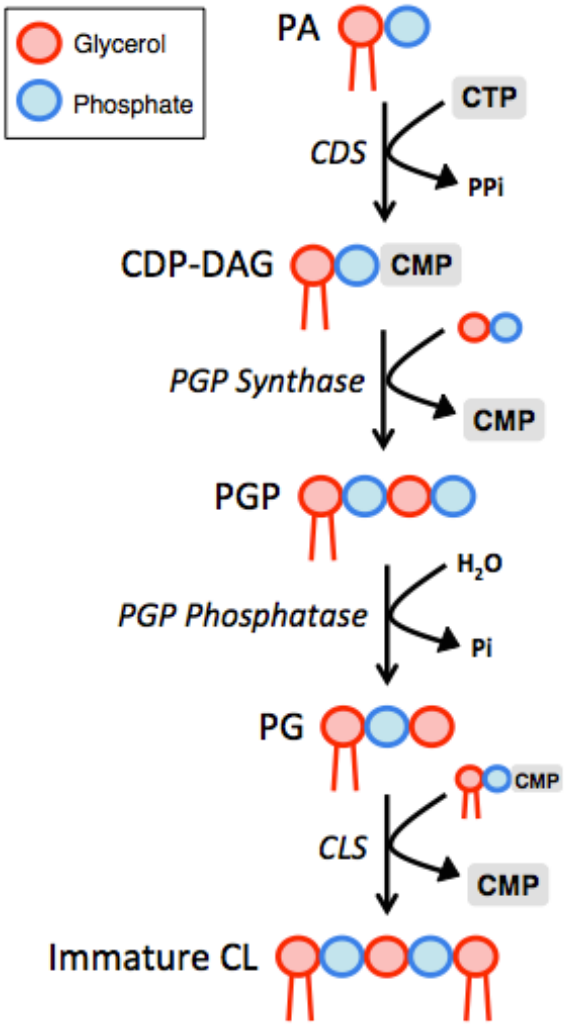

Figure 1.3. The *de novo* synthesis of cardiolipin. CDS = CDP-DAG synthetase, CDP-DAG = cytidine diphosphate-diacylglycerol, CL = cardiolipin, CLS = cardiolipin synthase, CMP = cytidine monophosphate, CTP = cytidine triphosphate, PA = phosphatidic acid, PG = phosphatidylglycerol, PGP = phosphatidylglycerol phosphate, Pi = inorganic phosphate, PPi = pyrophosphate.

The remodeling phase, which occurs shortly after the completion of *de novo* synthesis of immature cardiolipin, is responsible for transforming cardiolipin into its mature form (Schlame, 2013; Ye et al., 2016). During remodeling, the immature form of cardiolipin is deacylated, resulting in the formation of monolysocardiolipin. Monolysocardiolipin is reacylated by the activity of the tafazzin enzyme, which

utilizes fatty acid chains donated from surrounding phospholipids, including phosphatidylcholine and phosphatidylethanolamine, to produce mature cardiolipin (Schlame, 2013; Xu et al., 2003; Ye et al., 2016).

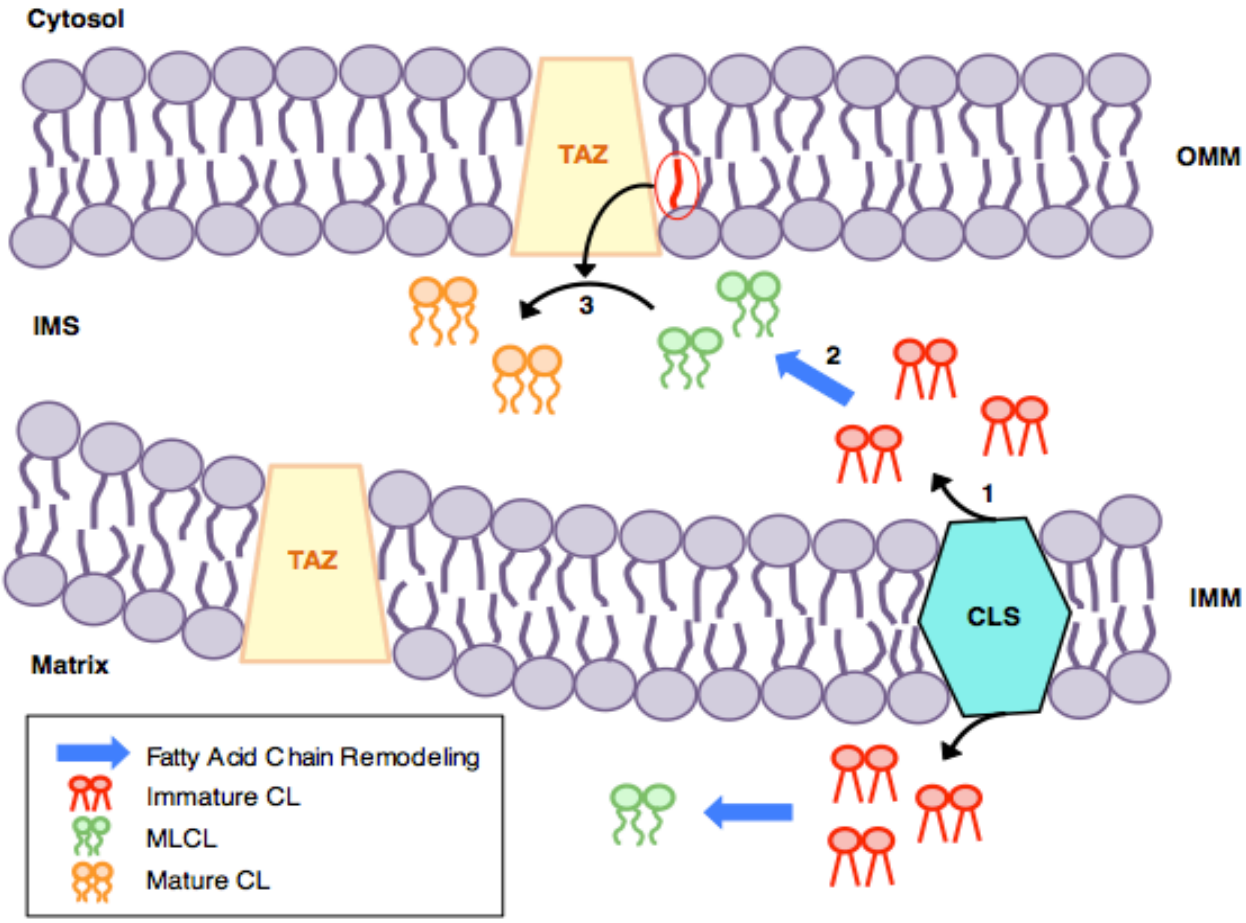

Figure 1.4. The remodeling phase of cardiolipin synthesis. 1) The immature form of cardiolipin (CL) is produced following the final step of *de novo* synthesis, which is catalyzed by the activity of cardiolipin synthase (CLS). 2) Monolysocardiolipin (MLCL) is formed following the deacytelation of immature cardiolipin. 3) Mature cardiolipin is formed following the reacytelation of monolysocardiolipin by the tafazzin (TAZ) enzyme, which utilizes fatty acid chains donated from surrounding phospholipids. IMS = intermembrane space, IMM = inner mitochondrial membrane, OMM = outer mitochondrial membrane.

Once synthesized, mature cardiolipin possesses a distinct structure that enables it to acquire a conical shape within the phospholipid bilayer. This configuration contributes to cardiolipin's ability to maintain mitochondrial membrane fluidity, as well as interact with various proteins located in both the mitochondria and cytosol of the cell (Sathappa and Alder, 2016; Schlame et al., 2000). However, the unique structure of cardiolipin, which contains four fatty acid side chains with higher level of unsaturation when compared to other phospholipids that only possess two fatty acid side chains, also increases its susceptibility to peroxidative damage (Chicco and Sparagna, 2007; Paradies et al., 2009; Pope et al., 2008). Due to its location in the mitochondria, cardiolipin is exposed to high levels of ROS, which are primarily formed during the excessive metabolism of oxygen via oxidative phosphorylation (Chong et al., 2005; Ott et al., 2007; Paradies et al., 2011). The extent of cardiolipin peroxidation, which depends on the degree of fatty acid unsaturation, affects the structure of cardiolipin. Structural changes in cardiolipin can interfere with various lipid-protein interactions required for proper mitochondrial functioning and/or result in lipid degradation, thereby, hindering the ability of cardiolipin to regulate various metabolic processes (Bielski et al., 1983; Ott et al., 2007; Paradies et al., 2011). Although the exact mechanisms by which peroxidized cardiolipin affects the activity of various mitochondrial enzymes are poorly understood, it has been shown that the altered structure of cardiolipin leads to mitochondrial dysfunction, further ROS production, and ultimately, cell death (Paradies et al., 2009; Pope et al., 2008).

1.3.2. Role of Cardiolipin in the Central Nervous System

Cardiolipin was initially discovered and isolated from the mammalian heart, where the most predominant form is tetralinoleoyl cardiolipin (Chicco and Sparagna, 2007; Pangborn, 1942). In this form, cardiolipin contains four fatty acid side chains with 18 carbon molecules and two double bonds (18:2) each (Chicco and Sparagna, 2007; Schlame et al., 2000). Following the heart, the second most prevalent location of cardiolipin is the brain, where there are over one hundred different molecular species of cardiolipin, each containing fatty acid side chains that have a different degree of saturation and/or length (Cheng et al., 2008; Kiebish et al., 2009). The most abundant forms of cardiolipin within the CNS contain palmitic (16:0), stearic (18:0), oleic (18:1) and arachidonic (20:4) fatty acid chains (Mancuso et al., 2009; Yabuuchi and O'Brien, 1968). Within the CNS, cardiolipin has been shown to support mitochondrial functioning, facilitate metabolic processes and regulate the viability of neurons and glial cells, including oligodendrocytes, astrocytes and microglia (Cheng et al., 2008; Chu et al., 2013; Fressinaud et al., 1990; Jacobson et al., 2002; Zhang et al., 2011). However, it has been demonstrated that the amount of cardiolipin is approximately two-fold higher in glial cells when compared to neurons (Kolomiytseva et al., 2010).

Cardiolipin is implicated in the regulation of various cellular functions, including intracellular and mitochondrial signaling, mitochondrial electron transport chain (ETC) efficiency, mitochondrial membrane fusion and fission, as well as the programmed death of cells by apoptosis (Chicco and Sparagna, 2007; Mancuso et al., 2009; Petrosillo et al., 2008). In healthy neurons and glial cells,

cardiolipin plays a pivotal role in regulating cellular metabolic processes through the binding and stabilization of various respiratory supercomplexes. These supercomplexes are formed following the aggregation of complex I, complex III and complex IV of the ETC (Figure 1.5) (Acin-Perez et al., 2008; Lapuente-Brun et al., 2013; Pfeiffer et al., 2003). By facilitating their formation, cardiolipin induces a conformational change that increases the enzymatic activity of the supercomplexes, which promotes the efficient transport of electrons between complexes, while simultaneously minimizing the production of excess ROS (Paradies et al., 2011; Pope et al., 2008). Additionally, its presence in the inner mitochondrial membrane enables cardiolipin to promote the transport of protons across the inner mitochondrial membrane, thereby generating a stable electrochemical gradient (Cui et al., 2014; Pfeiffer et al., 2003; Sen et al., 2006). Cardiolipin also regulates the synthesis of ATP by binding to, and stabilizing, complex V (ATP synthase) of the ETC (Acehan et al., 2011; Jonckheere et al., 2012). In this role, cardiolipin utilizes its anionic phosphate head-containing structure to trap protons and directly supply them to complex V, a process that contributes to the maintenance of mitochondrial membrane potentials, as well as to the efficiency of ATP synthesis (Haines and Dencher, 2002; Sen et al., 2006).

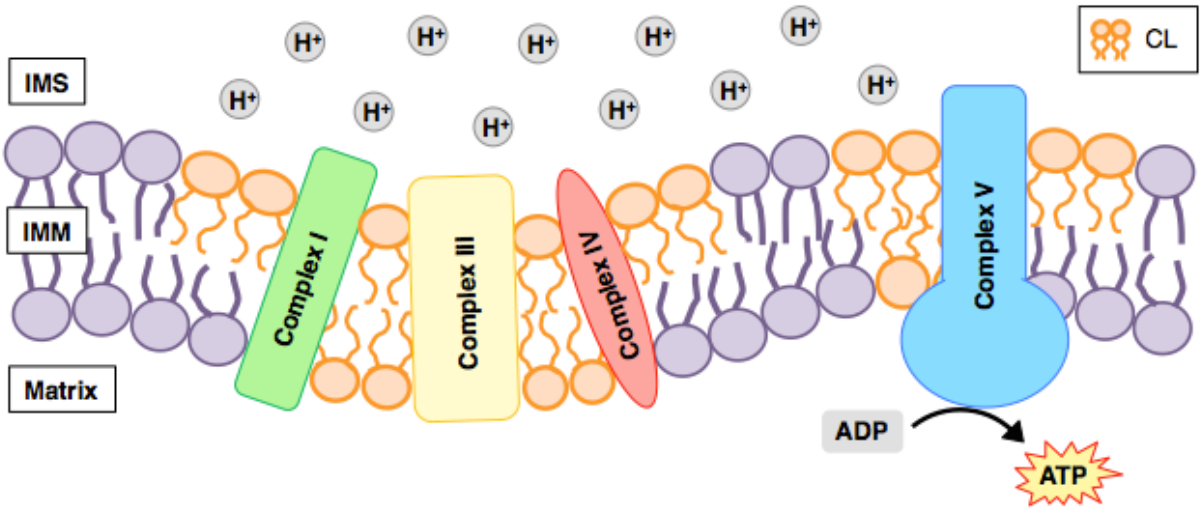

Figure 1.5. Cardiolipin binds to and stabilizes the electron transport chain (ETC) complexes. Cardiolipin (CL) plays a critical role in maintaining ETC efficiency by stabilizing the respiratory supercomplexes formed by the aggregation of complexes I, III and IV of the ETC. Complex V (ATP synthase) is also bound to and stabilized by cardiolipin, where it acts as a proton (H^+) trap and contributes to the maintenance of mitochondrial potentials, which are required for the synthesis of adenosine triphosphate (ATP). ADP = adenosine diphosphate, IMM = inner mitochondrial membrane, IMS = intermembrane space.

In damaged or dying neurons and glial cells, cardiolipin participates in the regulation of mitophagy, the selective degradation of malfunctioning mitochondria, and apoptotic cell death (Chu et al., 2013; Li et al., 2015; McMillin and Dowhan, 2002; Petrosillo et al., 2008). During mitophagy, dysfunctional mitochondria, which can produce excessive and harmful levels of ROS, are sequestered and degraded. This process, which is required to prevent oxidative damage to surrounding organelles and membranes, is mediated in part by cardiolipin following its redistribution from the inner mitochondrial membrane to the outer mitochondrial membrane (Garcia Fernandez et al., 2002). The translocation of cardiolipin between mitochondrial membranes is facilitated by the activity of the mitochondrial isoform

of creatine kinase (MtCK), which binds to cardiolipin on the outer face of the inner mitochondrial membrane and facilitates the formation of contact sites between the inner and outer mitochondrial membranes (Maniti et al., 2009; Schlattner et al., 2009; Speer et al., 2005). At the mitochondrial contact sites, MtCK induces the clustering of cardiolipin, and promotes the sequestration and transfer of cardiolipin from the inner to the outer mitochondrial membrane (Epand et al., 2007; Schlattner et al., 2009). Following its redistribution to the outer mitochondrial membrane, cardiolipin acts as an elimination signal and is recognized by various proteins involved in the initiation and propagation of mitophagic processes (Chu et al., 2014; Chu et al., 2013; Li et al., 2015; Paradies et al., 2009).

Cardiolipin also plays a critical role in cellular apoptosis (Figure 1.6). During this process, cardiolipin is redistributed from the inner mitochondrial membrane to the outer mitochondrial membrane (Li et al., 2015; McMillin and Dowhan, 2002; Raemy et al., 2016). Following translocation to the outer mitochondrial membrane, cardiolipin not only functions as a cytosolic signaling molecule, but also interacts with cytochrome *c*, a protein involved in the ETC, within the intermembrane space of the mitochondria (Anthonymuthu et al., 2016; Hong et al., 2012; Pope et al., 2008; Schlattner et al., 2009). The interaction of cationic cytochrome *c* with mitochondrial membrane constituents, such as cardiolipin, promotes the initiation of multiple types of apoptosis, including the perforin/granzyme and the intrinsic pathways (Cheng et al., 2008; Elmore, 2007; Kulikov et al., 2012; Schlattner et al., 2009). This interaction leads to the formation of a cardiolipin/cytochrome *c* complex, which functions to selectively oxidize cardiolipin. Once cardiolipin is oxidized, the

cardiolipin/cytochrome *c* complex dissociates, which increases the permeability of the outer mitochondrial membrane (Hong et al., 2012; Kagan et al., 2005; Tyurin et al., 2008; Vladimirov et al., 2013). This increase in membrane permeability permits the release of various molecules from the mitochondrial intermembrane space into the cytoplasm, including the pro-apoptotic factors cytochrome *c* and the second mitochondria-derived activator of caspase/direct inhibitor of apoptosis-binding protein with low pI (Smac/DIABLO) (Kagan et al., 2005; Petrosillo et al., 2008; Raemy et al., 2016).

Following its release into the cytoplasm, cytochrome *c* interacts with several caspases, which are known to positively regulate cell death by engaging other pro-apoptotic molecules, including BH3 interacting-domain death agonist (Bid) (Cheng et al., 2008; van Gurp et al., 2003). Bid normally resides in the cytosol, where it can be cleaved by caspase-2 or caspase-8 to induce its activation (Bonzon et al., 2006; Huang and Strasser, 2000). Following its cleavage, the active portion of Bid, known as truncated Bid (tBid), relocates from the cytosol to the mitochondria. tBid increases mitochondrial membrane permeability through the oligomerization of Bcl-2-associated X (Bax) and Bcl-2 homologous antagonist killer (Bak) proteins, which induce the release of cytochrome *c* from the mitochondria (Huang and Strasser, 2000; Kim et al., 2004; Kulikov et al., 2012). The migration and binding of tBid may be facilitated by cardiolipin, as it has been shown that tBid binding is restricted to the cardiolipin-enriched mitochondrial contact sites (Esposti et al., 2003; Kim et al., 2004). Additionally, it has been demonstrated that mitochondrial membranes deficient of cardiolipin result in impaired tBid binding, and

subsequently, reduced release of cytochrome *c* into the cytoplasm (Lutter et al., 2000; Lutter et al., 2001), which is an essential step in the apoptotic process of both neurons and glial cells (Camilleri et al., 2013; Jazvinscak Jembrek et al., 2015; Simon et al., 2000; Sparvero et al., 2010; Tyurin et al., 2008). Combined, these findings demonstrate that cardiolipin plays a critical role in apoptotic processes within the cells of the CNS.

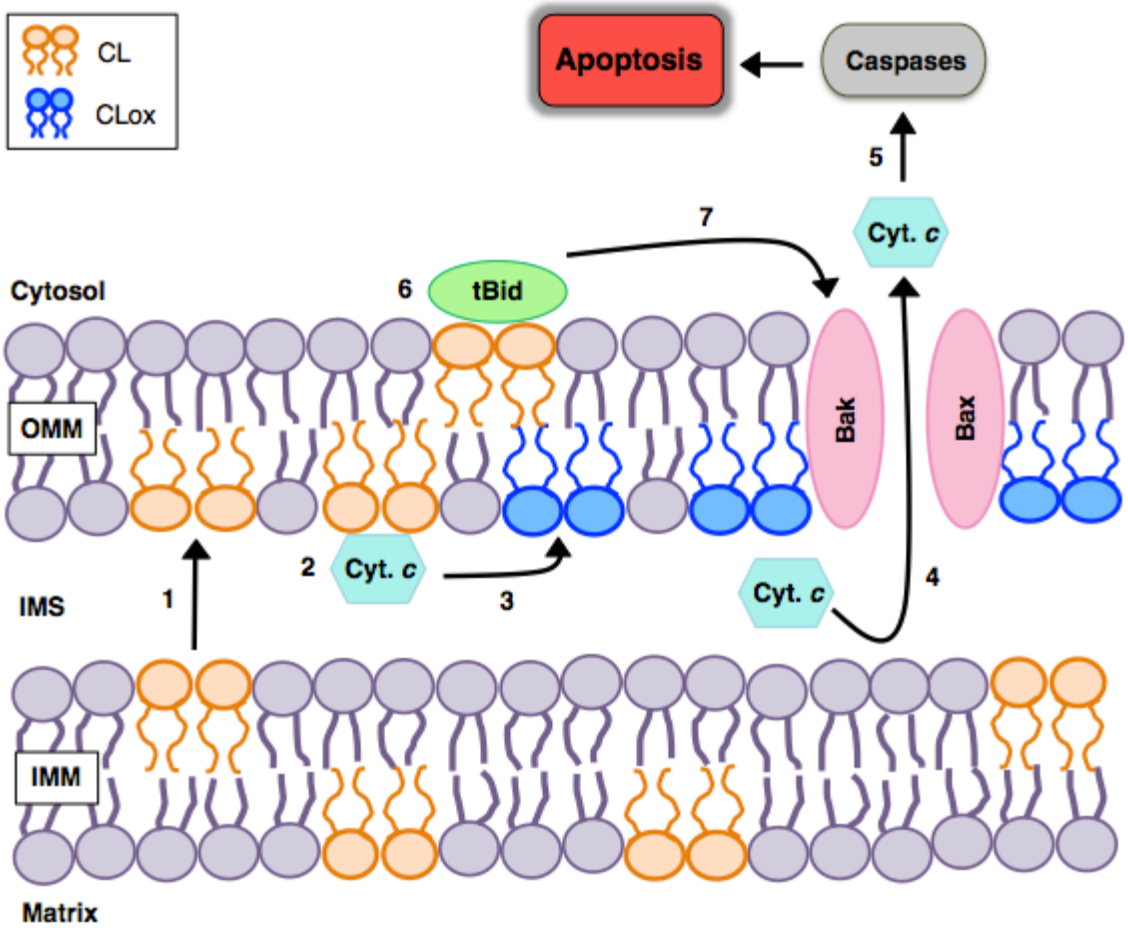

Figure 1.6. Cardiolipin plays a role in regulating cellular apoptosis. Following the initiation of apoptotic processes, 1) cardiolipin (CL) is redistributed from the inner mitochondrial membrane (IMM) to the outer mitochondrial membrane (OMM). Following its relocation, 2) cardiolipin interacts with cytochrome *c* (Cyt. *c*), which facilitates the formation of the cardiolipin/cytochrome *c* complex. 3) The formation of this complex results in the oxidation of cardiolipin (CLox), which subsequently causes the cardiolipin/cytochrome *c* complex to dissociate. This dissociation increases mitochondrial membrane permeability and 4) allows for cytochrome *c* to be released from the intermembrane space (IMS) into the cytoplasm. 5) Following its release from the mitochondria, cytochrome *c* interacts with various caspases, which positively regulate the apoptotic process by 6) promoting the migration and binding of truncated BH3 interacting-domain death agonist (tBid) to the outer mitochondrial membrane. Once bound to the mitochondria, 7) tBid further increases mitochondrial membrane permeability through the oligomerization of Bcl-2 homologous antagonist killer (Bak) and Bcl-2-associated X (Bax) proteins, which induces further cytochrome *c* release from the mitochondria.

1.3.3. Cardiolipin in Alzheimer's Disease

As a consequence of its high metabolic rate and significant proportion of unsaturated phospholipids, the brain is an organ that is particularly susceptible to oxidative stress and damage (Chong et al., 2005). It has been demonstrated that aging brains, particularly those affected by AD, are associated with an increase in the production of ROS (Mariani et al., 2005). This age-related increase in oxidative stress can result in extensive peroxidative damage to mitochondrial membrane constituents, including cardiolipin (Fang et al., 2016; Petrosillo et al., 2008; Zhou et al., 2008). Due to the pivotal role of cardiolipin in regulating various functions in both neurons and glial cells, modification to the structure of cardiolipin, or cardiolipin-associated molecules, can result in altered mitochondrial structure and functioning. Such changes can include enlarged, weakened or dysregulated mitochondria, which can have a detrimental effect on brain cell viability (Cheng et al., 2008; Fry and Green, 1981; Monteiro-Cardoso et al., 2015; Sathappa and Alder, 2016). For these reasons, adverse changes in the structure of cardiolipin, as well as decreased levels of functional cardiolipin, have been implicated in the pathogenesis of neurodegenerative disorders, including AD (Chicco and Sparagna, 2007; Honda et al., 2004; Mancuso et al., 2009). For example, it has been demonstrated that the brain mitochondria from aged rats contain 26% less cardiolipin when compared to the mitochondria from brains of young rats (Ruggiero et al., 1992). These findings were further confirmed by Petrosillo et al. (2008), who showed that, when compared to the brains of young rats, aged rats had a significant reduction in brain cardiolipin levels, which was accompanied by increased percentage of peroxidized

cardiolipin and a corresponding reduction in activity of complex I of the ETC. Furthermore, they demonstrated that the activity of mitochondrial complex could be completely restored to the control level following the application of exogenous cardiolipin, which was purified from the mitochondria of young rat brains (Petrosillo et al., 2008). Additionally, Monteiro-Cardoso et al. (2015) utilized a triple transgenic mouse model of AD (3x Tg-AD) to demonstrate that within AD brains, levels of mitochondrial cardiolipin were reduced by approximately 1.5-fold, which was accompanied by a decrease in complex I activity. Furthermore, this cardiolipin-related mitochondrial dysfunction was found to precede the deposition of Aβ plaques and formation of NFTs in 3x Tg-AD mice (Monteiro-Cardoso et al., 2015). Therefore, it is evident that maintaining the concentration of functional cardiolipin in the brain is critical for regulating essential mitochondrial processes, particularly within aging brains and those afflicted by neurodegenerative diseases, such as AD.

Due to its importance in regulating metabolic processes in the brain, the therapeutic potential of cardiolipin for the treatment of various neurodegenerative diseases has become an active area of study. For example, it has been demonstrated that liposomes with embedded cardiolipin, which can readily cross the BBB, have an affinity for Aβ peptides in the AD brain without producing toxic effects to the endothelial or phagocytic cells present in the CNS (Gobbi et al., 2010; Ordonez-Gutierrez et al., 2015; Orlando et al., 2013; Vieira and Gamarra, 2016). Additionally, it has been shown that the intraperitoneal injection of cardiolipin-embedded liposomes into double transgenic APP/PS1 AD model mice significantly reduced the presence of Aβ peptides in their plasma (Ordonez-Gutierrez et al., 2015). Although it

is promising that these liposomes have exhibited high affinity toward one of the cellular hallmarks of AD, further investigation is required to determine whether the association between these liposomes and Aβ peptides could lead to the clearance of the toxic aggregates from the AD brain (Gobbi et al., 2010). Furthermore, it has been shown that cardiolipin-containing liposomes are capable of delivering NGF across the BBB, which subsequently increased the survival of neurons that were previously damaged by neurotoxic Aβ peptides (Kuo and Liu, 2014). These findings indicate that cardiolipin-containing liposomes could be utilized as a therapeutic tool for the effective delivery of various drugs into the brains of AD patients (Orlando et al., 2013). However, additional studies are required to determine whether these liposomes will effectively reduce Aβ peptide aggregation, or enhance the clearance of the senile plaques, ultimately diminishing the extensive neurodegeneration and associated clinical symptoms observed in AD patients (Pointer and Klegeris, 2016).

1.4. Modeling Microglial Activation and Neuroinflammation

Microglial activation is a crucial immune response required for maintaining and regaining homeostatic conditions in the CNS. However, the over-activation of microglia has been implicated in chronic neuroinflammation, as well as in the development and progression of many neurodegenerative disorders, including AD (Akiyama et al., 2000; Cherry et al., 2014). For these reasons, many researchers have chosen to study microglia, in aims of better understanding the mechanisms involved in neuroinflammatory processes (Carson et al., 2008; Gresa-Arribas et al., 2012; Stansley et al., 2012). Since primary microglia, and especially those of human origin,

are difficult to obtain, microglia-like immortalized cell lines are often used. Immortalized cells are generally created following transfection with viral genes, which allow the cells to proliferate for prolonged periods of time, or following the extraction of immortal cancerous cells that can be cultured into cell lines (Masters, 2000; Mitra et al., 2013). Cell lines are an invaluable tool for laboratory research as they are readily available, inexpensive, easy to maintain, and can be used for high throughput assays (Kaur and Dufour, 2012; Pan et al., 2009). However, despite their availability and convenience of use, immortalized cell lines are prone to genetic drifting, which may contribute to variation in their genotype, causing cell phenotype that is divergent from the original (Horvath et al., 2008; Pan et al., 2009). Additionally, immortalized cell lines are often used in mono-culture, meaning that they are cultured in isolation, and do not directly interact with other cell types; therefore, the cell lines utilized in this study may behave and respond differently from the corresponding primary cell type in the CNS, where cells are continually communicating with one another (Miki et al., 2012; Regier et al., 2016). The use of primary cells, which are extracted directly from human or animal tissue, have limitations as well, including the difficulty of obtaining cells, the slow or absent rate of proliferation, as well as a limited life span.

The experiments described in this thesis were conducted using several types of immortalized cell lines to model the primary cells and cellular interactions of the CNS. Due to the limitations and limited availability of primary cells, only the key findings of this thesis were confirmed utilizing primary microglia, to ensure that the

results obtained were not due to the aforementioned differences between immortalized and primary cells.

In this study, microglial activation and neuroinflammation were modeled *in vitro* by using interferon (IFN)-γ and/or lipopolysaccharide (LPS) as the stimulating agents. These stimuli were chosen as they have been shown to induce an activation state similar to that seen in microglia in pathological conditions (Chao et al., 1992; Culbert et al., 2006; Klegeris and McGeer, 2000; Sheng et al., 2011; Wang et al., 2015). For example, it has been demonstrated that stimulation of cultured microglia with IFN-γ and/or LPS not only promotes the secretion of TNF-α, MCP-1 and nitric oxide (NO), but also induces neurotoxicity, which is a characteristic feature of the neuroinflammatory processes observed in several neurodegenerative diseases (Chao et al., 1992; Chow et al., 2012; Gresa-Arribas et al., 2012; Klegeris and McGeer, 2000, 2003; Leonard et al., 1993).

1.4.1. Model Cell Lines

In this study, human THP-1 monocytic cells, human HL-60 promyelocytic cells and murine BV-2 cells were used as microglia models, whereas human SH-SY5Y neuroblastoma cells were used as a neuron model. THP-1 cells, which were originally isolated from the blood of a one-year old male with acute monocytic leukemia, are widely-recognized as a microglia model due to their ability to perform various processes associated with microglial functioning, including phagocytosis and the secretion of inflammatory mediators (Diaz-Silvestre et al., 2005; Klegeris and McGeer, 2003; Tsuchiya et al., 1980). In this study, the THP-1 cells were utilized

in the microglia-mediated cytotoxicity experiments, as well as for the enzyme-linked immunosorbent assays (ELISAs), as previous studies have identified that these cells secrete cytokines and cytotoxic substances when stimulated with various pro-inflammatory molecules (Klegeris et al., 2005; Klegeris and McGeer, 2003).

HL-60 cells, which were originally derived from the blood of a female with acute promyelocytic leukemia, are routinely differentiated into macrophage-like cells that exhibit properties similar to those of primary microglia, such as the secretion of ROS (Birnie, 1988; Collins, 1987; Levy et al., 1990). Unlike THP-1 cells, differentiated HL-60 cells possess the subunits of the nicotinamide adenine dinucleotide phosphate (NADPH)-dependent oxidase, which is required for the generation of the respiratory burst, an immune response that involves the production of high amounts of ROS (Dahlgren and Karlsson, 1999; Forman and Torres, 2002; Levy et al., 1990). For this reason, the HL-60 cells, rather than the THP-1 cells, were utilized for the respiratory burst assay.

The BV-2 microglia cell line, which was generated following the transfection of murine microglial cells with a v-raf/v-myc recombinant retrovirus, is widely used as an *in vitro* model of primary murine microglia (Bocchini et al., 1992; Gresa-Arribas et al., 2012). Although not a perfect representation of microglia, BV-2 cells have been shown to secrete NO, as well as participate in phagocytosis, in a manner similar to that of primary murine microglia (He et al., 2002; Horvath et al., 2008; Pan et al., 2011; Watters et al., 2002). Therefore, the BV-2 cells were employed in the Griess assay, which is used to quantify NO secretion, as well as for the phagocytosis assay.

SH-SY5Y cells, which were originally isolated from the bone marrow of a female with neuroblastoma, are widely accepted as a model of neuronal cells (Biedler et al., 1973; Klegeris and McGeer, 2003; Kovalevich and Langford, 2013; Pahlman et al., 1990; Xie et al., 2010). SH-SY5Y cells have been shown to synthesize dopamine and noradrenaline, as well as possess various neuronal cell markers, including dopamine transporter (DAT), norepinephrine transporter (NET) and nicotinic acetylcholine receptors (nAChR); therefore, exhibiting similarities to primary human neurons (Kovalevich and Langford, 2013; Xicoy et al., 2017). In this study, SH-SY5Y cells were utilized in the microglia-mediated cytotoxicity experiments, as previous experiments have demonstrated that SH-SY5Y cells are susceptible to glial cell-mediated neurotoxicity (Klegeris et al., 2005; Klegeris and McGeer, 2003; Spielman et al., 2015).

1.5. Research Overview and Hypothesis

Since over-activated microglia are implicated in the propagation of the chronic neuroinflammation and extensive neurodegeneration observed in AD brains, identifying novel means of attenuating this detrimental microglial response may help to delay the onset and slow the progression of the disease. Previous studies have revealed that various phospholipids expressed on cell surfaces, including phosphatidylserine and phosphatidylcholine, regulate immune cell functioning and can reduce inflammatory responses within peripheral tissues, as well as in the CNS (Aabdallah and Eid, 2004; Hartmann et al., 2009; Jung et al., 2013; Segawa and Nagata, 2015; Tokes et al., 2011; Treede et al., 2007; Wu et al., 2006).

Therefore, externalized phospholipids, and their corresponding receptors, may represent a possible therapeutic target for the treatment of neurodegenerative diseases, such as AD, that are characterized by dysregulated microglial activation and extensive death of neurons.

Cardiolipin is primarily found within the inner mitochondrial membrane; however, studies have demonstrated that this phospholipid is not only relocated to the outer mitochondrial membrane and plasma membrane of the cell, but can also be released extracellularly during various cellular processes (Balasubramanian et al., 2015; Nakajima et al., 2008; Sorice et al., 2004; Sorice et al., 2000). Additionally, it has been shown that cardiolipin-containing liposomes are capable of modifying the function of peripheral macrophages (Balasubramanian et al., 2015). Although the critical role of cardiolipin in regulating mitochondrial metabolic processes within both the periphery and CNS is well defined, limited research is available regarding the effects of externalized cardiolipin on CNS cell functions. Therefore, we aimed to determine whether extracellular cardiolipin can alter CNS immune cell functioning and potentially impact the chronic neuroinflammation observed in AD brains.

The **central hypothesis** of this thesis proposes that extracellular cardiolipin regulates select microglial functions. To study the effects of extracellular cardiolipin on microglia *in vitro*, several cell culture techniques and biological assays were conducted using immortalized cell lines, as well as primary murine microglia.

The three main **research objectives** addressed in this thesis are:

1. To determine whether extracellular cardiolipin induces the phagocytic activity of microglia.
2. To determine whether extracellular cardiolipin affects microglial functions that impact neuronal viability.
    i. Investigate the effect of cardiolipin on microglia-mediated cytotoxicity.
    ii. Investigate the effect of cardiolipin on neurotrophic factor expression by microglia.
3. To determine whether extracellular cardiolipin alters the secretory profile of microglia.
    i. Investigate the effect of cardiolipin on RNS secretion by microglia.
    ii. Investigate the effect of cardiolipin on ROS secretion by microglia.
    iii. Investigate the effect of cardiolipin on the secretion of pro-inflammatory cytokines by microglia.

Chapter 2: Materials and Methods

2.1. Chemicals and Reagents

The following reagents were obtained from Sigma Aldrich (Oakville, ON, Canada): 3-(4,5-dimethylthiazol-2-yl)-2,5-diphenyltetrazolium bromide (MTT) beta-nicotinamide adenine dinucleotide (β-NAD), cytochalasin B, diaphorase (DPH, from *Clostridium kluyveri*), dimethyl sulfoxide (DMSO), DNase I, extravidin-alkaline phosphatase, fluoroshield with 4',6-diamidino-2-phenylindole (DAPI), N-formylmethionine-leucyl-phenylalanine (fMLP), D-(+)-glucose, iodonitrotetrazolium chloride (INT), LPS (from *Escherichia coli* 055:B5), luminol sodium salt, N-(1-napthyl)ethylenediamine dihydrochloride, paraformaldehyde, phosphoric acid, sodium L-lactate, sulfanilamide, D-(+)-trehalose dihydrate and Triton X-100.

The following reagents were obtained from ThermoFisher Scientific (Ottawa, ON, Canada): bovine serum albumin (BSA), calf bovine serum (CBS), dibasic sodium phosphate, diethanolamine, N,N-dimethylformamide (DMF), Dulbecco's modified Eagle medium: nutrient mixture F12 Ham (DMEM/F12), ethanol (EtOH), goat serum, Hanks' balanced salt solution without calcium/magnesium (HBSS), hydrogen chloride (HCl), monobasic sodium phosphate, papain, percoll, penicillin/streptomycin/amphotericin B solution, phenol-free DMEM/F12, phosphatase substrate tablets, sodium bicarbonate, sodium carbonate, sodium chloride, sodium dodecyl sulphate (SDS), sodium nitrite and 0.05% and 0.25% trypsin/ethylenediaminetetraacetic acid (EDTA) solutions.

Human recombinant IFN-γ, as well as TNF-α and MCP-1 ELISA kits were purchased from Peprotech (Rocky Hill, NJ, USA). Phosphate-buffered saline (PBS) tablets, Tween 20 and methanol were purchased from VWR International (Mississauga, ON, Canada). The rabbit anti-mouse BDNF antibody (Catalogue #SC-546), the rabbit anti-mouse GDNF antibody (Catalogue #SC-328), as well as the fluorescein isothiocyanate (FITC)-conjugated goat anti-rabbit antibody (Catalogue #SC-2012) were obtained from SantaCruz Biotechnology (San Jose, CA, USA). The rabbit anti-mouse ionized calcium-binding adaptor molecule (IBA)-1 antibody was purchased from WAKO (Catalogue #016-20001, Irving, CA, USA). Dako rabbit anti-mouse glial fibrillary acidic protein (GFAP) antibodies were purchased from Cedarlane Laboratories (Catalogue #Z033429-2, Burlington, ON, Canada).

The bovine heart cardiolipin utilized in this study was purchased from Sigma Aldrich (Catalogue #C1649). The cardiolipin solution contained a variety of molecular species of this phospholipid; however, 80% or greater of the cardiolipin molecules contained polyunsaturated fatty acid side chains.

2.2. Equipment and Supplies

All cell culture experiments were performed in a class 2, type IIA biological safety cabinet. Cell culture experiments were conducted using sterile 12-, 24- or 96-well plastic cell culture plates (Corning, Corning, NY, USA). The 12-well plates were utilized for the phagocytosis assay, the 24-well plates were utilized for seeding THP-1 and SH-SY5Y cells, and the 96-well plates were utilized when conducting ELISAs, the MTT and LDH assays, as well as for seeding HL-60 cells for use in the respiratory

burst assay. Sterile eight-well chamber slides (ThermoFisher Scientific) were used for the immunofluorescence and phagocytosis assays. Sterile petri dishes (10 cm, ThermoFisher Scientific) were used for the differentiation of HL-60 cells. Sterile tissue culture dishes (10 cm, Corning) were used for culturing primary murine microglia following extraction. Cell cultures were grown in T-75 flasks (Sarstedt, Montreal, QC, Canada) and incubated in a Steri-Cycle High-Efficiency Particulate Air (HEPA) Class 100 CO_2 incubator (Model #370, ThermoFisher Scientific). Cells were manually counted using a hemocytometer (ChangBioscience, Castro Valley, CA, USA). The Sorvall RT1 centrifuge (ThermoFisher Scientific) was used for primary murine microglia cell extraction, and prior to seeding cells for use in various protocols. The FLUOstar Omega microplate reader (BMG Labtech, Nepean, ON, Canada) was used for spectrophotometric and chemiluminescent measurements.

2.3. Cell Lines

The human THP-1 monocytic, the human HL-60 promyelocytic and the murine BV-2 microglia cell lines were used as microglia models. The human SH-SY5Y neuroblastoma cells were used to model neurons. The THP-1 cells and the HL-60 cells were obtained from the American Type Culture Collection (ATCC, Manassas, VA, USA), the BV-2 cells were generously donated by Dr. G. Garden (Center on Human Development and Disability, University of Washington, Seattle, WA, USA) and the SH-SY5Y cells were generously donated by Dr. Robert Ross (Department of Biological Sciences, Fordham University, Bronx, NY, USA). The cell lines were stored in liquid nitrogen in 1.2 ml cryovials (ThermoFisher Scientific) containing

DMEM/F12 media supplemented with 20% CBS and 10% DMSO, which acts as a cryoprotectant, as well as penicillin (100 U/ml), streptomycin (100 μg/ml) and amphotericin B (250 ng/ml). All cell lines were grown in T-75 flasks containing DMEM/F12 supplemented with 10% CBS, as well as penicillin (100 U/ml), streptomycin (100 μg/ml) and amphotericin B (250 ng/ml) (F10 medium). All flasks were incubated at 37^{O}C in humidified 5% CO_2 and 95% air atmosphere.

2.4. Primary Murine Microglia Extraction

Primary murine microglia were extracted from adult C57BL/6 mouse brains supplied by our collaborators Dr. D. Gibson and Dr. S. Ghosh from the UBC Okanagan Department of Biology, as previously described (Lee and Tansey, 2013). The composition of all reagents and solutions utilized during the extraction are listed in Appendix A. The mouse brain was placed into a sterile petri dish (10 cm, Corning) with 3 ml of DMEM/F12 supplemented with penicillin (100 U/ml), streptomycin (100 μg/ml) and amphotericin B (250 ng/ml) (F0 medium). The brain tissue was minced finely and transferred to a 50 ml conical tube containing 3 ml of dissociation medium. The conical tube was placed into a water bath at 37^{O}C for 20 min, following which 5 ml of F10 medium with glucose was added to neutralize the proteolytic enzymes present in the dissociation medium. The tube was then centrifuged for 5 min at 250 g, after which the supernatant was decanted. The pellet was re-suspended using F0 medium with glucose, and centrifuged again for 5 min at 250 g. The supernatant was decanted and 3 ml of F10 medium with glucose was added to the tube. The pellet was re-suspended, and repetitive suction and expulsion by a 10

ml pipette was utilized to break up the remaining pieces of brain tissue. Once the brain tissue easily passed through the pipette tip, an additional 5 ml of F10 medium with glucose was added to the tube containing the brain tissue. A 1 ml pipette tip and a 200 µl pipette tip were then used to further break up the tissue into a cell suspension. A 40 µm cell strainer (ThermoFisher Scientific), which was placed on the top of a new 50 ml tube, was wetted using 2 ml of F10 medium with glucose before the cell suspension was filtered through. The tube containing the filtered cell suspension was then centrifuged for 4 min at 250 g. After the supernatant was removed, the pellet was re-suspended in 5 ml of F10 medium with glucose, and the tube was centrifuged for an additional 4 min at 250 g. The pellet was re-suspended with 4 ml of 37% stock isotonic percoll (SIP) solution and transferred to a new 15 ml conical tube. 4 ml of 70% SIP solution was used to slowly underlay the 37% SIP layer. Subsequently, 4 ml of 30% SIP solution was slowly added on top of the 37% SIP layer, followed by the addition of 2 ml of 1x HBSS on top of the 30% SIP layer (Figure 2.1). The tube was then centrifuged for 40 min at 300 g (18^{0}C) without applying brakes to stop the spinning. Following centrifugation, a pipette was used to collect 3 ml of the 37-70% SIP interphase, which contained the extracted brain cells. This solution was transferred to a clean 15 ml tube, and 3 ml of 1x HBSS was added for every 1 ml of interphase collected (9 ml HBSS total). The tube was then centrifuged for 7 min at 500 g (4^{0}C) and the supernatant was removed. The pellet was re-suspended in 3 ml of 1x HBSS, and centrifuged for an additional 5 min at 800 g (4^{0}C). This step was repeated two additional times to ensure the cells were thoroughly washed. Finally, the cells were re-suspended in 10 ml of F10 media,

seeded in a sterile tissue culture dish (10 cm, Corning) and placed into the CO_2 incubator at 37^{0}C to allow for cell recovery and adherence to the plate surface. Two days following the extraction procedure, the medium above the adherent microglia was gently removed and 10 ml of fresh F10 media were added to the cells.

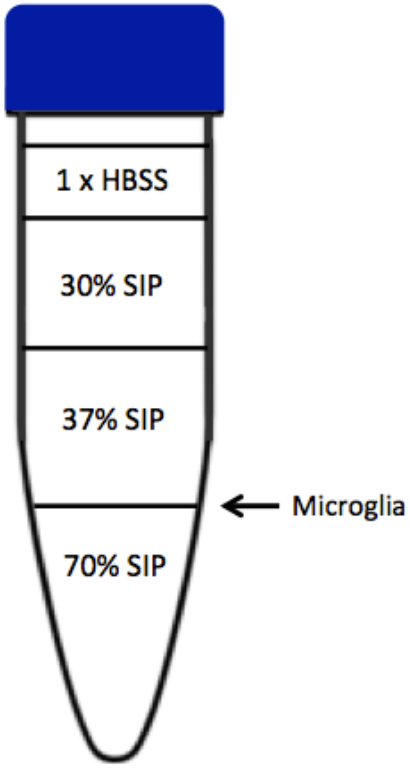

Figure 2.1. Stock isotonic percoll (SIP) solution gradient utilized in primary murine microglia extraction. HBSS = Hanks' balanced salt solution.

2.5. Phagocytic Activity of Microglia

2.5.1. Phagocytosis Assay using Murine BV-2 Cells

Murine BV-2 microglia were used to study the effect of cardiolipin on phagocytosis. BV-2 cells, which are adherent, were detached from the T-75 flasks by removing the media, adding 1.5 ml of 0.25% trypsin/EDTA and incubating for 3 min at 37^{0}C. Subsequently, the flasks were gently tapped to dislodge the cells from the

plastic. Once the majority of cells were detached from the flask, 10 ml of F10 media were added to neutralize the trypsin solution, and the cells were counted using a hemocytometer. The cells were placed in a 50 ml tube, centrifuged at 450 g for 7 min and subsequently re-suspended in DMEM/F12 supplemented with 5% CBS, penicillin (100 U/ml), streptomycin (100 μg/ml) and amphotericin B (250 ng/ml) (F5 medium) to a final concentration of 1 x 10^5 cells/ml. The cells were seeded at 500 μl/well into a sterile 12-well plate with sterile 18 mm glass cover slips (ThermoFisher Scientific) placed into each well. The plates were then placed in the CO_2 incubator for 24 h to allow for cell recovery and adherence to the glass cover slips. Following incubation, the media in each well was replaced with fresh F5 medium, and the cells were incubated for a 30 min period. The cells were then treated with cardiolipin (5 or 20 μg/ml) or its vehicle solution (1% v/v EtOH) and placed in the CO_2 incubator. Following 15 min incubation, the cells were stimulated with LPS (0.5 μg/ml), which was chosen as the inflammatory stimulus, as it has been shown to effectively induce the phagocytic activity of BV-2 cells (He et al., 2002; Majerova et al., 2014; Pan et al., 2011). Following stimulation, the BV-2 cells were placed in the CO_2 incubator for 24 h. Based on a study of similar nature (He et al., 2002), 0.8 μm latex beads in suspension (Sigma Aldrich) were added to each well at a concentration of 1 μl/ml. The BV-2 cells were incubated with the beads for 2.5 h, following which the cells were washed 1x with PBS and fixed for 20 min with 4% paraformaldehyde solution in PBS (pH = 6.9). Following fixation, the cover slips were removed from each well and placed cell side-down onto glass slides (ThermoFisher Scientific) for imaging using light microscopy.

The cells were visualized using a Zeiss AxioObserver.Z1 widefield microscope (Carl Zeiss, Toronto, ON, Canada) and imaged using Zen image acquisition software (version 2.0, Carl Zeiss). For each treatment condition, a minimum of 50 cells were examined. Cells containing greater than 10 beads were considered phagocytic (He et al., 2002), and the percentage of phagocytic cells was calculated using the following equation:

$$1)\ \%\ \text{Phagocytic Cells} = \frac{\#\ \text{of Phagocytic Cells}}{\text{Total \# of Cells}} \times 100\%$$

Phagocytosis was confirmed using cytochalasin B, a cell-permeable fungal toxin that has been shown to reversibly inhibit the phagocytic activity of various cell types, including BV-2 cells (Axline and Reaven, 1974; Malawista et al., 1971; Park et al., 2009; Zurier et al., 1973). Cytochalasin B exerts its effects by inhibiting the polymerization of actin, which interferes with the microfilament organization responsible for the formation of phagocytic vacuoles, or phagosomes (Axline and Reaven, 1974; Davis et al., 1971). BV-2 cells were seeded as described in section 2.5.1, and the plates were placed in the CO_2 incubator for 24 h to allow for cell recovery and adherence to the glass cover slips. Following incubation, the media in each well was replaced with fresh F5 medium, and the cells were incubated for a 30 min period. The cells were then treated with cytochalasin B (20 μM) and incubated for 1 h, following which either cardiolipin (5 or 20 μg/ml) or its vehicle solution (1% v/v EtOH) was added to the cells, and the plates were placed in the CO_2 incubator. Following 15 min incubation, the cells were stimulated with LPS (0.5 μg/ml), and placed in the CO_2 incubator for 24 h. Following incubation, the

phagocytosis assay, as well as cell visualization and analysis, were conducted exactly as described above.

2.5.2. Phagocytosis Assay using Primary Murine Microglia

Primary murine microglia were used to confirm the effects of cardiolipin on BV-2 cell phagocytosis. Primary murine microglia were extracted as described in section 2.4, and kept in the CO_2 incubator for 5-7 days prior to use in the phagocytosis assay. Primary murine microglia, which are adherent, were detached from the 10 cm tissue culture dishes by removing the media, adding 1.5 ml of 0.25% trypsin/EDTA solution for 5 min at 37^0C, and gently tapping the sides of the dish to aid in detachment of cells. The trypsin solution was neutralized by adding 10 ml of F10 medium, and the cells were counted using a hemocytometer. The cells were centrifuged at 450 g for 7 min and re-suspended in F5 medium to a final concentration of 5×10^4 cells/ml. The cells were seeded at 250 µl/well onto a sterile eight-well chamber slide, and the plates were placed in the CO_2 incubator for 24 h to allow for cell recovery and adherence to the well surface. Following incubation, the cells were treated with cardiolipin (5 or 20 µg/ml) or its vehicle solution (1% v/v EtOH) and incubated for an additional 24 h. Based on previous studies of a similar nature (Heo et al., 2015; Mayo et al., 2011), 1 µm Fluoresbrite® YG microspheres in suspension (Polysciences Inc., Warrington, PA, USA) were added to each well at a final concentration of 0.0025% v/v. Preliminary experiments using primary murine microglia revealed that untreated control cells were detectably phagocytic. When the primary murine microglia were incubated with latex beads, it was difficult to

accurately visualize and count the beads when analyzing the images due to the large number of beads internalized by the primary cells. For this reason, the fluorescent microspheres were used, rather than the latex beads, as a way to quantify the phagocytic activity of the primary murine microglia. The primary cells were incubated with the fluorescent microspheres for 1 h, following which the cells were washed 1x with PBS and fixed in the dark for 20 min in 4% paraformaldehyde solution. Following fixation, the cells were washed 2x with PBS, and 100 µl of fluoroshield with DAPI was added to each well prior to imaging with fluorescent microscopy.

The cells were visualized using a Zeiss AxioObserver.Z1 widefield epifluorescence microscope and imaged using Zen image acquisition software at an excitation/emission of 350/470 nm for DAPI (nuclei stain) and 470/520 nm for the fluorescent beads. For each treatment well, a minimum of 50 cells were examined. The mean fluorescence intensity (MFI) for each cell was measured using ImageJ software (version 2.0, National Institutes of Health, Bethesda, MD, USA), as previously described (McCloy et al., 2014). The corrected total cell fluorescence (CTCF) was calculated using the following formula:

1) CTCF = Integrated Density - (Area of the Cell x Background Fluorescence)

The integrated density is representative of each cell's fluorescence intensity, and was determined by multiplying area of the selected cell by the mean grey fluorescence intensity of the selected cell area. The background fluorescence is the average of three background fluorescence readings.

Additionally, to ensure the fluorescent beads were engulfed, rather than just adherent to the cell surface, the primary murine microglia were visualized using an Olympus FluoView confocal microscope (Model #FV1000, Olympus Inc., Richmond Hill, ON, Canada) and imaged using FV10-ASW software (version 3.1.2, Olympus Inc.).

2.6. Microglia-Mediated Cytotoxicity

2.6.1. Seeding and Stimulating Human THP-1 Cells

Human THP-1 and SH-SY5Y cells were used to study the effect of cardiolipin on microglia-mediated cytotoxicity. THP-1 cells, which are non-adherent, were harvested from T-75 flasks and counted using a hemocytometer. The cells were centrifuged at 450 g for 7 min and subsequently re-suspended in F5 medium to a final concentration of 5 x 10^5 cells/ml. The cells were seeded at 1 ml/well into a sterile 24-well plate and placed in the CO_2 incubator for 30 min to allow for cell recovery. The cells were then treated with varying concentrations of cardiolipin (2, 10, 20 or 25 μg/ml) or its vehicle solution (0.5% v/v DMSO) and placed in the CO_2 incubator. Following brief 15 min incubation, the cells were stimulated with IFN-γ (150 U/ml) plus LPS (0.2 ng/ml) and incubated for 48 h. These inflammatory stimuli were chosen due to their previously reported efficacy at inducing the secretion of pro-inflammatory mediators and cytotoxic compounds by THP-1 cells (Genin et al., 2015; Klegeris and McGeer, 2003). Following the 48 h incubation, supernatants were collected and THP-1 cell viability was assessed by the MTT and the lactate dehydrogenase (LDH) assays.

2.6.2. Seeding and Treating Human SH-SY5Y Cells

Human SH-SY5Y cells, which are a heterogeneous population of adherent and non-adherent cells, were detached from the T-75 flasks in the same manner as the BV-2 cells (see section 2.5.1), except that the 0.05% trypsin/EDTA solution was used instead of the 0.25% solution. The cells were counted using a hemocytometer, placed into a 50 ml tube and centrifuged at 450 g for 7 min. The SH-SY5Y cells were then re-suspended in F5 medium to a final concentration of 4×10^5 cells/ml and incubated for 24 h to allow for cell recovery and adherence to the plate surface. Following incubation, the media above the SH-SY5Y cells was removed from each well and 400 µl of THP-1 cell supernatants were transferred onto the SH-SY5Y cells. The SH-SY5Y cells were incubated with the THP-1 supernatants for an additional 72 h, following which SH-SY5Y cell viability was assessed by the MTT and LDH assays.

2.7. Cell Viability Assay: 3-(4,5-Dimethylthiazol-2-yl)-2,5-Diphenyltetrazolium Bromide (MTT)

The viability of human THP-1 and SH-SY5Y cells was assessed using the MTT assay. This assay evaluates the metabolic activity of mitochondrial enzymes, including succinate dehydrogenase, and is used as an indirect measure of cell viability (Ferrari et al., 1990; Gerlier and Thomasset, 1986; Liu et al., 1997). In the MTT assay, the mitochondrial enzymes reduce yellow MTT tetrazolium salt to form insoluble purple formazan crystals (Fotakis and Timbrell, 2006; Liu et al., 1997). Viable cells are generally more metabolically active than dying or dead cells, and will therefore reduce MTT tetrazolium salt more rapidly, which results in a higher

rate of production of purple formazan crystals that can be spectrophotometrically measured.

To measure cell viability, MTT was added to each well at a final concentration of 500 μg/ml, and cells were incubated at 37^{0}C for 1 h. SDS/DMF solution (20% SDS, 50% DMF in H_2O, pH = 4.7) was then added to each well at a 1:1 ratio, following which the plates were placed in a wetbox (a sealed plastic container containing moistened paper towel) and incubated at 37^{0}C for an additional 3 h. Following incubation, 100 μl were transferred from each well into a 96-well plate and an optical density (OD) measurement was taken at 570 nm using the FLUOstar Omega microplate reader. The percentage of cell viability was calculated using the following formulae:

1) Corrected OD (cOD) of Each Well = $OD_{sample} - OD_{lysis}$

2) % Cell Viability = $\frac{cOD_{sample}}{cOD_{control}} \times 100\%$

Where OD_{sample} represents the OD reading of each well, OD_{lysis} represents the OD reading of the wells treated with 1% Triton X-100 (100% cell death control), cOD_{sample} represents the corrected OD of each sample well and $cOD_{control}$ represents the corrected OD of the wells containing untreated cells (100% cell viability control).

2.8. Cell Death Assay: Lactate Dehydrogenase (LDH)

The percentage of dead or dying human THP-1 and SH-SY5Y cells was assessed using the LDH assay. This assay measures the activity of the LDH enzyme,

which is critical for the conversion of lactate to pyruvate (Buhl et al., 1978; Fotakis and Timbrell, 2006). LDH is typically found within the cytoplasm of a cell; however, following irreversible cellular damage or lysis, LDH is released into the extracellular space (Fotakis and Timbrell, 2006; Mitchell, 1980). In this assay, the enzymatically active LDH present in cell supernatant reacts with INT tetrazolium salt to form red formazan crystals. Higher concentration of LDH enzyme present in supernatant results in a more intense red color, which can be measured spectrophotometrically. This assay quantifies the relative amount of LDH released by damaged or dead cells, and is, therefore, representative of the percentage of dead and dying cells (Fotakis and Timbrell, 2006).

To conduct the LDH assay, 100 µl of THP-1 or SH-SY5Y supernatants were collected into a 96-well plate. INT was added to each well at a final concentration of 0.4 mg/ml, and the initial OD measurement was immediately taken at 492 nm using the FLUOstar Omega microplate reader. Subsequently, sodium L-lactate (0.9 mg/ml), β-NAD (0.75 mg/ml) and DPH (0.37 mg/ml) were added to each well, and the plate was placed in the dry incubator at 37^0C for 30 min. Following incubation, the final OD measurement was taken at 492 nm. The percentage of cell death was calculated using the following formulae:

1) Corrected OD (cOD) of Each Well = $OD_{final} - OD_{initial}$

2) % Cell Death = $\frac{cOD_{sample} - cOD_{media}}{cOD_{lysis} - cOD_{media}} \times 100\%$

Where OD_{final} represents the OD reading of each well following 30 min incubation, $OD_{initial}$ represents the initial OD reading of each well, cOD_{media}

represents the corrected OD of the wells containing only F5 media, and cOD_{lysis} represents the corrected OD of the wells treated with 1% Triton X-100 (100% cell death control).

2.9. Expression of Neurotrophic Factors by Microglia

2.9.1. Immunofluorescence Assay using Murine BV-2 Cells

Murine BV-2 microglia were used to investigate the effect of cardiolipin on microglial expression of BDNF and GDNF. BV-2 cells were detached from the T-75 flasks as described in section 2.5.1, and the cells were counted using a hemocytometer. The cells were centrifuged at 450 g for 7 min and subsequently re-suspended in F5 medium to a final concentration of 2×10^5 cells/ml. The cells were seeded at 200 µl/well onto a sterile eight-well chamber slide and incubated for 24 h to allow for cell recovery and adherence to well surface. Following incubation, the media in each well was replaced with fresh F5 medium and the plates were placed into the CO_2 incubator for a 30 min recovery period. The cells were then treated with varying concentrations of cardiolipin (5, 10 or 20 µg/ml) or its vehicle solution (1% v/v EtOH) and incubated for an additional 24 h prior to conducting the immunofluorescence assay.

The cells were washed 1x with PBS, fixed for 5 min with ice-cold methanol and then allowed to air dry. The cells were subsequently washed 3x with PBS, and 100 µl of blocking solution (10% goat serum in PBS) was added to each well for 20 min to ensure that non-specific binding of IgG to cells was suppressed. The cells were then washed 1x with PBS and incubated for 1 h with rabbit anti-mouse BDNF

or GDNF antibodies, which were diluted 50x in 1.5% goat serum (in PBS). Following incubation with the primary antibody, the cells were washed 3x for 5 min with PBS. The cells were then incubated for 45 min with FITC-conjugated goat anti-rabbit IgG antibody, which was diluted 100x in 1.5% goat serum. Following incubation with the secondary antibody, the cells were washed 3x with PBS, and 100 µl of fluoroshield with DAPI was added to each well prior to imaging using a fluorescent microscope.

Immunofluorescence was detected using an Olympus fluorescence microscope (Model #BX51, Olympus Inc.) and cells were imaged using MetaMorph software (version 7.7.8, MetaMorph Inc., Nashville, TN, USA) at an excitation/emission of 350/470 nm for DAPI (nuclei stain, blue) and 490/520 nm for FITC (BDNF and GDNF, green). Three images of the DAPI-stained nuclei, three images of the FITC-labeled anti-neurotrophic factor antibodies (either BDNF or GDNF) and three overlay images were captured for each treatment condition. The cell count and MFI for each image were analyzed using ImageJ software (version 2.0, National Institutes of Health), as previously described (McCloy et al., 2014). The CTCF and the MFI per cell were calculated using the following formulae:

1) CTCF = Integrated Density - (Selected Area x Background Fluorescence)

2) $\text{MFI/Cell} = \frac{\text{CTCF}}{\text{Total \# of Cells}}$

The integrated density is representative of the fluorescence intensity of the total selected area, and was determined by multiplying the total selected area by the mean grey fluorescence intensity of the selected area. The background fluorescence

is the average of three background fluorescence readings. To determine the MFI per cell, the CTCF for the selected region was divided by the total number of cells present in that area.

2.9.2. Immunofluorescence Assay using Primary Murine Microglia

Primary murine microglia were used to confirm the effect of cardiolipin on BV-2 cell expression of BDNF and GDNF. Primary murine microglia were extracted as described in section 2.4, and kept in the CO_2 incubator for 5-7 days prior to use in the immunofluorescence assay. Primary murine microglia were detached from the 10 cm tissue culture dishes as described in section 2.5.2, and the cells were counted using a hemocytometer. The cells were centrifuged at 450 g for 7 min and subsequently re-suspended in F5 medium to a final concentration of 1×10^5 cells/ml. The cells were seeded at 200 µl/well onto a sterile eight-well chamber slide and incubated for 24 h to allow for cell recovery and adherence to the well surface. The cells were then treated with varying concentrations of cardiolipin (5, 10 or 20 µg/ml) or its vehicle solution (1% v/v EtOH), and the chamber slides were placed in the CO_2 incubator for an additional 24 h prior to conducting the immunofluorescence assay.

The immunofluorescence assay using primary murine microglia was conducted as described for BV-2 cells in section 2.9.1. In conjunction with these experiments, rabbit anti-mouse IBA-1 antibody (microglia marker, diluted 1000x in 1.5% goat serum) and rabbit anti-mouse GFAP antibody (astrocyte marker, diluted 20,000x in 1.5% goat serum) were used as primary antibodies in the

immunofluorescence assay to confirm that the cells being studied were microglia and not astrocytes. The cells were visualized, and images were acquired and analyzed exactly as described in section 2.9.1.

2.10. Nitrite Secretion by Microglia

2.10.1. Seeding and Stimulating Murine BV-2 Cells

Murine BV-2 cells were used to investigate the effect of cardiolipin on the secretion of nitrite by microglia. BV-2 cells were detached from the T-75 flasks as described in section 2.5.1, and the cells were counted using a hemocytometer. The cells were centrifuged at 450 g for 7 min and subsequently re-suspended in F5 medium to a final concentration of 2×10^5 cells/ml. The cells were seeded at 500 µl/well into a sterile 24-well plate and incubated for 24 h to allow for cell recovery and adherence to the well surface. Following incubation, the media in each well was replaced with fresh F5 medium and the plates were placed in the CO_2 incubator for an additional 30 min recovery period. The cells were then treated with varying concentrations of cardiolipin (2, 10 or 20 µg/ml) or its vehicle solution (1% v/v EtOH) and placed in the CO_2 incubator. Following 15 min incubation, the cells were stimulated with LPS (0.5 µg/ml) and placed in the CO_2 incubator for an additional 24 h prior to conducting the Griess assay.

2.10.2. Griess Assay

The Griess assay is used to quantify the secretion of nitrite, a stable metabolite of NO (Ding et al., 1988; Miranda et al., 2001). In this assay, the Griess

reagents react with the nitrite present in cell supernatants to form a pink azo product, which is measured spectrophotometrically. NO, a well-defined RNS molecule, has been implicated in a variety of physiological processes, including neuronal communication and immune cell activation (Miranda et al., 2001). However, NO has a very short half-life and is, therefore, difficult to directly measure accurately using biochemical assays (Liu et al., 1998). The Griess assay has been previously used to measure nitrite secretion by various cell types, and is generally accepted as an indirect measure of NO secretion (Bryan and Grisham, 2007).

To conduct the Griess assay, 50 µl of BV-2 cell supernatants were transferred into a 96-well plate. 50 µl of the sodium nitrite standards (0.01-40 µM in F5 medium) were prepared and added to the plate in duplicate. Additionally, 50 µl of F5 media only were added to five wells of the plate and used as blank controls. Solution C was made by combining a 1:1 ratio of Solution A (2% sulfanilamide, 5% phosphoric acid in H_2O) and Solution B (0.2% N-(1-napthyl)ethylenediamine dihydrochloride in H_2O). 50 µl of Solution C were added to each well containing samples, standards, or blanks and the OD measurement was immediately taken at 550 nm using the FLUOstar Omega microplate reader. The corrected OD of each sample (cOD_{sample}) was calculated using the following formula:

1) $cOD_{sample} = OD_{sample} - OD_{blank}$

Where OD_{sample} represents the OD reading of each well, and OD_{blank} represents the mean OD reading of the five blank control wells containing F5 media only.

To determine the nitrite concentration in each well, a calibration curve was constructed using the cOD values of the standards (0.01-40 μM), and a linear trend line for the standard curve was plotted. The concentration of nitrite (μM) in each sample, as well as the detection limit (μM) for the assay, were calculated using the following formulae:

2) Nitrite Concentration = $\frac{cOD_{sample}}{m}$

3) Detection Limit = $\frac{\text{Mean } OD_{blank} + 2(\text{Standard Deviation } OD_{blank})}{m}$

Where m represents the slope of the linear trend line for the standard curve.

2.11. Superoxide Anion Secretion by Microglia

2.11.1. Differentiation and Seeding of Human HL-60 Cells

Differentiated human HL-60 cells were used as a microglia model, as they have been shown to express functional subunits of the NADPH oxidase enzyme, which is critical for producing respiratory bursts (Levy et al., 1990). HL-60 cells, which are non-adherent, were harvested from T-75 flasks and counted using a hemocytometer. The cells were centrifuged at 450 g for 7 min, re-suspended in 12 ml of F10 medium to a final concentration of 2 x 10^5 cells/ml and seeded into a 10 cm sterile petri dish. To differentiate the HL-60 cells, DMSO was added to the plate in a drop-wise manner to a final concentration of 1.3% v/v, and the plates were placed in the CO_2 incubator at 37^{0}C for 5 days.

Following differentiation, the HL-60 cells were harvested from the 10 cm dishes and centrifuged at 450 g for 7 min. The cells were seeded at a final

concentration of 1 x 10^6 cells/ml in 250 µl clear (phenol red free) DMEM/F12 supplemented with 2% CBS (F2 medium) into a sterile 96-well plate, which was placed in the CO_2 incubator for a 30 min recovery period. The cells were then treated with varying concentrations of cardiolipin (2, 10 or 20 µg/ml) or its vehicle solution (1% v/v EtOH) and placed in the CO_2 incubator. Following 15 min incubation, the cells were primed using LPS (0.5 µg/ml) and incubated for 24 h prior to conducting the respiratory burst assay.

2.11.2. Respiratory Burst Assay

The respiratory burst is a beneficial immune response performed by a variety of cell types, including neutrophils and macrophages. Following cellular activation, the NADPH oxidase enzyme subunits assemble to produce and secrete high amounts of ROS (Hermann et al., 2004; Richardson et al., 1998). The respiratory burst assay is used to quantify the secretion of superoxide anion, the most commonly occurring oxygen free radical (Chong et al., 2005; Dahlgren and Karlsson, 1999; Levy et al., 1990). In this assay, cells are stimulated with fMLP, a bacterial peptide, to induce the release of superoxide anion, which reacts with luminol to produce photons of light. The light produced can be detected using a plate reader and quantified as a chemiluminescence (CHL) value, which is representative of the quantity of secreted ROS (Dahlgren and Karlsson, 1999).

To conduct the respiratory burst assay, varying amounts of supernatant were removed from each sample to ensure each well of the 96-well plate contained a total volume of 85 µl. The plate was then placed in the dry incubator at 37^{0}C for 5 min.

The luminol solution (10 mg/ml luminol sodium salt in PBS) and the fMLP solution (fMLP in PBS) were prepared and placed in the dry incubator at 37^0C for 5 min. Following incubation, the luminol solution was loaded into the first injector and the fMLP solution was loaded into the second injector of the FLUOstar Omega microplate reader. The 96-well plate containing the differentiated and primed HL-60 cells was then placed into the plate reader, which was programmed to measure light intensity at each 21-second cycle over a 60-cycle period. 10 µl of the luminol solution were added to each well during cycle 5, and 5 µl of the fMLP solution were added to each well during cycle 15. The measurements taken at each cycle were plotted over time to produce a graph, which was analyzed using the Mars Analysis Software (BMG Labtech). Data were expressed as percent CHL of the control well, which was calculated using the following formulae:

1) $nCHL = CHL_{cycles15\text{-}39} - CHL_{cycles40\text{-}60}$

2) $$\% \text{ CHL} = \frac{nCHL_{sample}}{nCHL_{control}} \times 100\%$$

In each of the experiments, the light signal emitted after 40 cycles was equivalent to background light intensity; therefore, the values from cycles 40-60 ($CHL_{cycles40\text{-}60}$) were averaged to obtain the mean background value. To determine the normalized CHL (nCHL) value for each well, the mean background value was subtracted from the values obtained during the respiratory burst response, which was observed during cycles 15-39 ($CHL_{cycles15\text{-}39}$). CHL values were calculated by summing the area under the curve (light measurement vs. time) at each cycle. The percent CHL value was then determined by dividing the nCHL value of each sample

well ($nCHL_{sample}$) by the nCHL value of the control well ($nCHL_{control}$), and multiplying this number by 100%.

2.12. Secretion of Pro-Inflammatory Cytokines by Microglia

To determine the concentrations of TNF-α and MCP-1 secreted by human THP-1 cells, ELISA kits were obtained from Peprotech and the assays were conducted as per the manufacturer's instructions. THP-1 cells were harvested from T-75 flasks and counted using a hemocytometer. The cells were centrifuged at 450 g for 7 min and subsequently re-suspended in F5 medium to a final concentration of 5 x 10^5 million cells/ml. The cells were seeded at 500 µl/well into a sterile 24-well plate, which was placed in the CO_2 incubator for 30 min to allow for cell recovery. The cells were then treated with varying concentrations of cardiolipin (2, 10, 20 or 25 µg/ml) or its vehicle solution (0.5% v/v DMSO) and placed in the CO_2 incubator. Following 15 min incubation, the cells were stimulated with IFN-γ (150 U/ml) plus LPS (0.5 µg/ml or 0.2 ng/ml for the TNF-α or MCP-1 ELISAs, respectively) and placed in the CO_2 incubator for 48 h. Preliminary experiments revealed that THP-1 cell stimulation with LPS at 0.5 µg/ml resulted in excessive secretion of MCP-1. Therefore, the MCP-1 ELISA experiments were conducted using LPS at a concentration of 0.2 ng/ml, which optimally induced the secretion of MCP-1 to a level where any effects of cardiolipin could be observed. Following incubation, the THP-1 supernatants were collected for use in the ELISAs. The composition of all reagents and solutions utilized in the ELISA are listed in Appendix B.

On the first day of the ELISA, each well of a 96-well plate was coated with 50 µl of the primary antibody (diluted 100x and 400x for TNF-α and MCP-1, respectively) in coating buffer. The plate was then covered with parafilm and incubated overnight at 4^{O}C.

On the second day of the ELISA, the coating buffer was discarded and 180 µl of blocking solution were added to each well. The plate was placed in a wetbox and incubated at 37^{O}C for 1 h, following which the blocking solution was discarded. The plate was then washed 2x with PBS-Tween, leaving the solution in the wells after the second wash. The solution was aspirated from each individual well, and 100 µl of the sample (THP-1 supernatant) or standards were added to the corresponding wells. The concentrations of the standards ranged from 0.0032-10 ng/ml in F5 medium, and four additional wells containing F5 media only were used as blank controls. The plate was then covered with parafilm and incubated overnight at 4^{O}C.

On the third day of the ELISA, the samples were discarded and the plate was washed 3x with PBS-Tween. Subsequently, 100 µl of the secondary antibody (diluted 200x for both TNF-α and MCP-1) in blocking solution were added to each well. The plate was then placed in a wetbox and incubated at 37^{O}C for 45 min. Following incubation, the plate was washed 4x with PBS-Tween and 100 µl of extravidin-alkaline phosphatase (diluted 10,000x) in blocking solution were added to each well. The plate was placed in a wetbox and incubated at 37^{O}C for an additional 45 min, following which the plate was washed 5x with PBS-Tween and 100 µl of the alkaline phosphatase substrate solution were added to each well. The OD was immediately measured at 405 nm using the FLUOstar Omega microplate

reader, and the plate was placed in the dry incubator. The OD was then measured each subsequent hour, for 3 h or until a distinct color change was observed.

Analysis of the data was conducted as per the manufacturer's instructions (Peprotech) using the following formulae:

1) $dOD_{sample} = OD_{final} - OD_{initial}$

2) $cOD_{sample} = dOD_{sample} - dOD_{blank}$

Where dOD_{sample} represents the change in OD of each sample, cOD_{sample} represents the corrected OD of each sample and dOD_{blank} represents the change in OD of the blank control wells containing F5 media only.

To determine the concentration of either TNF-α or MCP-1 in each well, a calibration curve was constructed using the cOD values of the standards (0.0032-10 ng/ml), and a linear trend line for the standard curve was plotted. The cytokine concentration (ng/ml) in each sample, as well as the detection limit (ng/ml) for the assay were calculated using the following formulae:

3) $$\text{Cytokine Concentration} = \frac{cOD_{sample}}{m}$$

4) $$\text{Detection Limit} = \frac{\text{Mean } dOD_{blank} + 2(\text{Standard Deviation } dOD_{blank})}{m}$$

Where m represents the slope of the linear trend line for the standard curve.

2.13. Statistical Analyses

GraphPad Prism software (version 7.0, GraphPad Software Inc., La Jolla, CA, USA) was used to conduct statistical analyses. Data obtained were analyzed using the randomized block design one-way analysis of variance (ANOVA), which accounts

for the high variability of data collected on different days. The one-way ANOVA was followed by Fisher's least significant difference (LSD) post-hoc test, which was performed to detect differences between the individual treatments, and has been utilized in previous studies of a similar nature (Asanuma et al., 2003; Calviello et al., 2004; Klegeris et al., 2005; Klegeris et al., 2008). The two-way ANOVA was followed by Dunnett's post-hoc test. Data are presented as means ± standard error of the mean (SEM). Significance was established at $P < 0.05$.

Chapter 3: Results

3.1. Effect of Cardiolipin on Phagocytic Activity of Microglia

3.1.1. Phagocytic Activity of Murine BV-2 Cells

Since microglial phagocytosis plays an important role in regulating homeostatic conditions in the brain (Brown and Vilalta, 2015; Fu et al., 2014; Yang et al., 2010), we evaluated the effect of cardiolipin on the phagocytic activity of murine BV-2 cells. Experiments were conducted as described in section 2.5.1. Cardiolipin was added to the BV-2 cells at 5 or 20 μg/ml in the absence or presence of LPS, as this stimulating agent has been shown to effectively induce phagocytosis in BV-2 cells (He et al., 2002; Majerova et al., 2014; Pan et al., 2011). Following 24 h incubation, 0.8 μm latex beads were added to the BV-2 cells for 2.5 h. Subsequently, the cells were imaged under the light microscope (Figure 3.3) and the phagocytosed latex beads were counted. The results were compared to the data obtained from cardiolipin vehicle-treated cells.

Additionally, as a measure to ensure that the latex beads were being engulfed, rather than just adhering to the BV-2 cells, cytochalasin B was utilized as an inhibitor of phagocytosis (Axline and Reaven, 1974; Malawista et al., 1971; Zurier et al., 1973). Cytochalasin B was added to the cells prior to treatment with cardiolipin, and the experiments were conducted as described in section 2.5.1. The results were compared to the data obtained from cells pre-incubated with cytochalasin B and treated with the cardiolipin or LPS vehicle solution.

We confirm that stimulation with LPS induces the phagocytic activity of BV-2 cells, and demonstrate, for the first time, that cardiolipin on its own can trigger

phagocytosis by BV-2 cells (Figures 3.1 and 3.3). However, when combined with LPS, cardiolipin does not further increase the phagocytic activity of BV-2 cells (Figure 3.2). Additionally, we authenticate our results by demonstrating that cardiolipin-induced phagocytosis of latex beads by BV-2 cells can be attenuated when the cells are pre-incubated with cytochalasin B. Figure 3.4 illustrates that adding cardiolipin to cytochalasin B-treated cells does not result in an increase in the phagocytic activity of BV-2 cells. This, therefore, demonstrates that the beads are engulfed by BV-2 cells, and have not just adhered to these cells.

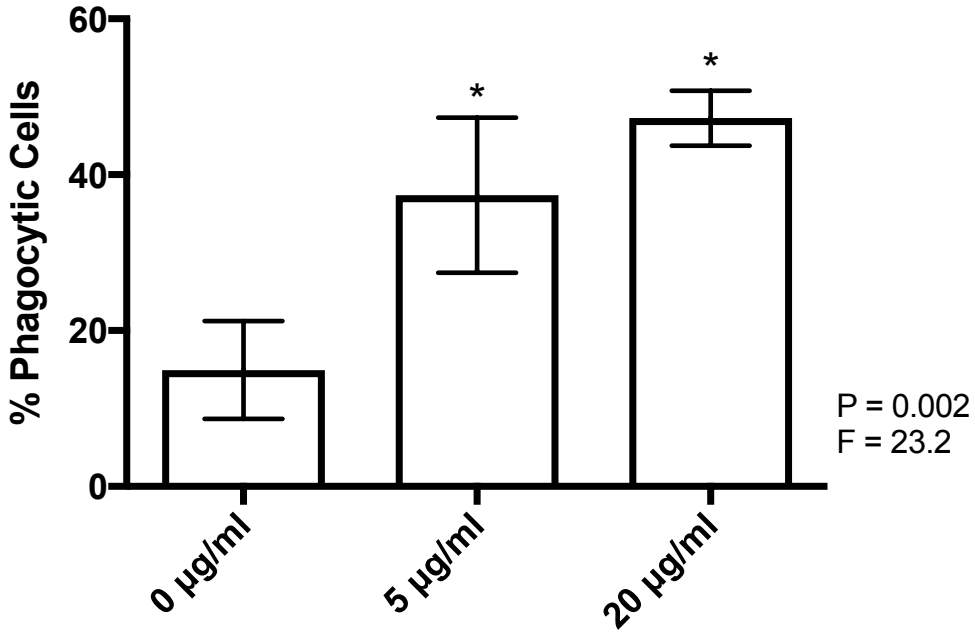

Figure 3.1. Cardiolipin induces the phagocytic activity of murine BV-2 microglia. BV-2 cells were treated with varying concentrations of cardiolipin (shown on the abscissa) or its vehicle solution (1% v/v EtOH). Following 24 h incubation, BV-2 cell phagocytosis of 0.8 µm latex beads was assessed using light microscopy. Data from four independent experiments are presented (means ± S.E.M). * $P < 0.01$, different from cardiolipin vehicle-treated cells (0 µg/ml), according to the randomized block one-way ANOVA (P and F values indicated on figure), followed by Fisher's LSD post-hoc test.

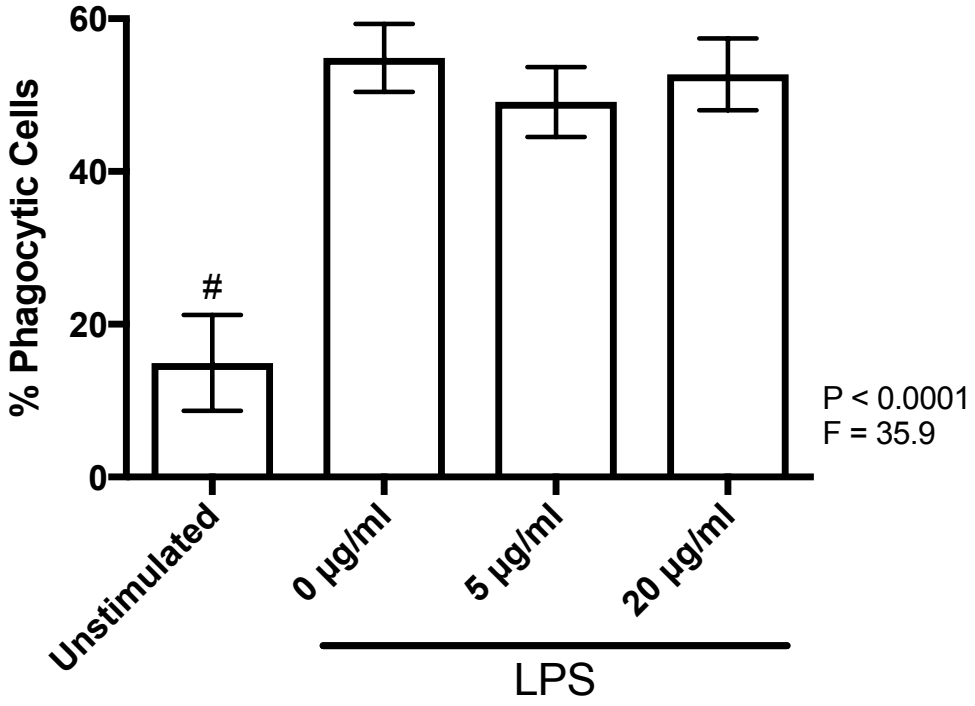

Figure 3.2. Cardiolipin does not affect the phagocytic activity of stimulated murine BV-2 microglia. BV-2 cells were treated with varying concentrations of cardiolipin (shown on the abscissa) or its vehicle solution (1% v/v EtOH) prior to stimulation with LPS (0.5 µg/ml). In addition, control cells (unstimulated) were seeded in the absence of cardiolipin or LPS. Following 24 h incubation, BV-2 cell phagocytosis of 0.8 µm latex beads was assessed using light microscopy. Data from four independent experiments are presented (means ± S.E.M). # $P < 0.01$, different from cardiolipin vehicle-treated cells (0 µg/ml) stimulated with LPS, according to the randomized block one-way ANOVA (P and F values indicated on figure), followed by Fisher's LSD post-hoc test.

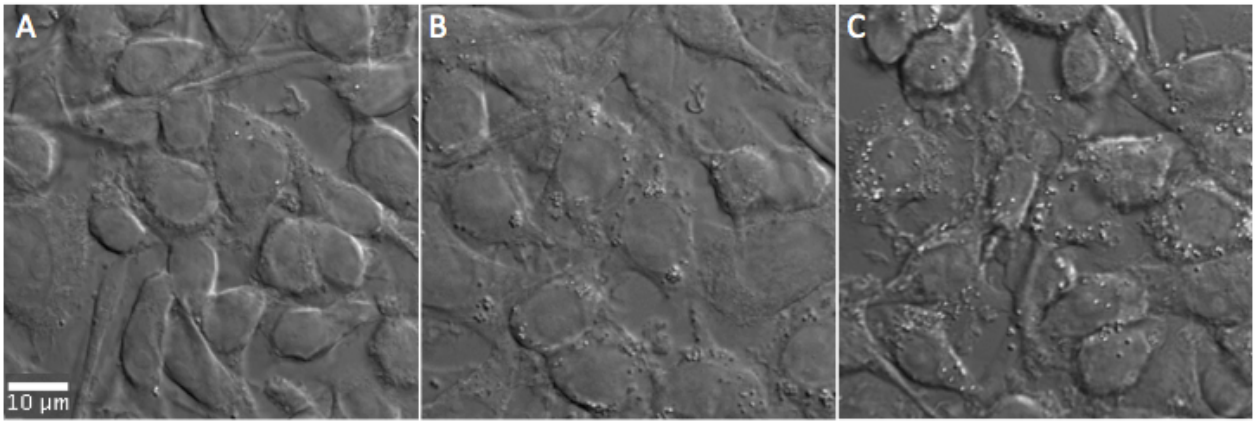

Figure 3.3. Cardiolipin induces the phagocytic activity of murine BV-2 microglia. BV-2 cells were treated with the cardiolipin vehicle solution (1% v/v EtOH) (A) or cardiolipin at 5 µg/ml (B) or 20 µg/ml (C) for 24 h prior the addition of 0.8 µm latex beads. Following 2.5 h incubation with the latex beads, cells were imaged under the light microscope. The scale bar represents 10 µm on all panels.

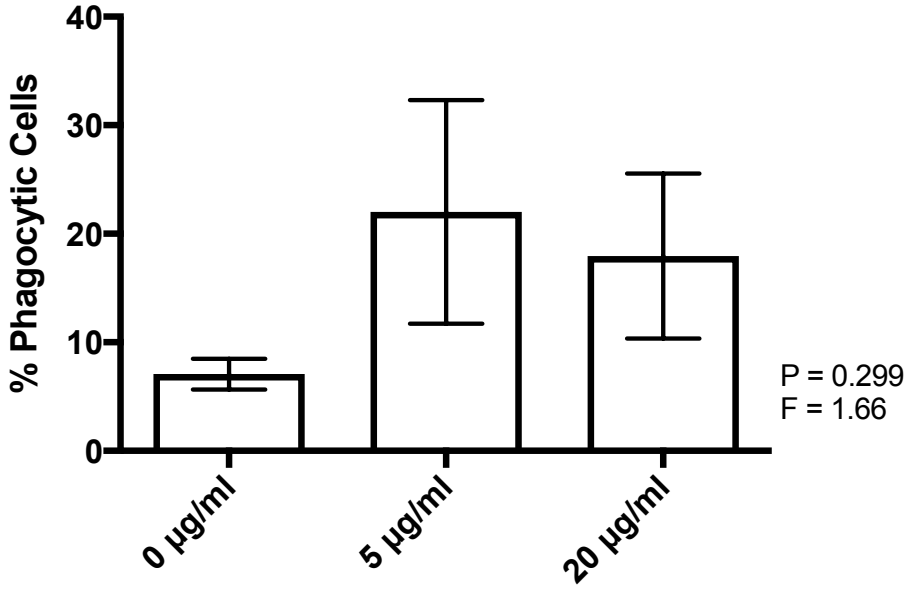

Figure 3.4. Cytochalasin B inhibits the cardiolipin-induced phagocytic activity of murine BV-2 microglia. Cytochalasin B (20 µM) was added to the BV-2 cells 1 h prior to treatment with varying concentrations of cardiolipin (shown on the abscissa) or its vehicle solution (1% v/v EtOH). Following 24 h incubation, BV-2 cell phagocytosis of 0.8 µm latex beads was assessed using light microscopy. Data from three independent experiments are presented (means ± S.E.M). Data were analyzed using the randomized block one-way ANOVA (P and F values indicated on figure).

3.1.2. Phagocytic Activity of Primary Murine Microglia

The effect of cardiolipin on the phagocytic activity of primary murine microglia was evaluated. Experiments were conducted as described in section 2.5.2. Cardiolipin was added to the primary murine microglia at 5 or 20 µg/ml. Following 24 h incubation, 1 µm Fluoresbrite® YG microspheres were added to the primary murine microglia for 1 h. Subsequently, the cells were imaged under the light microscope (Figure 3.6) and the phagocytosis of the fluorescent microspheres by primary murine microglia was analyzed. The results were compared to the data obtained from cardiolipin vehicle-treated cells.

Here we demonstrate, for the first time, that cardiolipin increases the phagocytic activity of primary murine microglia (Figures 3.5 and 3.6). Additionally, we utilized confocal microscopy to confirm that the fluorescent microspheres were engulfed by the primary murine microglia, and not just adhered to the surface of cells (Figure 3.7).

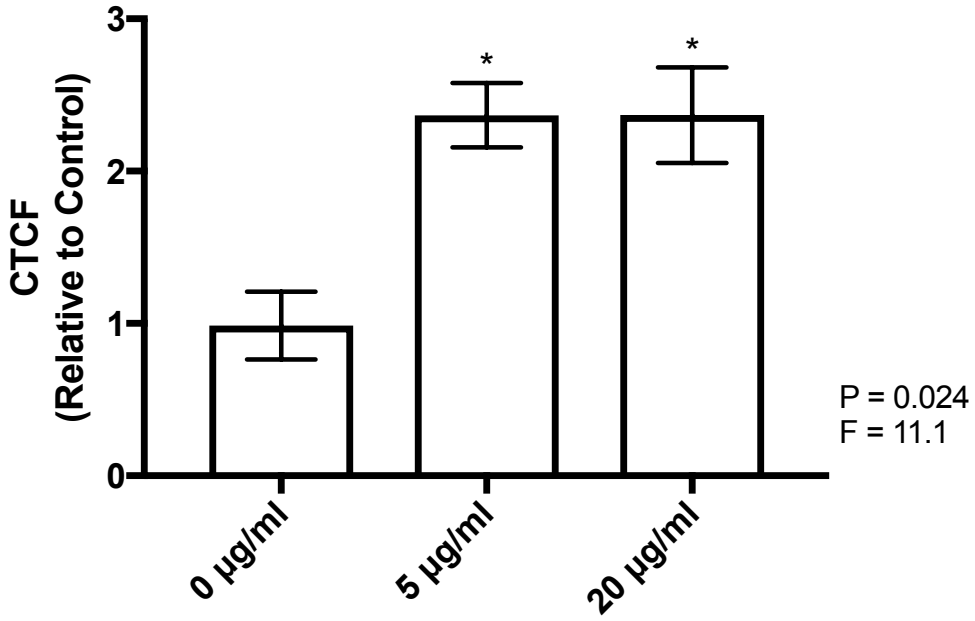

Figure 3.5. Cardiolipin increases the phagocytic activity of primary murine microglia. Primary murine microglia were treated with varying concentrations of cardiolipin (shown on the abscissa) or its vehicle solution (1% v/v EtOH). Following 24 h incubation, light microscopy was used to assess primary murine microglia phagocytosis of 1 µm Fluoresbrite® YG microspheres. Results are expressed as corrected total cell fluorescence (CTCF) relative to control values, which were obtained from cells in the absence of cardiolipin or its vehicle solution. Data from three independent experiments are presented (means ± S.E.M). * $P < 0.05$, different from cardiolipin vehicle-treated cells (0 µg/ml), according to the randomized block one-way ANOVA (P and F values indicated on figure), followed by Fisher's LSD post-hoc test.

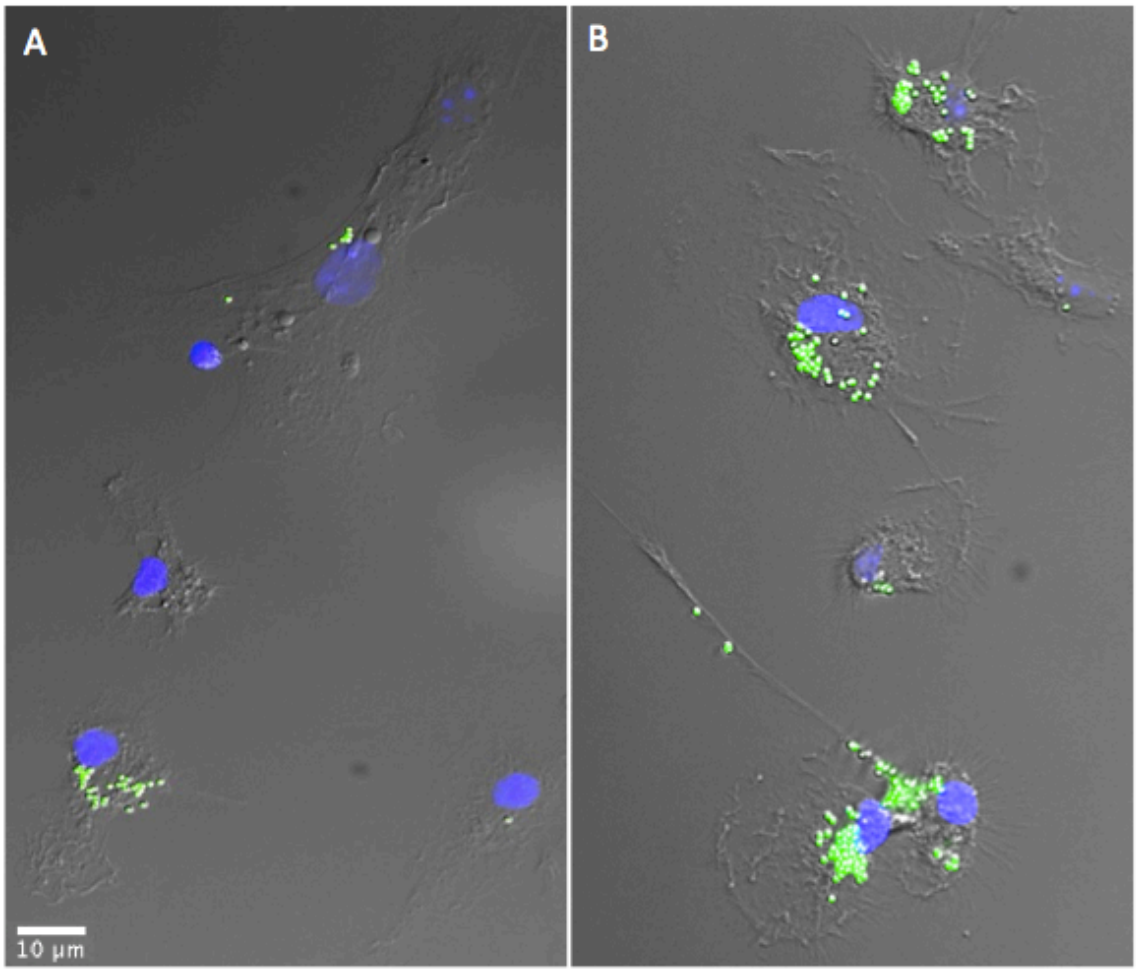

Figure 3.6. Cardiolipin increases the phagocytic activity of primary murine microglia. Primary murine microglia were treated with the cardiolipin vehicle solution (1% v/v EtOH) (A) or cardiolipin at 20 µg/ml (B) for 24 h prior the addition of 1 µm Fluoresbrite® YG microspheres. Following 1 h incubation with the fluorescent microspheres, cells were imaged under the light microscope (blue = DAPI-stained nuclei, green = fluorescent microspheres). The scale bar represents 10 µm on both panels.

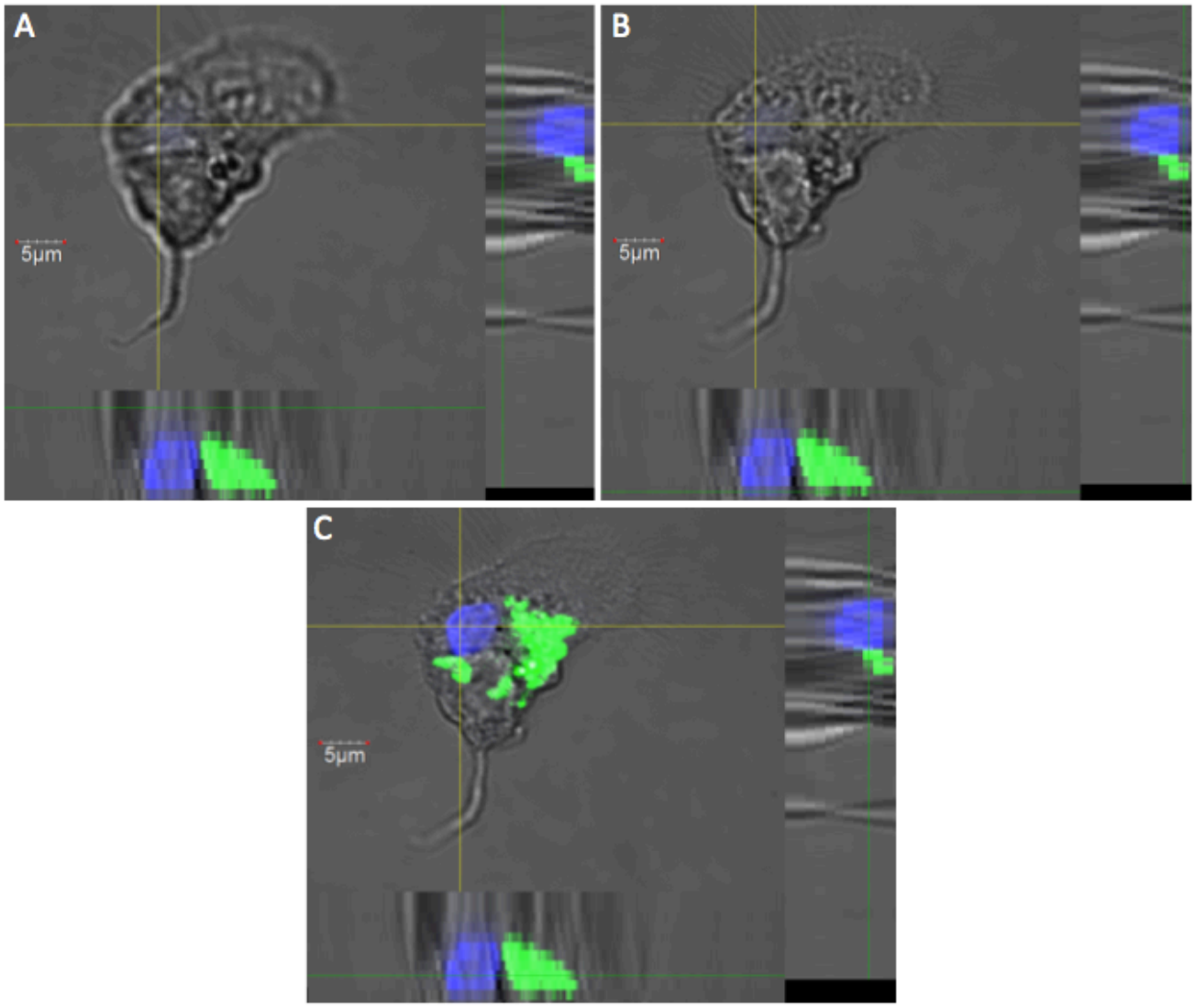

Figure 3.7. Phagocytosis of fluorescent microspheres by primary murine microglia was confirmed by confocal microscopy. Primary murine microglia were treated with cardiolipin at 20 µg/ml for 24 h prior the addition of 1 µm Fluoresbrite® YG microspheres. Following 1 h incubation with the fluorescent microspheres, cells were imaged by confocal microscopy. Images were taken at the top (A), bottom (B) and mid-point (C) of the cell (blue = DAPI-stained nuclei, green = fluorescent microspheres). The scale bars represent 5 µm on all panels.

3.2. Effect of Cardiolipin on Microglia-Mediated Cytotoxicity

3.2.1. Human THP-1 Cell Viability

The effect of cardiolipin on human THP-1 cell viability was determined prior to conducting the microglia-mediated cytotoxicity assay. Experiments were performed as described in section 2.6.1. Cardiolipin was added to THP-1 cells at 2, 10, 20 or 25 μg/ml in the absence or presence of IFN-γ plus LPS. As in previous studies, IFN-γ plus LPS were used as stimulating agents to induce microglial activation and subsequent microglia-mediated cytotoxicity (Genin et al., 2015; Klegeris and McGeer, 2000). Following 48 h incubation, the viability of the THP-1 cells was assessed using the MTT and LDH assays (Figure 3.8 and 3.9, respectively). The results were compared to data obtained from cardiolipin vehicle-treated cells in the presence of IFN-γ plus LPS.

Here we demonstrate that the addition of IFN-γ plus LPS significantly affects THP-1 cell viability (Figure 3.8) and cell death (Figure 3.9). However, the addition of cardiolipin alone (data not shown) or cardiolipin in combination with IFN-γ plus LPS does not significantly affect THP-1 cell viability (Figure 3.8) or cell death (Figure 3.9).

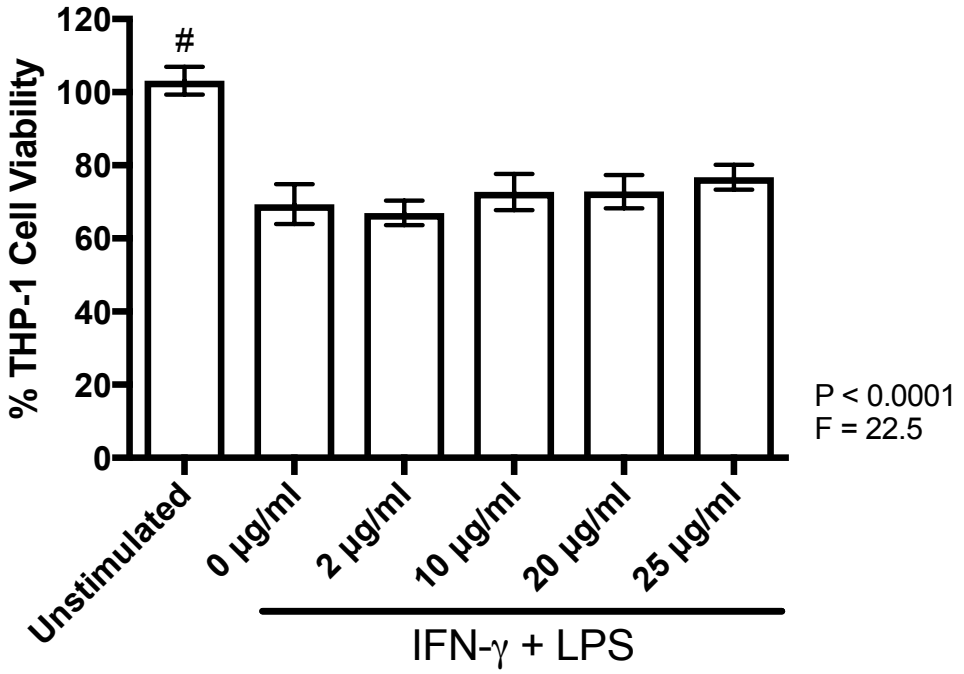

Figure 3.8. Cardiolipin does not significantly affect the viability of stimulated human THP-1 monocytic cells. THP-1 cells were treated with varying concentrations of cardiolipin (shown on the abscissa) or its vehicle solution (0.5% v/v DMSO) and stimulated with IFN-γ (150 U/ml) plus LPS (0.2 ng/ml). In addition, control cells (unstimulated) were seeded in the absence of vehicle, cardiolipin, IFN-γ or LPS. Following 48 h incubation, THP-1 cell viability was assessed using the MTT assay. Data from six independent experiments are presented (means ± S.E.M). # $P < 0.01$, different from cardiolipin vehicle-treated cells (0 µg/ml) stimulated with IFN-γ plus LPS, according to the randomized block one-way ANOVA (P and F values indicated on figure), followed by Fisher's LSD post-hoc test.

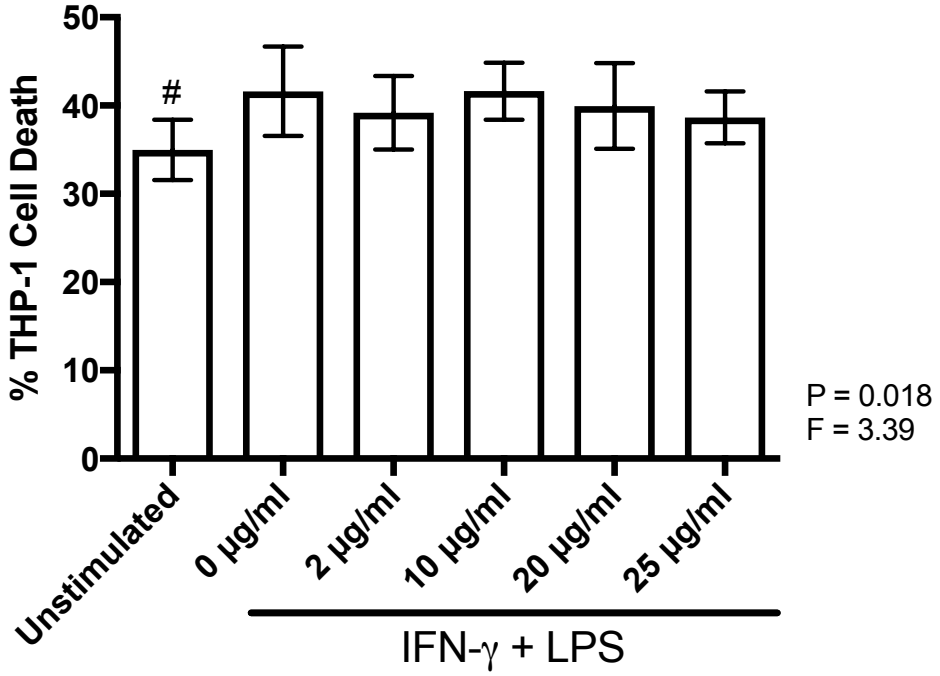

Figure 3.9. Cardiolipin does not significantly affect the death of stimulated human THP-1 monocytic cells. THP-1 cells were treated with varying concentrations of cardiolipin (shown on the abscissa) or its vehicle solution (0.5% v/v DMSO) and stimulated with IFN-γ (150 U/ml) plus LPS (0.2 ng/ml). In addition, control cells (unstimulated) were seeded in the absence of vehicle, cardiolipin, IFN-γ or LPS. Following 48 h incubation, THP-1 cell death was assessed using the LDH assay. Data from six independent experiments are presented (means ± S.E.M). # $P < 0.01$, different from cardiolipin vehicle-treated cells (0 µg/ml) stimulated with IFN-γ plus LPS, according to the randomized block one-way ANOVA (P and F values indicated on figure), followed by Fisher's LSD post-hoc test.

3.2.2. Human SH-SY5Y Cell Viability

Since microglia-mediated neuron death is a characteristic feature of neuroinflammation (Klegeris and McGeer, 2000; Kraft and Harry, 2011), we investigated whether cardiolipin affected microglia-mediated cytotoxicity towards human SH-SY5Y neuronal cells. Once it was established that cardiolipin did not significantly affect THP-1 cell viability, experiments were conducted as described in

section 2.6.2. Cardiolipin was added to THP-1 cells at 2, 10, 20 or 25 μg/ml in the absence or presence of IFN-γ plus LPS. THP-1 cell supernatants were transferred onto human SH-SY5Y cells, following which the viability of the SH-SY5Y cells was assessed using the MTT and LDH assays (Figure 3.10 and 3.11, respectively). The results were compared to the data obtained from cardiolipin vehicle-treated cells in the presence of IFN-γ plus LPS.

The addition of cardiolipin to unstimulated THP-1 cells, followed by transfer of their supernatants onto SH-SY5Y cells, does not significantly affect the viability of the SH-SY5Y neuronal cells (data not shown). Here we demonstrate that stimulation with IFN-γ plus LPS induces THP-1 cell cytotoxicity towards SH-SY5Y neuronal cells, thereby, resulting in decreased viability (Figure 3.10) and increased death (Figure 3.11) of the SH-SY5Y cells. However, when THP-1 cells are stimulated with IFN-γ plus LPS in the presence of cardiolipin, a decrease in THP-1 cell cytotoxicity is observed at all concentrations of cardiolipin studied, which is evidenced by an increase in viability (Figure 3.10) and decrease in death (Figure 3.11) of SH-SY5Y cells, when compared to cells incubated with supernatants from THP-1 cells stimulated with IFN-γ plus LPS in the absence of cardiolipin.

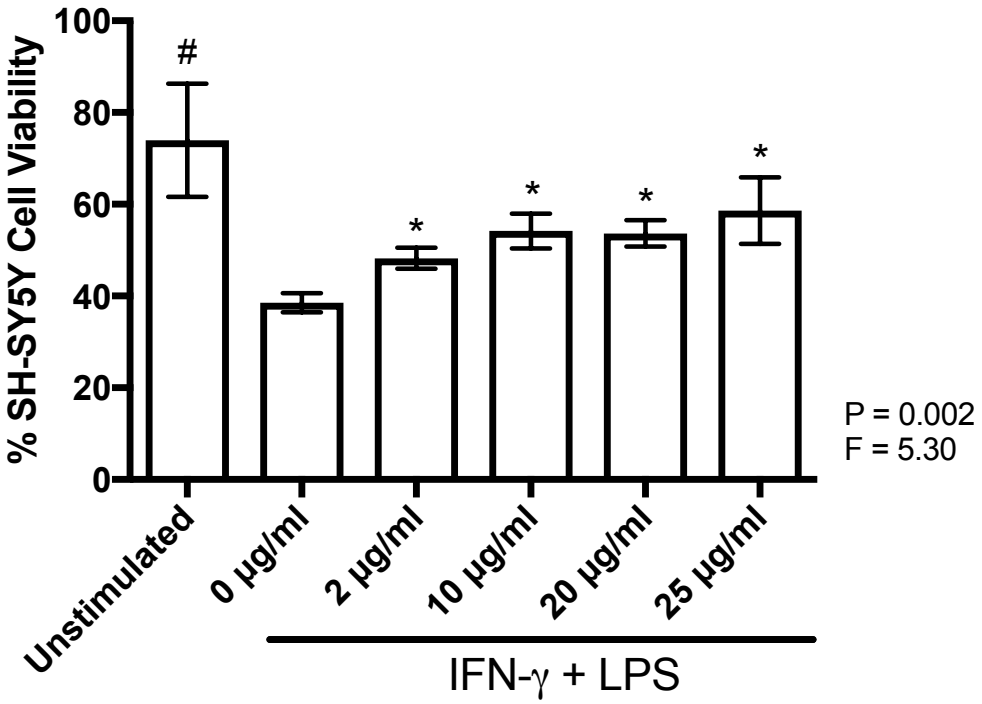

Figure 3.10. Cardiolipin inhibits the cytotoxicity of stimulated human THP-1 monocytic cells and increases human SH-SY5Y neuronal cell viability. THP-1 cells were treated with varying concentrations of cardiolipin (shown on the abscissa) or its vehicle solution (0.5% v/v DMSO) and stimulated with IFN-γ (150 U/ml) plus LPS (0.2 ng/ml). In addition, control cells (unstimulated) were seeded in the absence of vehicle, cardiolipin, IFN-γ or LPS. Following 48 h incubation, THP-1 cell supernatants were transferred onto SH-SY5Y cells. Following 72 h exposure to the THP-1 cell supernatants, SH-SY5Y cell viability was assessed using the MTT assay. Data from six independent experiments are presented (means ± S.E.M). $^{\#}$ $P < 0.01$, * $P < 0.05$, different from cardiolipin vehicle-treated cells (0 µg/ml) stimulated with IFN-γ plus LPS, according to the randomized block one-way ANOVA (P and F values indicated on figure), followed by Fisher's LSD post-hoc test.

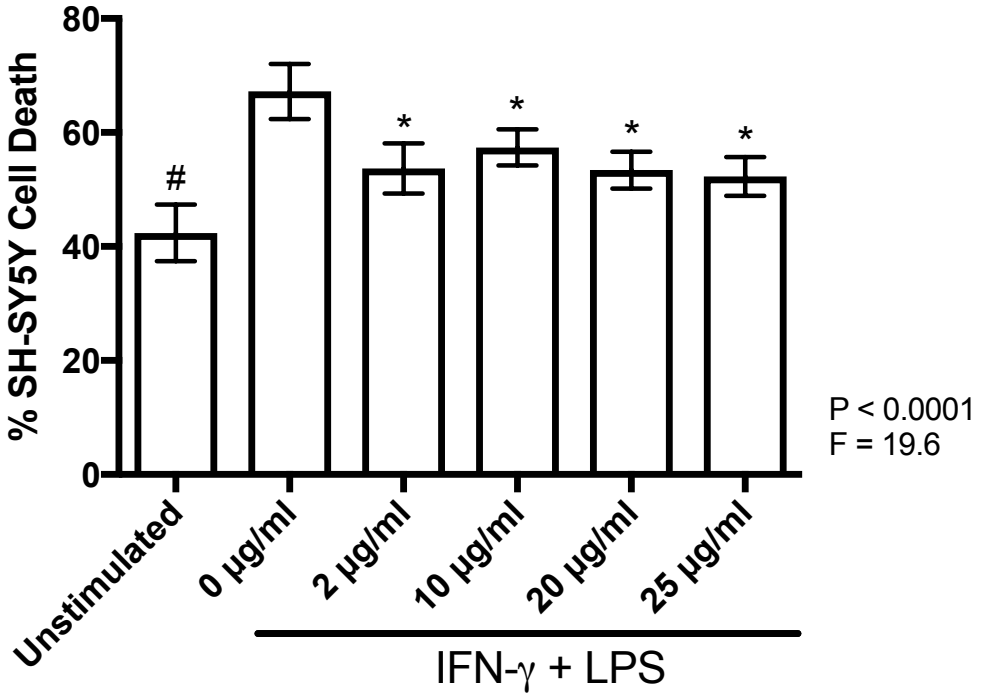

Figure 3.11. Cardiolipin inhibits the cytotoxicity of stimulated human THP-1 monocytic cells and decreases human SH-SY5Y neuronal cell death. THP-1 cells were treated with varying concentrations of cardiolipin (shown on the abscissa) or its vehicle solution (0.5% v/v DMSO) and stimulated with IFN-γ (150 U/ml) plus LPS (0.2 ng/ml). In addition, control cells (unstimulated) were seeded in the absence of vehicle, cardiolipin, IFN-γ or LPS. Following 48 h incubation, THP-1 cell supernatants were transferred onto SH-SY5Y cells. Following 72 h exposure to the THP-1 cell supernatants, SH-SY5Y cell death was assessed using the LDH assay. Data from six independent experiments are presented (means ± S.E.M). # $P < 0.01$, * $P < 0.01$, different from cardiolipin vehicle-treated cells (0 µg/ml) stimulated with IFN-γ plus LPS, according to the randomized block one-way ANOVA (P and F values indicated on figure), followed by Fisher's LSD post-hoc test.

3.3. Effect of Cardiolipin on Neurotrophic Factor Expression by Microglia

3.3.1. Expression of Brain-Derived Neurotrophic Factor (BDNF) and Glial Cell Line-Derived Neurotrophic Factor (GDNF) by Murine BV-2 Cells

Since cardiolipin exhibited neuroprotective effects against microglia-mediated cytotoxicity (see section 3.2), we hypothesized that cardiolipin may also induce the expression of the critical neurotrophic factors BDNF and GDNF by microglia. Experiments were conducted as described in section 2.9.1. Cardiolipin was added to BV-2 cells at a concentration of 5, 10 or 20 μg/ml. Following 24 h incubation, the immunofluorescence assay was conducted to evaluate the effect of cardiolipin on BDNF and GDNF expression by BV-2 cells. The results were compared to the data obtained from the cardiolipin vehicle-treated cells.

Here we demonstrate, for the first time, that incubation with cardiolipin increases the expression of both BDNF (Figure 3.12) and GDNF (Figure 3.13) by BV-2 cells.

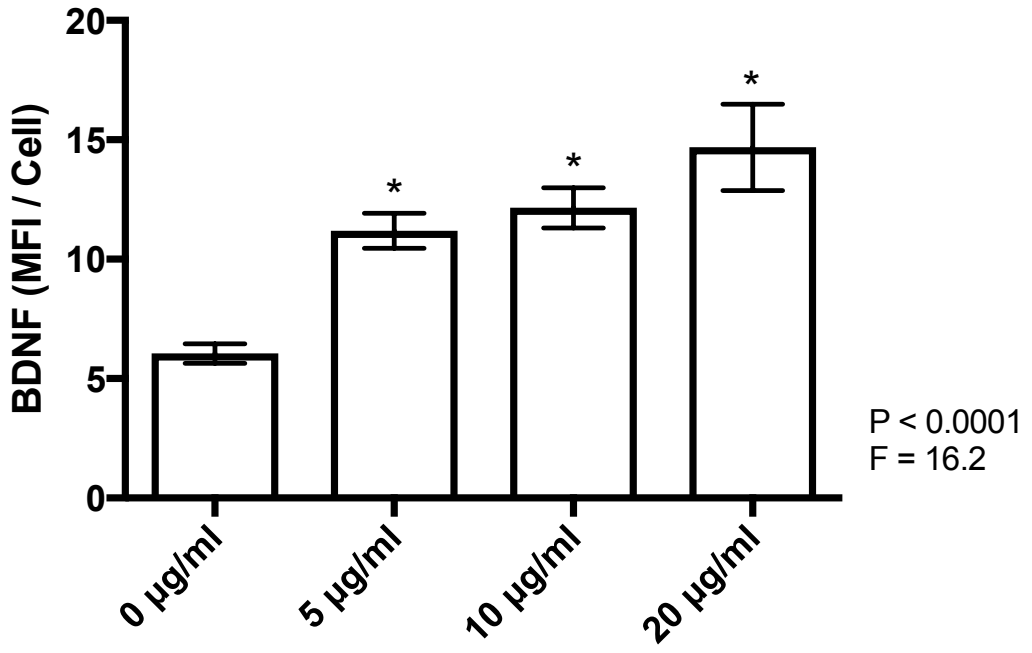

Figure 3.12. Cardiolipin induces the expression of brain-derived neurotrophic factor (BDNF) by murine BV-2 microglia. BV-2 cells were treated with varying concentrations of cardiolipin (shown on the abscissa) or its vehicle solution (1% v/v EtOH). Following 24 h incubation, the immunofluorescence assay was conducted to assess the expression of BDNF (mean fluorescence intensity (MFI)/cell) by BV-2 cells. Data from six independent experiments are presented (means ± S.E.M). * $P < 0.01$, different from cardiolipin vehicle-treated cells (0 µg/ml), according to the randomized block one-way ANOVA (P and F values indicated on figure), followed by Fisher's LSD post-hoc test.

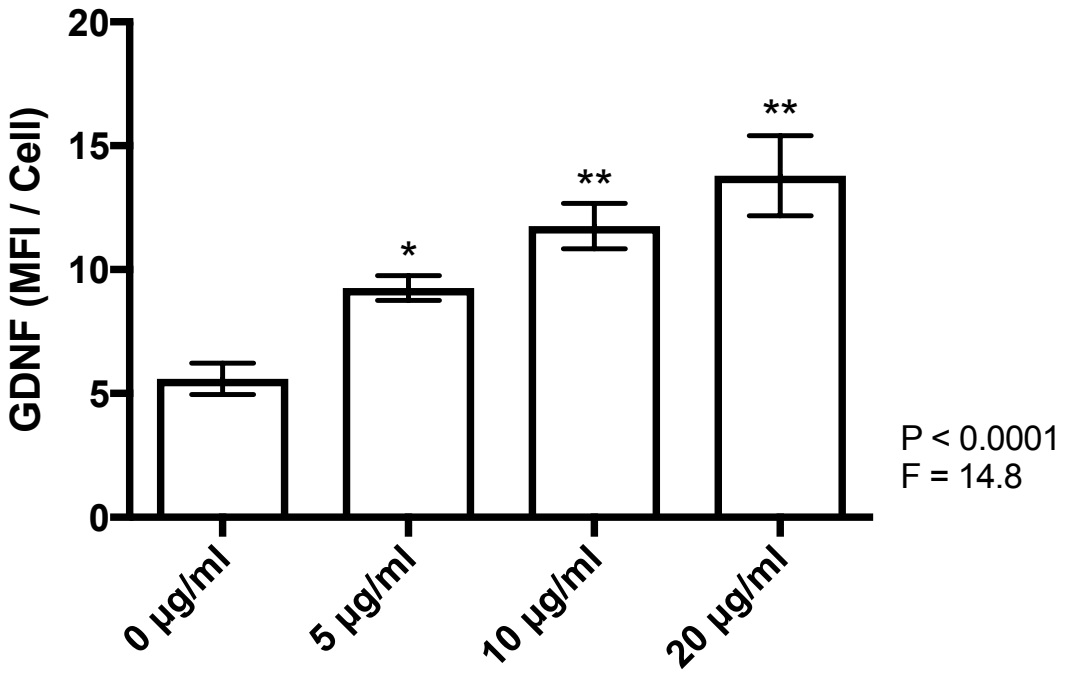

Figure 3.13. Cardiolipin induces the expression of glial cell line-derived neurotrophic factor (GDNF) by murine BV-2 microglia. BV-2 cells were treated with varying concentrations of cardiolipin (shown on the abscissa) or its vehicle solution (1% v/v EtOH). Following 24 h incubation, the immunofluorescence assay was conducted to assess the expression of GDNF (mean fluorescence intensity (MFI)/cell) by BV-2 cells. Data from six independent experiments are presented (means ± S.E.M). * $P < 0.05$, ** $P < 0.01$, different from cardiolipin vehicle-treated cells (0 µg/ml), according to the randomized block one-way ANOVA (P and F values indicated on figure), followed by Fisher's LSD post-hoc test.

3.3.2. Expression of Brain-Derived Neurotrophic Factor (BDNF) and Glial Cell Line-Derived Neurotrophic Factor (GDNF) by Primary Murine Microglia

Next, we assessed the effect of cardiolipin on the expression of BDNF and GDNF by primary murine microglia. Experiments were conducted as described in section 2.9.2. Cardiolipin was added to primary murine microglia at 5, 10 or 20 µg/ml. Following 24 h incubation, the immunofluorescence assay was conducted.

The results were compared to the data obtained from the cardiolipin vehicle-treated cells.

Here we demonstrate that, similar to the effect observed in BV-2 cells, incubation of primary murine microglia with cardiolipin increases their expression of BDNF (Figure 3.14) and GDNF (Figure 3.15). Additionally, we confirm that the cells utilized in these experiments were primary murine microglia, as they are positive for the IBA-1 microglia marker (Figure 3.16).

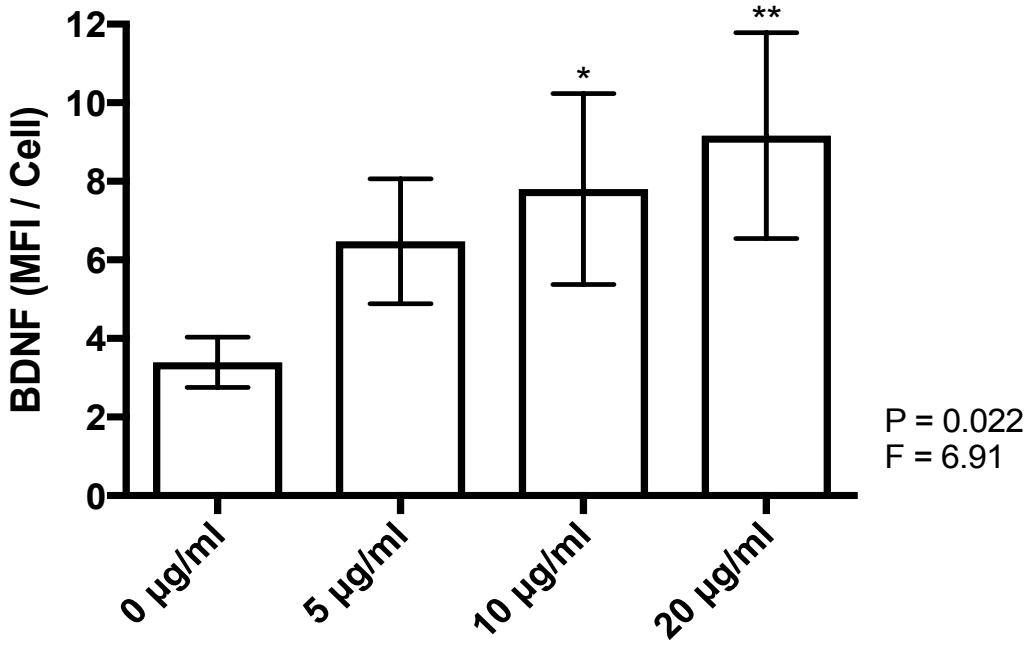

Figure 3.14. Cardiolipin increases the expression of brain-derived neurotrophic factor (BDNF) by primary murine microglia. Primary murine microglia were treated with varying concentrations of cardiolipin (shown on the abscissa) or its vehicle solution (1% v/v EtOH). Following 24 h incubation, the immunofluorescence assay was conducted to assess the expression of BDNF (mean fluorescence intensity (MFI)/cell) by primary murine microglia. Data from three independent experiments are presented (means ± S.E.M). * $P < 0.05$, ** $P < 0.01$, different from cardiolipin vehicle-treated cells (0 µg/ml), according to the randomized block one-way ANOVA (P and F values indicated on figure), followed by Fisher's LSD post-hoc test.

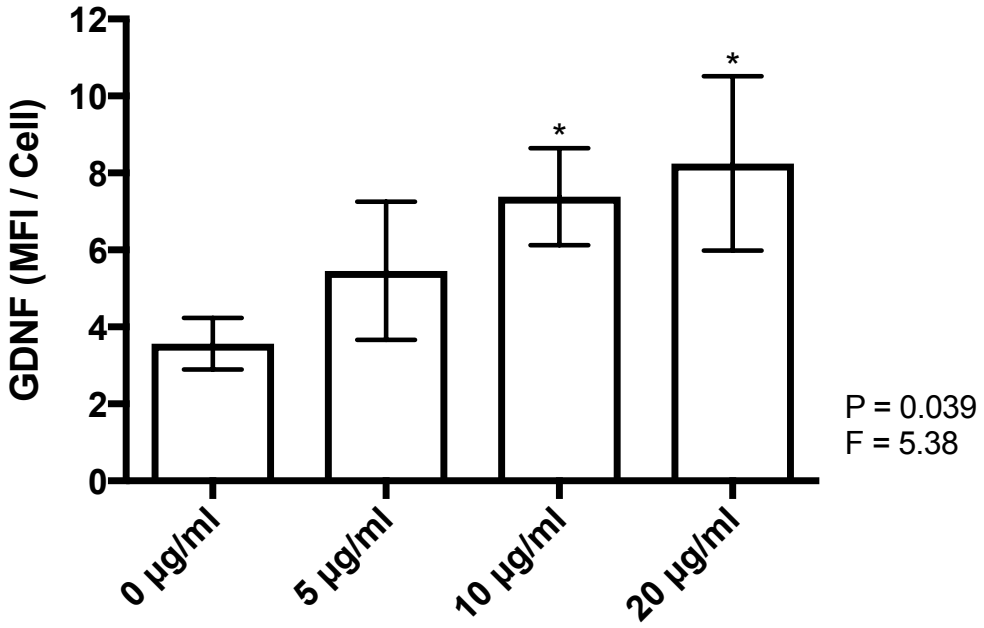

Figure 3.15. Cardiolipin increases the expression of glial cell line-derived neurotrophic factor (GDNF) by primary murine microglia. Primary murine microglia were treated with varying concentrations of cardiolipin (shown on the abscissa) or its vehicle solution (1% v/v EtOH). Following 24 h incubation, the immunofluorescence assay was conducted to assess the expression of GDNF (mean fluorescence intensity (MFI)/cell) by primary murine microglia. Data from three independent experiments are presented (means ± S.E.M). * $P < 0.05$, different from cardiolipin vehicle-treated cells (0 µg/ml), according to the randomized block one-way ANOVA (P and F values indicated on figure), followed by Fisher's LSD post-hoc test.

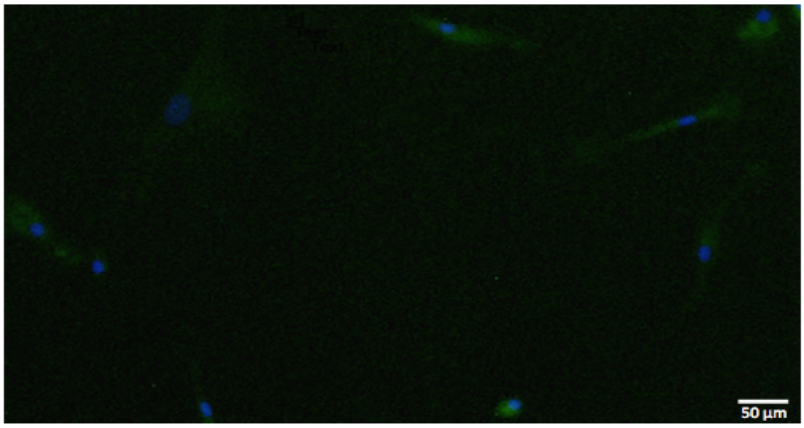

Figure 3.16. Primary murine microglia utilized in the immunofluorescence assay are ionized calcium-binding adaptor molecule (IBA)-1-positive. The immunofluorescence assay was conducted to assess expression of IBA-1 by primary murine microglia. Immunostaining was performed using the anti-IBA-1 antibody and DAPI nuclear stain. Two separate images were obtained and combined to create the overlay image presented in this figure (green = IBA-1 staining, blue = DAPI-stained nuclei). The scale bar represents 50 µm.

3.4. Effect of Cardiolipin on the Secretory Profile of Microglia

Since cardiolipin modulates microglia-mediated cytotoxicity, we next assessed the effect of cardiolipin on the secretory profile of activated microglia. We examined the effect of cardiolipin on microglial secretion of RNS, ROS, TNF-α and MCP-1, all of which are upregulated following the pro-inflammatory activation of microglia, as well as in the chronic neuroinflammatory state observed in neurodegenerative diseases, such as AD (Jessen, 2004; Lull and Block, 2010; Parpura et al., 2012; Saijo and Glass, 2011; Yang et al., 2010).

3.4.1. Effect of Cardiolipin on Nitrite Secretion by Murine BV-2 Cells

We first evaluated the effect of cardiolipin on the secretion of RNS by microglia. Experiments were conducted as described in section 2.10. Cardiolipin

was added to BV-2 cells at 2, 10 or 20 μg/ml in the absence or presence of LPS, as this stimulating agent has been shown to induce the RNS secretion by BV-2 cells (Horvath et al., 2008; Hu et al., 2007). Following 24 h incubation, the Griess assay was conducted to assess BV-2 cell secretion of nitrite. The results were compared to the data obtained from cardiolipin vehicle-treated cells in the presence of LPS.

The addition of cardiolipin alone does not induce nitrite secretion by BV-2 cells (data not shown). Here we confirm that BV-2 cell stimulation with LPS induces the secretion of nitrite; however, when the cells are stimulated with LPS in the presence of cardiolipin, nitrite secretion is reduced at all concentrations of cardiolipin studied (Figure 3.17).

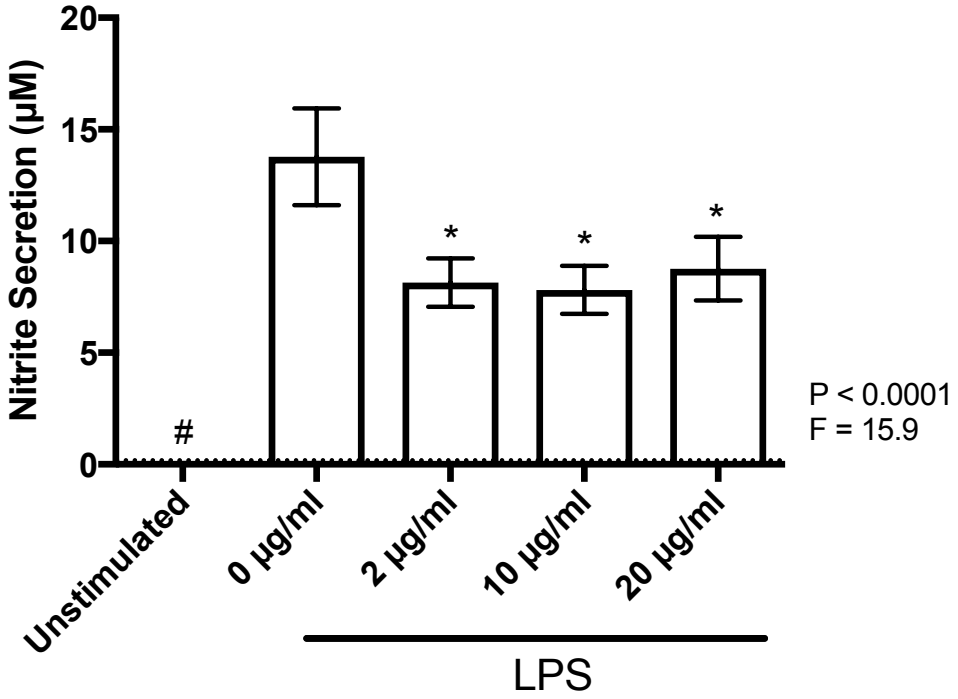

Figure 3.17. Cardiolipin reduces the secretion of nitrite by stimulated murine BV-2 microglia. BV-2 cells were treated with varying concentrations of cardiolipin (shown on the abscissa) or its vehicle solution (1% v/v EtOH) prior to stimulation with LPS (0.5 μg/ml). In addition, control cells (unstimulated) were seeded in the absence of vehicle, cardiolipin or LPS. Following 24 h incubation, the Griess assay was conducted to measure the concentration of nitrite (μM) in BV-2 cell supernatants. Data from six independent experiments are presented (means ± S.E.M.). The detection limit of the Griess assay (0.06 ± 0.002 μM) is shown as a dotted line. # $P < 0.01$, * $P < 0.01$, different from cardiolipin vehicle-treated cells (0 μg/ml) stimulated with LPS, according to the randomized block one-way ANOVA (P and F values indicated on figure), followed by Fisher's LSD post-hoc test.

3.4.2. Effect of Cardiolipin on Superoxide Anion Secretion by Human HL-60 Cells

Since the production and secretion of ROS is significantly upregulated during neuroinflammatory events, we aimed to evaluate the effect of cardiolipin on microglial secretion of superoxide anion, a well-defined ROS. Experiments were conducted as described in section 2.11. Human HL-60 cells were differentiated for 5

days to induce the expression of the NADPH oxidase subunits, which are required for the generation of the respiratory burst (Hermann et al., 2004; Richardson et al., 1998). Cardiolipin was added to the differentiated cells at 2, 10 or 20 μg/ml in the absence or presence of LPS, which was used as a priming agent. Following 24 h incubation, luminol solution was added to the cells prior to stimulation with fMLP, a bacterial peptide that induces respiratory burst. The results are expressed as CHL intensity relative to the data obtained from the control wells, which contained differentiated HL-60 cells in the absence of vehicle, cardiolipin or LPS.

The addition of cardiolipin alone does not affect the secretion of superoxide anion by differentiated HL-60 cells (data not shown). Here we demonstrate that when differentiated HL-60 cells are primed with LPS, there is a significant increase in superoxide anion secretion in response to fMLP-stimulation (Figure 3.18). The addition of cardiolipin to LPS-primed cells just prior to stimulation with fMLP does not affect superoxide anion secretion (data not shown). However, when the cells are primed with LPS in the presence of cardiolipin, there is a significant reduction in superoxide anion secretion following fMLP-stimulation (Figure 3.18). This, therefore, demonstrates that the addition of cardiolipin inhibits the priming, rather than the stimulation, of the respiratory burst.

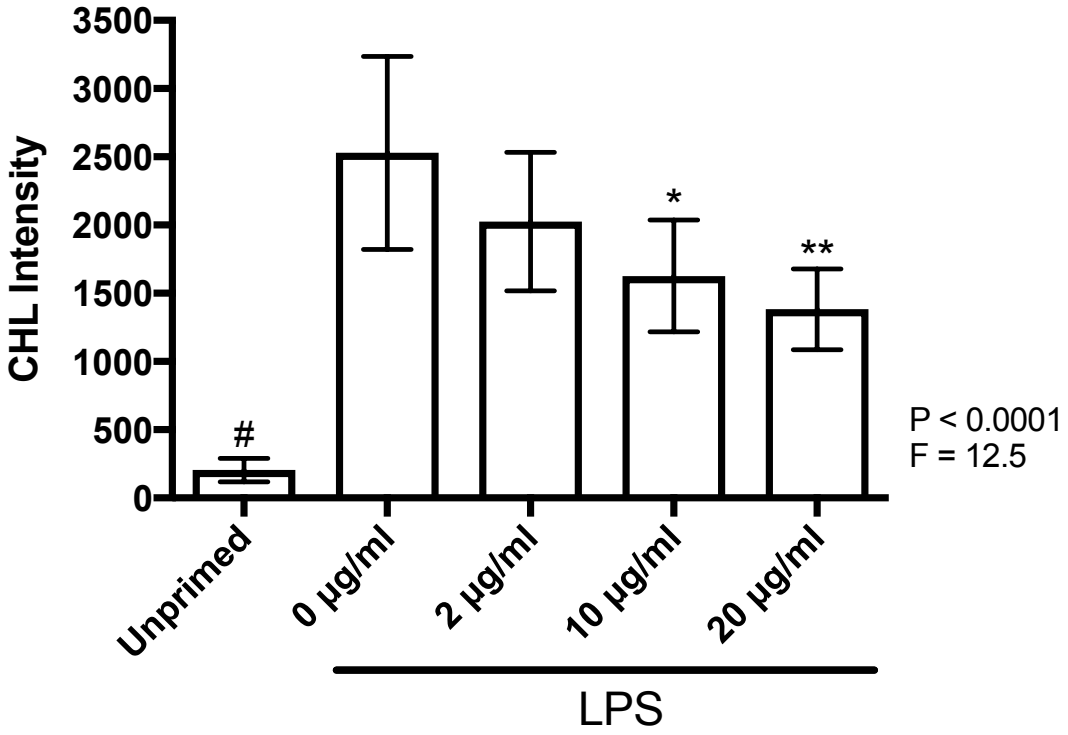

Figure 3.18. Cardiolipin reduces the secretion of ROS by LPS-primed and fMLP-stimulated human HL-60 promyelocytic cells. HL-60 cells were differentiated with DMSO prior to conducting the experiment. The cells were treated with varying concentrations of cardiolipin (shown on the abscissa) or its vehicle solution (1% v/v EtOH) prior to priming with LPS (0.5 µg/ml). In addition, control cells (unprimed) were seeded in the absence of cardiolipin or LPS. Following 24 h incubation, the cells were stimulated with fMLP and the luminol-dependent chemiluminescence (CHL) response of the HL-60 cells was measured. Results are expressed as percentage of control values, which were obtained from cells in the absence of vehicle, cardiolipin or LPS. Data from seven independent experiments are presented (means ± S.E.M.). * $P < 0.05$, # $P < 0.01$, ** $P < 0.01$, different from cardiolipin vehicle-treated cells (0 µg/ml) primed with LPS, according to the randomized block one-way ANOVA (P and F values indicated on figure), followed by Fisher's LSD post-hoc test.

3.4.3. Effect of Cardiolipin on the Secretion of Tumor Necrosis Factor (TNF)-α and Monocyte Chemoattractant Protein (MCP)-1 by Human THP-1 Cells

Next, we assessed the effect of cardiolipin on microglial secretion of TNF-α, a well-defined pro-inflammatory cytokine, and MCP-1, a cytokine implicated in mediating immune responses in the brain. Experiments were conducted as described in section 2.12. Cardiolipin was added to THP-1 cells at 2, 10 or 20 μg/ml in the absence or presence of IFN-γ plus LPS. Following 48 h incubation, ELISAs were conducted to determine the concentrations of TNF-α and MCP-1 in THP-1 cell supernatants. The results were compared to the data obtained from cardiolipin vehicle-treated cells in the presence of IFN-γ plus LPS.

The addition of cardiolipin alone does not significantly affect the secretion of TNF-α by THP-1 cells, as the concentration of TNF-α in THP-1 supernatants was below the detection limit in the presence of all concentrations of cardiolipin studied (data not shown). However, THP-1 cell stimulation with IFN-γ plus LPS significantly increases the secretion of TNF-α by THP-1 cells, which was reduced when the cells were co-incubated with cardiolipin (Figure 3.19).

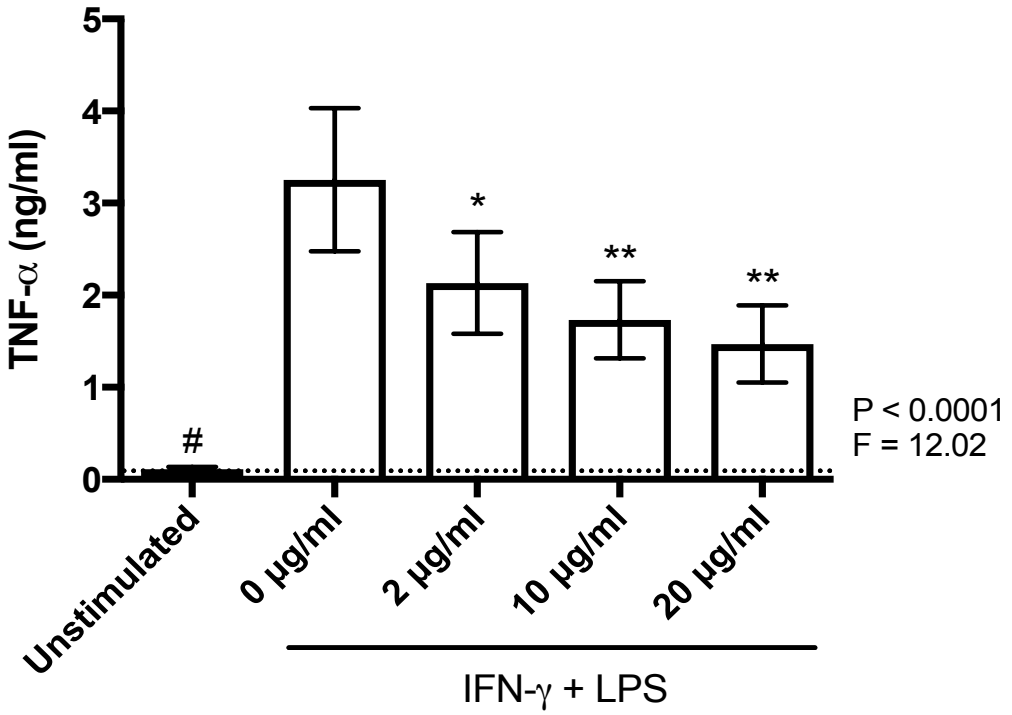

Figure 3.19. Cardiolipin inhibits the secretion of tumor necrosis factor (TNF)-α by stimulated human THP-1 monocytic cells. THP-1 cells were treated with varying concentrations of cardiolipin (shown on the abscissa) or its vehicle solution (0.5% v/v DMSO) prior to stimulation with IFN-γ (150 U/ml) plus LPS (0.5 µg/ml). In addition, control cells (unstimulated) were seeded in the absence of vehicle, cardiolipin, IFN-γ or LPS. Following 48 h incubation, an ELISA was used to measure the concentration of TNF-α (ng/ml) in THP-1 cell supernatants. Data from eight independent experiments are presented (means ± S.E.M.). The detection limit of the ELISA (0.05 ± 0.01 ng/ml) is shown as a dotted line. * $P < 0.05$, # $P < 0.01$, ** $P < 0.01$, different from cardiolipin vehicle-treated cells (0 µg/ml) stimulated with IFN-γ plus LPS, according to the randomized block one-way ANOVA (P and F values indicated on figure), followed by Fisher's LSD post-hoc test.

Here we demonstrate that the addition of cardiolipin on its own upregulates the secretion of MCP-1 by THP-1 cells (Figure 3.20). Additionally, we show that THP-1 cell stimulation with IFN-γ plus LPS significantly increases the secretion of MCP-1 by THP-1 cells, which was slightly, yet significantly, reduced at all

concentrations of cardiolipin studied when the cells were co-incubated with cardiolipin (Figure 3.21).

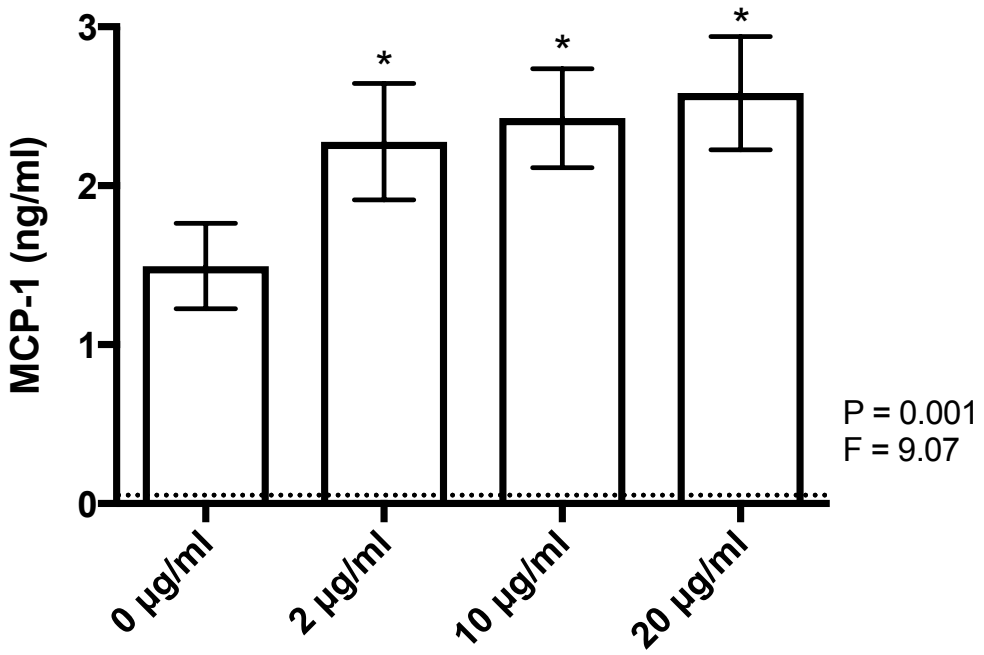

Figure 3.20. Cardiolipin increases the secretion of monocyte chemoattractant protein (MCP)-1 by human THP-1 monocytic cells. THP-1 cells were treated with varying concentrations of cardiolipin (shown on the abscissa) or its vehicle solution (0.5% v/v DMSO). Following 48 h incubation, an ELISA was used to measure the concentration of MCP-1 (ng/ml) in THP-1 cell supernatants. Data from eight independent experiments are presented (means ± S.E.M.). The detection limit of the ELISA (0.062 ± 0.009 ng/ml) is shown as a dotted line. * $P < 0.01$, different from cardiolipin vehicle-treated cells (0 µg/ml), according to the randomized block one-way ANOVA (P and F values indicated on figure), followed by Fisher's LSD post-hoc test.

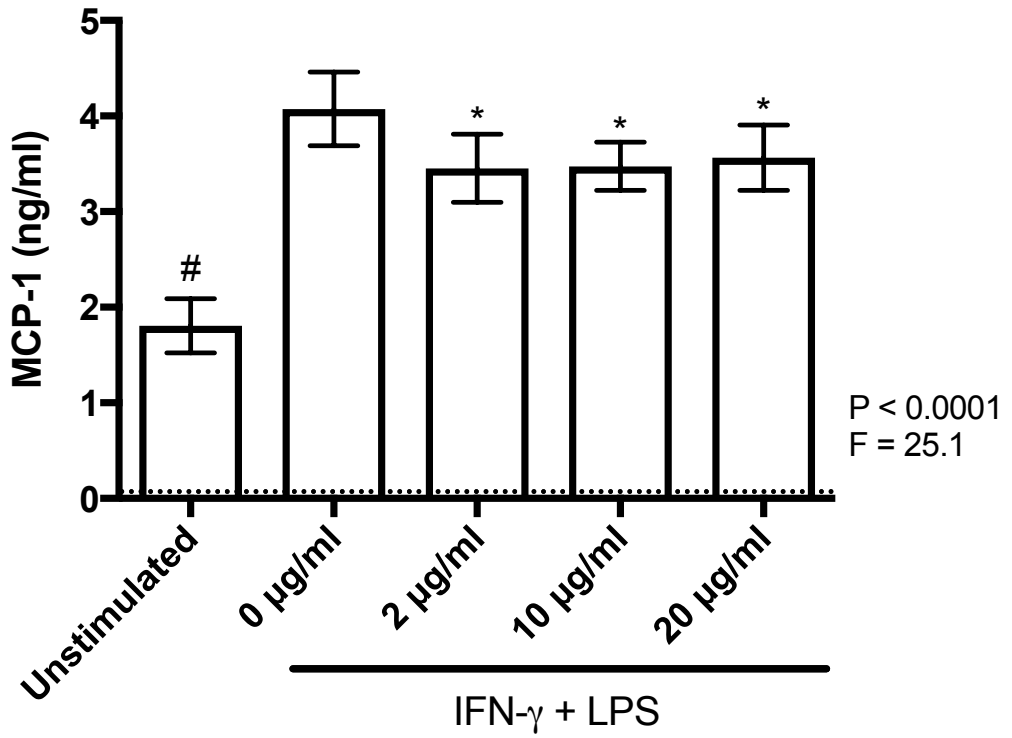

Figure 3.21. Cardiolipin decreases the secretion of monocyte chemoattractant protein (MCP)-1 by stimulated human THP-1 monocytic cells. THP-1 cells were treated with varying concentrations of cardiolipin (shown on the abscissa) or its vehicle solution (0.5% v/v DMSO) prior to stimulation with IFN-γ (150 U/ml) plus LPS (0.2 ng/ml). In addition, control cells (unstimulated) were seeded in the absence of vehicle, cardiolipin, IFN-γ or LPS. Following 48 h incubation, an ELISA was used to measure the concentration of MCP-1 (ng/ml) in THP-1 cell supernatants. Data from eight independent experiments are presented (means ± S.E.M.). The detection limit of the ELISA (0.062 ± 0.009 ng/ml) is shown as a dotted line. # $P < 0.01$, * $P < 0.05$, different from cardiolipin vehicle-treated cells (0 µg/ml) stimulated with IFN-γ plus LPS, according to the randomized block one-way ANOVA (P and F values indicated on figure), followed by Fisher's LSD post-hoc test.

Chapter 4: Discussion

4.1. Cardiolipin Induces the Phagocytic Activity of Microglia

Phagocytosis, a process performed by select types of immune cells, including microglia, is critical for maintaining homeostatic conditions in both the periphery and CNS. This process involves the recognition, engulfment and clearance of organisms and detrimental substances, including foreign pathogens and cellular debris, as a means of resolving inflammation and protecting the body from potentially harmful stimuli (Fu et al., 2014; Maderna and Godson, 2003; Prinz and Priller, 2017; Sierra et al., 2013). Within the periphery, the phagocytosis of damaged and dying cells is frequently initiated by phosphatidylserine, a phospholipid found in most cellular membranes, which is recognized by phagocytic cells (Segawa and Nagata, 2015; Wu et al., 2006). However, mitochondrial membranes contain very low levels of phosphatidylserine, and instead contain substantial amounts of the phospholipid cardiolipin (Balasubramanian et al., 2015; Vance and Tasseva, 2013). Additionally, it has been demonstrated that cardiolipin, as well as cardiolipin-containing mitochondria, can relocate during cellular processes in peripheral tissues. For example, cardiolipin can be translocated from the mitochondrial membranes to the plasma membrane during apoptotic events, and cardiolipin-presenting mitochondria can be released from peripheral cells following necrosis or acute trauma, as well as during pathological conditions (Balasubramanian et al., 2015; Nakajima et al., 2008; Sorice et al., 2004; Sorice et al., 2000). Therefore, researchers have been interested in determining whether externalized cardiolipin

can mediate the phagocytic actions of surrounding peripheral cells in a manner similar to that of phosphatidylserine. For example, Balasubramanian et al. (2015) demonstrated that cardiolipin-presenting mitochondria, as well as cardiolipin-containing liposomes, upregulated the phagocytic activity of peripheral macrophages by up to four-fold and 18-fold, respectively (Balasubramanian et al., 2015). Therefore, in addition to its role in regulating mitochondrial processes, cardiolipin may also function as an intercellular signaling molecule in the periphery. Studies have shown that externalized cardiolipin can regulate select peripheral immune cell functions; however, the effect of extracellular cardiolipin on phagocytosis in the CNS has yet to be investigated.

Within the CNS, phagocytosis is performed by microglia in both healthy and diseased brains. For example, normal brain development requires the apoptotic death of millions of neurons, and it has been demonstrated that microglia participate in the clearance of these dead neurons via phagocytosis (Wakselman et al., 2008; Witting et al., 2000). Additionally, in AD brains, microglia migrate towards, and participate in, the phagocytosis of toxic Aβ deposits (Ard et al., 1996; Frackowiak et al., 1992; Koenigsknecht and Landreth, 2004; Rogers and Lue, 2001).

Due to the critical role of microglia in maintaining CNS homeostasis, we assessed the effect of extracellular cardiolipin on the phagocytic activity of microglia. We hypothesized that the addition of cardiolipin to microglial cells in culture would induce the phagocytic activity of microglia. To test this hypothesis, we conducted the phagocytosis assay using murine BV-2 microglia and primary murine microglia. We discovered that the addition of extracellular cardiolipin induces the

phagocytic activity of microglia. More specifically, the addition of cardiolipin at 5 and 20 μg/ml increases the phagocytic activity of BV-2 microglia by 2.5-fold and 3-fold, respectively, when compared to cardiolipin vehicle-treated cells. Additionally, primary murine microglia experienced a 2.4-fold increase in phagocytic activity following their exposure to cardiolipin at both 5 and 20 μg/ml concentrations, when compared to cardiolipin vehicle-treated cells. This is consistent with the outcomes of a previous study, which found that extracellular cardiolipin enhanced the phagocytic activity of peripheral macrophages (Balasubramanian et al., 2015).

When investigating potential therapeutic targets for the treatment of neurodegenerative diseases such as AD, it is important to ensure that the phagocytic functions of microglia are preserved, as this process is essential for returning the brain to a homeostatic state. Here we show, for the first time, that the addition of cardiolipin induces microglial phagocytosis, which is necessary for the clearance of damaged and dying neurons. Additionally, by upregulating the intrinsic phagocytic capabilities of microglia, cardiolipin may contribute to improved efficacy at engulfing and clearing of the Aβ deposits present in AD brains. Therefore, extracellular cardiolipin may represent a novel therapeutic agent for the treatment of neurodegenerative diseases, such as AD, which are characterized by extensive neuronal death and reduced microglial ability to phagocytose pathological structures (Hickman et al., 2008; Theriault et al., 2015). However, further investigation is required to determine the concentration of cardiolipin that will optimally induce microglial phagocytosis without resulting in further neurodegeneration through non-specific phagoptosis, or the death of viable neurons

induced by excessive phagocytic activity of microglia, which has been observed following the over-activation of microglia by Aβ plaques (Neniskyte et al., 2011; Sierra et al., 2013).

4.2. Cardiolipin Alters Microglial Functions that Impact Neuron Viability

4.2.1. Cardiolipin Inhibits Microglia-Mediated Cytotoxicity towards Neurons

Next, cardiolipin was investigated for its potential to modify microglia-mediated cytotoxicity towards neurons. Microglial activation is an essential process that is responsible for mounting an immune response in the CNS (Akiyama et al., 2000; Streit et al., 1999). However, microglial activation becomes dysregulated in AD brains due to the continued presence of pathological structures, as well as extensive neuron death. This over-activation of microglia results in the persistent release of cytotoxic molecules, which can have damaging effects to surrounding brain cells, including neurons and other glial cells (Akiyama et al., 2000; Banati et al., 1993; Brown and Vilalta, 2015; Lull and Block, 2010; Mrak and Griffin, 2005). Therefore, researchers have been interested in identifying molecules that are capable of attenuating the detrimental effects associated with chronic microglial activation in aims of preventing the onset and slowing the progression of AD.

Phosphatidylcholine is a phospholipid found abundantly within cellular membranes, including the mitochondrial membranes. Phosphatidylcholine has been extensively studied for its ability to reduce the damaging effects of chronic inflammation in the periphery, and recent studies have revealed that phosphatidylcholine may exert similar effects within the CNS (Aabdallah and Eid,

2004; Hartmann et al., 2009; Jung et al., 2013; Treede et al., 2007). For example, it has been shown that phosphatidylcholine can reduce microglial activation and migration to the hippocampus, as well as promote neurogenesis (Hashioka et al., 2007; Tokes et al., 2011), thus, demonstrating that phosphatidylcholine is capable of regulating microglial responses and exerting neuroprotective effects.

Since the cytotoxic effects of over-activated microglia are implicated in the propagation of the chronic neuroinflammatory state observed in AD, we investigated the effect of extracellular cardiolipin on microglia-mediated cytotoxicity towards neurons. We hypothesized that the addition of cardiolipin to microglial cells in culture would lead to neuroprotective effects in a manner similar to that of phosphatidylcholine. To test this hypothesis, we utilized an *in vitro* assay, which involved the transfer of THP-1 cell supernatants onto SH-SY5Y cells, as this model has been successfully utilized to study the interactions between microglial and neuronal cells (Klegeris and McGeer, 2001, 2003). In this study, we confirmed that THP-1 cell stimulation with IFN-γ plus LPS induces the secretion of cytotoxic molecules that reduce SH-SY5Y neuronal cell viability. We also discovered that the addition of extracellular cardiolipin to THP-1 cells, in the absence of IFN-γ plus LPS, does not induce THP-1 cytotoxicity towards SH-SY5Y cells. However, when the THP-1 cells were treated with extracellular cardiolipin prior to stimulation with IFN-γ plus LPS, a neuroprotective effect was observed. More specifically, the addition of cardiolipin increases the viability of SH-SY5Y cells at all concentrations studied, with the maximum 1.5-fold increase in cell viability observed at the concentration of 25 μg/ml, when compared to cardiolipin vehicle-treated cells in the presence of IFN-γ

plus LPS. Furthermore, the addition of cardiolipin to THP-1 cells decreases the death of SH-SY5Y cells at all concentrations studied, with the maximum 1.3-fold decrease in cell death observed at the concentration of 25 μg/ml, when compared to cardiolipin vehicle-treated cells in the presence of IFN-γ plus LPS. These findings are consistent with previous studies, which identified that phosphatidylcholine modified microglial functions in a neuroprotective manner (Hashioka et al., 2007; Tokes et al., 2011).

It has been suggested that within AD brains, it is not the deposition of Aβ plaques that directly contributes to neuron death, but rather the resultant over-activation of microglia that occurs following their interaction with pathological structures (Weldon et al., 1998). Therefore, reducing the chronic activation of microglia has been an active area of research, as such intervention may prevent the subsequent neurodegeneration observed in AD (Gao and Hong, 2008; Martin-Moreno et al., 2011; Solito and Sastre, 2012). Here we show, for the first time, that the addition of cardiolipin prior to the activation of microglia reduces subsequent microglia-mediated cytotoxicity towards neurons, which could be a major cause of neurodegeneration in AD brains. Therefore, extracellular cardiolipin may represent a novel therapeutic agent for the treatment of neurodegenerative diseases, such as AD, which are characterized by microglia-mediated neuron death.

4.2.2. Cardiolipin Induces Microglial Expression of Neurotrophic Factors

In addition to regulating the neuroimmune status of the brain, microglia also play a direct role in supporting neuronal survival. Neurons rely on microglia to

express and secrete a variety of trophic factors, including BDNF and GDNF, which are required for neuronal growth and development, as well as for synaptic remodeling (Allen et al., 2013; Huang and Reichardt, 2001; Skaper, 2012). However, it has yet to be determined whether extracellular cardiolipin can regulate trophic factor expression by microglia.

Since BDNF and GDNF are essential for neuronal survival, we examined the effect of extracellular cardiolipin on the expression of these trophic factors by microglia. Due to the neuroprotective effects cardiolipin exhibited against microglia-mediated cytotoxicity (see section 3.2), we hypothesized that cardiolipin would induce the expression of BDNF and GDNF by microglia. To test this hypothesis, we conducted immunofluorescence experiments using murine BV-2 microglia and primary murine microglia. Here we show, for the first time, that the addition of extracellular cardiolipin induces the expression of BDNF and GDNF by microglia. The addition of cardiolipin to BV-2 cells results in a 1.8-fold, 2-fold and 2.4-fold increase in BDNF expression at the concentrations of 5, 10 and 20 μg/ml, respectively; whereas, the addition of cardiolipin to BV-2 cells results in a 1.7-fold, 2.1-fold and 2.5-fold increase in expression of GDNF at the concentrations of 5, 10 and 20 μg/ml, respectively, when compared to cardiolipin vehicle-treated cells. Furthermore, the addition of cardiolipin to primary murine microglia results in a 1.9-fold, 2.3-fold and 2.7-fold increase in BDNF expression at the concentrations of 5, 10 and 20 μg/ml, respectively; whereas the addition of cardiolipin to primary murine microglia results in a 1.5-fold, 2-fold and 2.3-fold increase in GDNF expression at the concentrations of 5, 10 and 20 μg/ml, respectively, when

compared to cardiolipin vehicle-treated cells. These findings, therefore, support the neuroprotective properties of extracellular cardiolipin.

In AD patients, levels of BDNF and GDNF are significantly reduced (Budni et al., 2015; Forlenza et al., 2015). This reduction in trophic factor expression contributes to neuronal death, and results in the exacerbation of the cognitive decline associated with AD (Budni et al., 2015; Forlenza et al., 2015). Multiple studies utilizing mouse models of AD have demonstrated that increasing levels of BDNF and GDNF can exert neuroprotective effects through the reduction of oxidative stress, which thereby results in improved cognitive functioning (Allen et al., 2013; Han et al., 2013; Hsiao et al., 2014; Revilla et al., 2014; Shin et al., 2014). Our data indicate that the addition of cardiolipin can induce the expression of BDNF and GDNF by microglia. Therefore, these findings represent an additional reason why extracellular cardiolipin may act as a possible therapeutic agent for the treatment of neurodegenerative diseases, such as AD, which are partially characterized by a decline in expression of critical brain trophic factors. However, further investigation is required to determine whether extracellular cardiolipin also induces the secretion of BDNF and GDNF by microglia, as the release of these neurotrophic factors is crucial for neuronal survival.

4.3. Cardiolipin Alters the Secretory Profile of Activated Microglia

Finally, cardiolipin was investigated for its ability to modify the secretory profile of microglia. Activated microglia have been shown to release various pro-inflammatory mediators, including RNS, ROS, TNF-α and MCP-1, as a means of

mounting an immune response (Akiyama et al., 2000; Jessen, 2004; Lull and Block, 2010; Parpura et al., 2012; Saijo and Glass, 2011; Yang et al., 2010). Acute microglial activation is required for maintaining homeostatic conditions in the CNS; however, when this response becomes prolonged, such as in AD brains, cytotoxic molecules are continually released, which has damaging effects and results in extensive brain cell death and disease propagation (Banati et al., 1993; Brown and Vilalta, 2015; Lull and Block, 2010). Therefore, researchers have been interested in modulating the secretion of these immune mediators, as a means of preventing the extensive neuron death observed following the over-activation of microglia.

Previous studies have demonstrated that externalized phospholipids may act to alter the secretory profile of microglia. For example, Balasubramanian et al. (2015) found that the LPS-induced secretion of the pro-inflammatory cytokines interleukin (IL)-6 and IL-12 by peripheral macrophages could be reduced by treatment with cardiolipin-embedded liposomes (Balasubramanian et al., 2015). Additionally, due to its protective effects against chronic inflammation in both the periphery and CNS, phosphatidylcholine has been extensively investigated for its ability to mediate the secretory profile of peripheral macrophages and microglia. Previous studies have shown that phosphatidylcholine can down-regulate the immunological responses of both peripheral macrophages and microglia by reducing their activation, as well as decreasing their production of ROS, RNS and TNF-α (Aabdallah and Eid, 2004; Gilbreath et al., 1985; Hashioka et al., 2007; Nishiyama-Naruke and Curi, 2000; Tokes et al., 2011).

We investigated the effect of extracellular cardiolipin on the secretory profile of activated microglia. Since we established that extracellular cardiolipin can attenuate microglia-mediated cytotoxicity towards neurons, we hypothesized that the addition of cardiolipin would decrease the secretion of pro-inflammatory mediators and cytotoxic molecules. Specifically, we assessed the effect of cardiolipin on the secretion of RNS, ROS, TNF-α and MCP-1, all of which are released in excess during the neuroinflammatory processes implicated in AD (Dawson and Dawson, 1996; Galimberti et al., 2003; Hickman et al., 2008; Multhaup et al., 1997; Porcellini et al., 2013).

4.3.1. Cardiolipin Reduces the Secretion of Reactive Nitrogen Species (RNS) by Microglia

NO, a well-defined RNS, is implicated in a variety of physiological processes within the CNS, including neuronal communication, synaptic plasticity, regulation of gene expression and immune cell activation (Dawson and Dawson, 1996; Miranda et al., 2001). Despite its important role as a messenger molecule within the CNS, when NO is secreted superfluously, it can exert neurotoxic effects; therefore, excessive NO production is implicated in the pathogenesis of neurodegenerative disorders, such as AD, that are characterized by extensive death of neurons (Chao et al., 1992; Combs et al., 2001; Dawson and Dawson, 1996). For example, it has been demonstrated that within AD brains, the recognition of aggregated Aβ plaques by microglia results in increased expression of inducible nitric oxide synthase (iNOS), an enzyme that catalyzes the excess production of NO (Aktan, 2004; Combs et al., 2001; Maezawa et al., 2011; Weldon et al., 1998). Previous studies have also

demonstrated that inhibiting the activity of iNOS minimizes production of NO, thereby, preventing the associated nitrosative stress and subsequent microglia-mediated neurotoxicity (Combs et al., 2001; Maezawa et al., 2011). Therefore, reducing the excess production of RNS by activated microglia may help to prevent the extensive neurodegeneration observed in AD brains.

To determine whether extracellular cardiolipin affects the production and release of RNS by activated microglia, we utilized murine BV-2 cells in the Griess assay, which measures the secretion of nitrite, a stable metabolite of NO (Ding et al., 1988; Miranda et al., 2001). Here we show, for the first time, that the addition of extracellular cardiolipin reduces nitrite secretion by activated microglia. The addition of cardiolipin decreases the LPS-induced secretion of nitrite by BV-2 cells at all concentrations studied, with the maximum 1.7-fold decrease in nitrite secretion observed at the concentration of 10 μg/ml, when compared to cardiolipin vehicle-treated cells in the presence of LPS. Therefore, we have demonstrated that cardiolipin can reduce the nitrosative stress of microglia, which has significant implications for a number of CNS diseases, including AD. These findings are consistent with previous studies, which identified similar effects of extracellular phosphatidylcholine on microglial secretion of nitrite (Hashioka et al., 2007). Therefore, extracellular cardiolipin may represent a possible therapeutic agent for the treatment of neurodegenerative diseases, such as AD, that are characterized by excessive RNS production.

4.3.2. Cardiolipin Reduces the Secretion of Reactive Oxygen Species (ROS) by Microglia

The brain is particularly susceptible to oxidative stress due to its high content of unsaturated phospholipids (Chong et al., 2005). In AD brains, there is a significant increase in ROS production due to age-related mitochondrial dysfunction, as well as the over-activation of microglia due to the presence of Aβ deposits (Canevari et al., 2004; Emerit et al., 2004; Mariani et al., 2005; Multhaup et al., 1997). This excessive production of ROS results in the oxidative damage to lipids, proteins and DNA, thereby hindering cellular functioning and resulting in extensive brain cell death (Barnham et al., 2004; Mariani et al., 2005). Additionally, it has been shown that this increase in oxidative stress contributes to the peroxidation of mitochondrial membrane components, including cardiolipin (Fang et al., 2016; Petrosillo et al., 2008; Zhou et al., 2008). Following its peroxidation, the structure of cardiolipin is modified in a way that further hinders mitochondrial functioning, and results in decreased brain cell viability (Cheng et al., 2008; Fry and Green, 1981; Monteiro-Cardoso et al., 2015; Sathappa and Alder, 2016). Therefore, decreasing ROS production is critical for reducing the peroxidation of cardiolipin and associated mitochondrial dysfunctioning, as well as for preventing the oxidative stress and extensive brain cell death observed in AD brains.

To determine whether extracellular cardiolipin affects the release of ROS by activated microglia, we utilized differentiated human HL-60 cells in the respiratory burst assay, which was conducted to measure the secretion of superoxide anion, the most commonly occurring oxygen free radical (Chong et al., 2005). Here we show, for the first time, that the addition of extracellular cardiolipin reduces superoxide

anion secretion by primed microglia. The addition of cardiolipin results in a 1.2-fold, 1.5-fold and 1.8-fold decrease in the secretion of superoxide anion by human HL-60 cells at the concentrations of 2, 10 and 20 μg/ml, respectively, when compared to cardiolipin vehicle-treated cells primed with LPS. Therefore, these findings demonstrate that cardiolipin can reduce microglia-mediated oxidative stress. This is consistent with the outcomes of previous studies that found similar effects of phosphatidylcholine on ROS production in the CNS (Aabdallah and Eid, 2004; Hashioka et al., 2007). Therefore, extracellular cardiolipin may represent a possible therapeutic agent for the treatment of neurodegenerative diseases, such as AD, that are characterized by excessive ROS production.

4.3.3. Cardiolipin Modifies the Secretion of Pro-Inflammatory Cytokines by Microglia

Pro-inflammatory cytokines, including TNF-α and MCP-1, are secreted by activated microglia during immune responses in aims of communicating with other cells of the CNS (Deshmane et al., 2009; Mennicken et al., 1999; Olson and Miller, 2004; Wang et al., 2015). TNF-α is a well-defined pro-inflammatory cytokine that is significantly upregulated following microglial activation. Despite its important physiological role in mounting inflammatory responses in the CNS, TNF-α has also been implicated in AD pathogenesis, as it can exert neurotoxic effects when produced in excess (Dickson et al., 1993; Hickman et al., 2008; Wang et al., 2015). For example, Combs et al. (2001) demonstrated that microglial recognition of Aβ plaques resulted in a 3-fold increase in TNF-α expression, which was associated with a subsequent decrease in neuronal viability (Combs et al., 2001). MCP-1, a

crucial pro-inflammatory cytokine that is constitutively produced by microglia, is responsible for mediating inflammatory responses in the CNS by regulating the chemotaxis of monocytes and microglia (Deshmane et al., 2009; Olson and Miller, 2004; Porcellini et al., 2013). However, it has been demonstrated that within AD brains, the over-activation of microglia results in the excessive secretion of MCP-1, which is associated with a further increase in Aβ plaque deposition, thereby exacerbating AD pathology (Galimberti et al., 2003; Yamamoto et al., 2013). Therefore, it is evident that controlling the secretion of these pro-inflammatory mediators is critical for preserving the beneficial immune responses required in the CNS, as well as for preventing the extensive neurodegeneration present in AD brains.

To determine whether extracellular cardiolipin regulates the secretion of TNF-α and MCP-1 by microglia, we quantified their concentration in human THP-1 cell supernatants. Here we show, for the first time, that the addition of extracellular cardiolipin reduces TNF-α secretion by activated microglia. The addition of cardiolipin results in a 1.5-fold, 1.9-fold and 2.2-fold decrease in the secretion of TNF-α by stimulated human THP-1 cells at the concentrations of 2, 10 and 20 μg/ml, respectively, when compared to cardiolipin vehicle-treated cells in the presence of IFN-γ plus LPS; therefore, demonstrating that cardiolipin is able to reduce this aspect of neuroinflammation. These observations are consistent with the outcomes of previous studies that found similar effects of extracellular phosphatidylcholine on the secretion of TNF-α by activated microglia, as well as the effects of extracellular

cardiolipin on the secretion of pro-inflammatory cytokines by peripheral macrophages (Balasubramanian et al., 2015; Hashioka et al., 2007).

Furthermore, we show that extracellular cardiolipin on its own induces the secretion of MCP-1 by THP-1 cells. The addition of cardiolipin, in the absence of IFN-γ plus LPS, results in a 1.5-fold, 1.6-fold and 1.7-fold increase in the secretion of MCP-1 by human THP-1 cells at the concentrations of 2, 10 and 20 μg/ml, respectively, when compared to cardiolipin vehicle-treated cells. However, the addition of cardiolipin to THP-1 cells prior to their stimulation with IFN-γ plus LPS results in a 1.1-fold decrease in the secretion of MCP-1 by microglia at all concentrations studied, when compared to cardiolipin vehicle-treated cells in the presence of IFN-γ plus LPS. Therefore, these data indicate that extracellular cardiolipin may induce the inflammatory responses of resting microglia; however, in AD brains, where microglia become over-activated, extracellular cardiolipin may prevent the exacerbation of AD pathogenesis by reducing excess production of MCP-1 by microglia.

Taken together, these findings demonstrate that cardiolipin modifies the secretory profile of microglia. Therefore, extracellular cardiolipin may represent a possible therapeutic agent for the treatment of neurodegenerative diseases, such as AD, that are characterized by the excessive production of pro-inflammatory cytokines.

Chapter 5: Conclusion

5.1. Limitations of the Research

One of the main limitations of this study is the use of immortalized cell lines, including human THP-1 monocytic cells, human HL-60 promyelocytic cells, murine BV-2 cells and human SH-SY5Y neuroblastoma cells, as models of primary CNS cells. These cell lines were originally derived either from cancerous cells or through transfection with viral genes, as a means of ensuring prolonged proliferation of the cells (Birnie, 1988; Bocchini et al., 1992; Pahlman et al., 1990; Tsuchiya et al., 1980). Thus, the cell lines utilized in this study may differ in genotype and phenotype compared to their primary cell counterpart, which can result in differential morphology and physiological responses (Horvath et al., 2008; Pan et al., 2009). In this study, I attempted to overcome this limitation by repeating key experiments using primary murine microglia.

An additional limitation of this study is the use of mono-culture, rather than co-culture or *in vivo* experiments. For example, in the microglia-mediated cytotoxicity experiments, I utilized human THP-1 monocytic cells and human SH-SY5Y neuroblastoma cells to model microglia and neurons, respectively. This experiment required culturing the two cell types in isolation, following which THP-1 cell supernatants were transferred onto SH-SY5Y cells. However, by culturing these cells separately, they did not physically interact with one another, which might have resulted in behavior and responses that differ from those that occur during cellular interactions in the CNS (Miki et al., 2012; Regier et al., 2016). For example, it has

been shown that cells in mono-culture and co-culture differentially express various cell surface receptor genes, which may result in discrepancies in cellular responses following interaction with various stimuli (Regier et al., 2016). Therefore, the experiments presented in this thesis, such as the cytotoxicity experiment, may over-simplify the interactions that occur within the CNS, where cells are in constant communication with one another, as these experiments only examined unidirectional effects of microglia on neurons. Despite this drawback, the microglia-mediated cytotoxicity experiment, as well as the other experiments described in this study, allow for the investigation and discovery of single variables that may represent key factors of neuroinflammation, and thus, act as a valuable tool for the collection of preliminary data that are necessary for the development of more complex models and experiments.

5.2. Future Directions of Research

This thesis provides substantial evidence that extracellular cardiolipin modifies select microglial functions. However, additional studies are required to examine and identify the molecular mechanisms through which extracellular cardiolipin exerts its effects. In order to address this knowledge gap, several receptors, including the triggering receptor expressed on myeloid cells (TREM)-2, should be explored as potential binding sites for extracellular cardiolipin. The TREM-2 receptor is of relevance, as it is expressed on peripheral macrophages, as well as microglia, and following its activation by anionic phospholipids, it is responsible for mediating phagocytosis, reducing the secretion of inflammatory

cytokines and preventing cell death (Hickman and El Khoury, 2014; Painter et al., 2015). Additionally, due to its phospholipid structure, cardiolipin could directly alter membrane fluidity, which can thereby affect various down-stream signaling cascades involved in microglial activation (Ibarguren et al., 2014). Therefore, further investigation is required to elucidate which, if any, of these mechanisms are utilized by extracellular cardiolipin to exert its effects on microglia.

5.3. Research Objectives Addressed and Future Directions

Objective 1: To address the first research objective, I established that extracellular cardiolipin induced the phagocytic activity of both murine BV-2 cells and primary murine microglia. However, further studies are required to confirm these findings *in vivo*, as well as to determine the optimal concentration of cardiolipin required to induce microglial phagocytosis without causing detrimental neuronal death via phagoptosis, which has been observed following the over-activation of microglia by Aβ plaques (Neniskyte et al., 2011; Sierra et al., 2013).

Objective 2: I determined that extracellular cardiolipin reduced microglia-mediated cytotoxicity towards neurons. Since these experiments were conducted using human THP-1 and SH-SY5Y cells as models of CNS cells, the results should be confirmed using primary human microglia and neurons, or through *in vivo* studies. Additionally, I demonstrated that extracellular cardiolipin increased the expression of BDNF and GDNF by both murine BV-2 cells and primary murine microglia. However, additional studies are required to determine whether upregulated expression of BDNF and GDNF induced by extracellular cardiolipin leads to

increased microglial secretion of these brain trophic factors, as they are required for neuronal survival and are significantly decreased in AD brains (Budni et al., 2015).

Objective 3: I established that extracellular cardiolipin altered the secretory profile of microglia. Since these experiments were conducted using microglia model cells, additional studies should be conducted to confirm these findings using primary microglia *in vitro*, or through *in vivo* studies.

Previous studies have demonstrated that cardiolipin-containing liposomes are capable of crossing the BBB in mice (Ordonez-Gutierrez et al., 2015; Vieira and Gamarra, 2016). Therefore, additional *in vivo* studies using liposomes with varying concentrations of embedded cardiolipin could determine the optimal concentration of this phospholipid necessary to alter physiological responses in the CNS. Additionally, cardiolipin-embedded liposomes could be administered to AD model mice to determine whether increasing levels of extracellular cardiolipin in the CNS modifies the detrimental microglial responses and extensive neuron death observed in AD model brains. Such experiments would assess the effects of extracellular cardiolipin in a model system that is more representative of the human AD brain than *in vitro* studies with cultured cells, and could, therefore, determine whether extracellular cardiolipin regulates microglial functions and exerts neuroprotective effects in AD brains.

5.4. Significance of Findings

This thesis confirms that extracellular cardiolipin regulates several microglial functions that potentially impact select aspects of neuroinflammation.

Previous studies have demonstrated that extracellular cardiolipin mediates select functions of peripheral immune cells (Balasubramanian et al., 2015); however, to the best of my knowledge, the effects of extracellular cardiolipin on the immune cells of the CNS have not been investigated. In this study, I have shown for the first time that extracellular cardiolipin induces the phagocytic activity of microglia, decreases microglia-mediated cytotoxicity towards neurons, as well as alters the secretory profile of activated microglia towards a less pro-inflammatory profile. Therefore, extracellular cardiolipin, or cardiolipin-embedded liposomes, may represent novel therapeutic agents for preventing the over-activation of microglia and subsequent extensive neurodegeneration observed in AD brains.

As our global population ages, it is estimated that the prevalence of neurodegenerative diseases, which are partially characterized by chronic neuroinflammation and dysregulated microglial activation, will reach over 131 million by the year 2050 if no effective treatment is identified (Prince et al., 2015). Since there are currently no viable strategies available to delay the onset or slow the progression of AD, discovering novels means of attenuating the over-activation of microglia may reduce the chronic neuroinflammation and extensive neurodegeneration observed in AD brains. In addition to broadening the knowledge of molecules involved in regulating microglial functioning and CNS homeostasis, this study identifies novel molecular targets and potential therapeutic strategies for the treatment of neurodegenerative disorders, such as AD, which are characterized by dysregulated microglial functioning and subsequent death of neurons.

References:

Aabdallah DM, Eid NI (2004) Possible neuroprotective effects of lecithin and alpha-tocopherol alone or in combination against ischemia/reperfusion insult in rat brain. J Biochem Mol Toxicol 18:273-278. doi:10.1002/jbt.20037

Acehan D, Malhotra A, Xu Y, Ren M, Stokes DL, Schlame M (2011) Cardiolipin affects the supramolecular organization of ATP synthase in mitochondria. Biophys J 100:2184-2192. doi:10.1016/j.bpj.2011.03.031

Acin-Perez R, Fernandez-Silva P, Peleato ML, Perez-Martos A, Enriquez JA (2008) Respiratory active mitochondrial supercomplexes. Mol Cell 32:529-539. doi:10.1016/j.molcel.2008.10.021

Akiyama H et al. (2000) Inflammation and Alzheimer's disease. Neurobiol Aging 21:383-421

Aktan F (2004) iNOS-mediated nitric oxide production and its regulation. Life Sci 75:639-653. doi:10.1016/j.lfs.2003.10.042

Allen SJ, Watson JJ, Shoemark DK, Barua NU, Patel NK (2013) GDNF, NGF and BDNF as therapeutic options for neurodegeneration. Pharmacol Ther 138:155-175. doi:10.1016/j.pharmthera.2013.01.004

Anthonymuthu TS, Kenny EM, Bayir H (2016) Therapies targeting lipid peroxidation in traumatic brain injury. Brain Res. doi:10.1016/j.brainres.2016.02.006

Ard MD, Cole GM, Wei J, Mehrle AP, Fratkin JD (1996) Scavenging of Alzheimer's amyloid beta-protein by microglia in culture. J Neurosci Res 43:190-202. doi:10.1002/(SICI)1097-4547(19960115)43:2<190::AID-JNR7>3.0.CO;2-B

Asanuma M, Tsuji T, Miyazaki I, Miyoshi K, Ogawa N (2003) Methamphetamine-induced neurotoxicity in mouse brain is attenuated by ketoprofen, a non-steroidal anti-inflammatory drug. Neurosci Lett 352:13-16

Axline SG, Reaven EP (1974) Inhibition of phagocytosis and plasma membrane mobility of the cultivated macrophage by cytochalasin B. Role of subplasmalemmal microfilaments. J Cell Biol 62:647-659

Balasubramanian K et al. (2015) Dichotomous roles for externalized cardiolipin in extracellular signaling: promotion of phagocytosis and attenuation of innate immunity. Sci Signal 8:ra95. doi:10.1126/scisignal.aaa6179

Bamberger ME, Landreth GE (2002) Inflammation, apoptosis, and Alzheimer's disease. Neuroscientist 8:276-283

Banati RB, Gehrmann J, Schubert P, Kreutzberg GW (1993) Cytotoxicity of microglia. Glia 7:111-118. doi:10.1002/glia.440070117

Barnham KJ, Masters CL, Bush AI (2004) Neurodegenerative diseases and oxidative stress. Nat Rev Drug Discov 3:205-214. doi:10.1038/nrd1330

Biedler JL, Helson L, Spengler BA (1973) Morphology and growth, tumorigenicity, and cytogenetics of human neuroblastoma cells in continuous culture. Cancer Res 33:2643-2652

Bielski BH, Arudi RL, Sutherland MW (1983) A study of the reactivity of HO2/O2- with unsaturated fatty acids. J Biol Chem 258:4759-4761

Birnie GD (1988) The HL60 cell line: a model system for studying human myeloid cell differentiation. Br J Cancer Suppl 9:41-45

Blasko I, Stampfer-Kountchev M, Robatscher P, Veerhuis R, Eikelenboom P, Grubeck-Loebenstein B (2004) How chronic inflammation can affect the brain and support the development of Alzheimer's disease in old age: the role of microglia and astrocytes. Aging Cell 3:169-176. doi:10.1111/j.1474-9728.2004.00101.x

Bocchini V, Mazzolla R, Barluzzi R, Blasi E, Sick P, Kettenmann H (1992) An immortalized cell line expresses properties of activated microglial cells. J Neurosci Res 31:616-621. doi:10.1002/jnr.490310405

Bonzon C, Bouchier-Hayes L, Pagliari LJ, Green DR, Newmeyer DD (2006) Caspase-2-induced apoptosis requires bid cleavage: a physiological role for bid in heat shock-induced death. Mol Biol Cell 17:2150-2157. doi:10.1091/mbc.E05-12-1107

Breedlove SM, Watson NV (2013) Biological psychology: an introduction to behavioral, cognitive and clinical neuroscience. Seventh Edition. Sinauer Associates, Inc.

Brown GC, Vilalta A (2015) How microglia kill neurons. Brain Res 1628:288-297. doi:10.1016/j.brainres.2015.08.031

Bryan NS, Grisham MB (2007) Methods to detect nitric oxide and its metabolites in biological samples. Free Radic Biol Med 43:645-657. doi:10.1016/j.freeradbiomed.2007.04.026

Budni J, Bellettini-Santos T, Mina F, Garcez ML, Zugno AI (2015) The involvement of BDNF, NGF and GDNF in aging and Alzheimer's disease. Aging Dis 6:331-341. doi:10.14336/AD.2015.0825

Buhl SN, Jackson KY, Graffunder B (1978) Optimal reaction conditions for assaying human lactate dehydrogenase pyruvate-to-lactate at 25, 30, and 37 degrees C. Clin Chem 24:261-266

Calviello G et al. (2004) n-3 PUFAs reduce VEGF expression in human colon cancer cells modulating the COX-2/PGE2 induced ERK-1 and -2 and HIF-1alpha induction pathway. Carcinogenesis 25:2303-2310. doi:10.1093/carcin/bgh265

Camilleri A et al. (2013) Mitochondrial membrane permeabilisation by amyloid aggregates and protection by polyphenols. Biochim Biophys Acta 1828:2532-2543. doi:10.1016/j.bbamem.2013.06.026

Canevari L, Abramov AY, Duchen MR (2004) Toxicity of amyloid beta peptide: tales of calcium, mitochondria, and oxidative stress. Neurochem Res 29:637-650

Carson MJ, Crane J, Xie AX (2008) Modeling CNS microglia: the quest to identify predictive models. Drug Discov Today Dis Models 5:19-25. doi:10.1016/j.ddmod.2008.07.006

Chao CC, Hu S, Molitor TW, Shaskan EG, Peterson PK (1992) Activated microglia mediate neuronal cell injury via a nitric oxide mechanism. J Immunol 149:2736-2741

Cheng H et al. (2008) Shotgun lipidomics reveals the temporally dependent, highly diversified cardiolipin profile in the mammalian brain: temporally coordinated postnatal diversification of cardiolipin molecular species with neuronal remodeling. Biochemistry 47:5869-5880. doi:10.1021/bi7023282

Cherry JD, Olschowka JA, O'Banion MK (2014) Neuroinflammation and M2 microglia: the good, the bad, and the inflamed. J Neuroinflammation 11:98. doi:10.1186/1742-2094-11-98

Chicco AJ, Sparagna GC (2007) Role of cardiolipin alterations in mitochondrial dysfunction and disease. Am J Physiol Cell Physiol 292:C33-44. doi:10.1152/ajpcell.00243.2006

Chong ZZ, Li F, Maiese K (2005) Oxidative stress in the brain: novel cellular targets that govern survival during neurodegenerative disease. Prog Neurobiol 75:207-246. doi:10.1016/j.pneurobio.2005.02.004

Chow YL, Lee KH, Vidyadaran S, Lajis NH, Akhtar MN, Israf DA, Syahida A (2012) Cardamonin from Alpinia rafflesiana inhibits inflammatory responses in IFN-gamma/LPS-stimulated BV2 microglia via NF-kappaB signalling pathway. Int Immunopharmacol 12:657-665. doi:10.1016/j.intimp.2012.01.009

Chu CT, Bayir H, Kagan VE (2014) LC3 binds externalized cardiolipin on injured mitochondria to signal mitophagy in neurons: implications for Parkinson disease. Autophagy 10:376-378. doi:10.4161/auto.27191

Chu CT et al. (2013) Cardiolipin externalization to the outer mitochondrial membrane acts as an elimination signal for mitophagy in neuronal cells. Nat Cell Biol 15:1197-1205. doi:10.1038/ncb2837

Collins SJ (1987) The HL-60 promyelocytic leukemia cell line: proliferation, differentiation, and cellular oncogene expression. Blood 70:1233-1244

Colton CA, Gilbert DL (1987) Production of superoxide anions by a CNS macrophage, the microglia. FEBS Lett 223:284-288

Combs CK, Karlo JC, Kao SC, Landreth GE (2001) beta-Amyloid stimulation of microglia and monocytes results in TNFalpha-dependent expression of inducible nitric oxide synthase and neuronal apoptosis. J Neurosci 21:1179-1188

Cui TZ, Conte A, Fox JL, Zara V, Winge DR (2014) Modulation of the respiratory supercomplexes in yeast: enhanced formation of cytochrome oxidase increases the stability and abundance of respiratory supercomplexes. J Biol Chem 289:6133-6141. doi:10.1074/jbc.M113.523688

Culbert AA et al. (2006) MAPK-activated protein kinase 2 deficiency in microglia inhibits pro-inflammatory mediator release and resultant neurotoxicity. Relevance to neuroinflammation in a transgenic mouse model of Alzheimer disease. J Biol Chem 281:23658-23667. doi:10.1074/jbc.M513646200

Dahlgren C, Karlsson A (1999) Respiratory burst in human neutrophils. J Immunol Methods 232:3-14

Dai X et al. (2003) The trophic role of oligodendrocytes in the basal forebrain. J Neurosci 23:5846-5853

Davis AT, Estensen R, Quie PG (1971) Cytochalasin B. 3. Inhibition of human polymorphonuclear leukocyte phagocytosis. Proc Soc Exp Biol Med 137:161-164

Dawson VL, Dawson TM (1996) Nitric oxide neurotoxicity. J Chem Neuroanat 10:179-190

Deshmane SL, Kremlev S, Amini S, Sawaya BE (2009) Monocyte chemoattractant protein-1 (MCP-1): an overview. J Interferon Cytokine Res 29:313-326. doi:10.1089/jir.2008.0027

Dheen ST, Kaur C, Ling EA (2007) Microglial activation and its implications in the brain diseases. Curr Med Chem 14:1189-1197

Diaz-Silvestre H et al. (2005) The 19-kDa antigen of Mycobacterium tuberculosis is a major adhesin that binds the mannose receptor of THP-1 monocytic cells and promotes phagocytosis of mycobacteria. Microb Pathog 39:97-107. doi:10.1016/j.micpath.2005.06.002

Dickson DW, Lee SC, Mattiace LA, Yen SH, Brosnan C (1993) Microglia and cytokines in neurological disease, with special reference to AIDS and Alzheimer's disease. Glia 7:75-83. doi:10.1002/glia.440070113

Ding AH, Nathan CF, Stuehr DJ (1988) Release of reactive nitrogen intermediates and reactive oxygen intermediates from mouse peritoneal macrophages. Comparison of activating cytokines and evidence for independent production. J Immunol 141:2407-2412

Edgar JM, Nave KA (2009) The role of CNS glia in preserving axon function. Curr Opin Neurobiol 19:498-504. doi:10.1016/j.conb.2009.08.003

Elkabes S, DiCicco-Bloom EM, Black IB (1996) Brain microglia/macrophages express neurotrophins that selectively regulate microglial proliferation and function. J Neurosci 16:2508-2521

Elmore S (2007) Apoptosis: a review of programmed cell death. Toxicol Pathol 35:495-516. doi:10.1080/01926230701320337

Emerit J, Edeas M, Bricaire F (2004) Neurodegenerative diseases and oxidative stress. Biomed Pharmacother 58:39-46

Epand RF, Tokarska-Schlattner M, Schlattner U, Wallimann T, Epand RM (2007) Cardiolipin clusters and membrane domain formation induced by mitochondrial proteins. J Mol Biol 365:968-980. doi:10.1016/j.jmb.2006.10.028

Esposti MD, Cristea IM, Gaskell SJ, Nakao Y, Dive C (2003) Proapoptotic Bid binds to monolysocardiolipin, a new molecular connection between mitochondrial membranes and cell death. Cell Death Differ 10:1300-1309. doi:10.1038/sj.cdd.4401306

Etkin A, Buchel C, Gross JJ (2015) The neural bases of emotion regulation. Nat Rev Neurosci 16:693-700. doi:10.1038/nrn4044

Fang D et al. (2016) Increased Electron Paramagnetic Resonance Signal Correlates with Mitochondrial Dysfunction and Oxidative Stress in an Alzheimer's disease Mouse Brain. J Alzheimers Dis 51:571-580. doi:10.3233/JAD-150917

Fernandez M, Gobartt AL, Balana M, Group CS (2010) Behavioural symptoms in patients with Alzheimer's disease and their association with cognitive impairment. BMC Neurol 10:87. doi:10.1186/1471-2377-10-87

Ferrari M, Fornasiero MC, Isetta AM (1990) MTT colorimetric assay for testing macrophage cytotoxic activity in vitro. J Immunol Methods 131:165-172

Forlenza OV, Miranda AS, Guimar I, Talib LL, Diniz BS, Gattaz WF, Teixeira AL (2015) Decreased neurotrophic support is associated with cognitive decline in non-demented subjects. J Alzheimers Dis 46:423-429. doi:10.3233/JAD-150172

Forman HJ, Torres M (2002) Reactive oxygen species and cell signaling: respiratory burst in macrophage signaling. Am J Respir Crit Care Med 166:S4-8. doi:10.1164/rccm.2206007

Fotakis G, Timbrell JA (2006) In vitro cytotoxicity assays: comparison of LDH, neutral red, MTT and protein assay in hepatoma cell lines following exposure to cadmium chloride. Toxicol Lett 160:171-177. doi:10.1016/j.toxlet.2005.07.001

Frackowiak J, Wisniewski HM, Wegiel J, Merz GS, Iqbal K, Wang KC (1992) Ultrastructure of the microglia that phagocytose amyloid and the microglia that produce beta-amyloid fibrils. Acta Neuropathol 84:225-233

Fressinaud C, Vallat JM, Rigaud M, Cassagne C, Labourdette G, Sarlieve LL (1990) Investigation of myelination in vitro: polar lipid content and fatty acid composition of myelinating oligodendrocytes in rat oligodendrocyte cultures. Neurochem Int 16:27-39

Fry M, Green DE (1981) Cardiolipin requirement for electron transfer in complex I and III of the mitochondrial respiratory chain. J Biol Chem 256:1874-1880

Fu R, Shen Q, Xu P, Luo JJ, Tang Y (2014) Phagocytosis of microglia in the central nervous system diseases. Mol Neurobiol 49:1422-1434. doi:10.1007/s12035-013-8620-6

Galimberti D, Schoonenboom N, Scarpini E, Scheltens P, Dutch-Italian Alzheimer Research G (2003) Chemokines in serum and cerebrospinal fluid of Alzheimer's disease patients. Ann Neurol 53:547-548. doi:10.1002/ana.10531

Gao HM, Hong JS (2008) Why neurodegenerative diseases are progressive: uncontrolled inflammation drives disease progression. Trends Immunol 29:357-365. doi:10.1016/j.it.2008.05.002

Garcia Fernandez M et al. (2002) Early changes in intramitochondrial cardiolipin distribution during apoptosis. Cell Growth Differ 13:449-455

Genin M, Clement F, Fattaccioli A, Raes M, Michiels C (2015) M1 and M2 macrophages derived from THP-1 cells differentially modulate the response of cancer cells to etoposide. BMC Cancer 15:577. doi:10.1186/s12885-015-1546-9

Gerlier D, Thomasset N (1986) Use of MTT colorimetric assay to measure cell activation. J Immunol Methods 94:57-63

Gilbreath MJ, Nacy CA, Hoover DL, Alving CR, Swartz GM, Jr., Meltzer MS (1985) Macrophage activation for microbicidal activity against Leishmania major: inhibition of lymphokine activation by phosphatidylcholine-phosphatidylserine liposomes. J Immunol 134:3420-3425

Giulian D (1999) Microglia and the immune pathology of Alzheimer disease. Am J Hum Genet 65:13-18. doi:10.1086/302477

Gobbi M et al. (2010) Lipid-based nanoparticles with high binding affinity for amyloid-beta1-42 peptide. Biomaterials 31:6519-6529. doi:10.1016/j.biomaterials.2010.04.044

Gomez-Isla T et al. (1997) Neuronal loss correlates with but exceeds neurofibrillary tangles in Alzheimer's disease. Ann Neurol 41:17-24. doi:10.1002/ana.410410106

Gorlovoy P, Larionov S, Pham TT, Neumann H (2009) Accumulation of tau induced in neurites by microglial proinflammatory mediators. FASEB J 23:2502-2513. doi:10.1096/fj.08-123877

Gotz J, Lim YA, Ke YD, Eckert A, Ittner LM (2010) Dissecting toxicity of tau and beta-amyloid. Neurodegener Dis 7:10-12. doi:10.1159/000283475

Gresa-Arribas N, Vieitez C, Dentesano G, Serratosa J, Saura J, Sola C (2012) Modelling neuroinflammation in vitro: a tool to test the potential neuroprotective effect of anti-inflammatory agents. PLoS One 7:e45227. doi:10.1371/journal.pone.0045227

Haines TH, Dencher NA (2002) Cardiolipin: a proton trap for oxidative phosphorylation. FEBS Lett 528:35-39

Halliday G, Robinson SR, Shepherd C, Kril J (2000) Alzheimer's disease and inflammation: a review of cellular and therapeutic mechanisms. Clin Exp Pharmacol Physiol 27:1-8

Han K, Jia N, Li J, Yang L, Min LQ (2013) Chronic caffeine treatment reverses memory impairment and the expression of brain BNDF and TrkB in the PS1/APP double transgenic mouse model of Alzheimer's disease. Mol Med Rep 8:737-740. doi:10.3892/mmr.2013.1601

Hartmann P et al. (2009) Anti-inflammatory effects of phosphatidylcholine in neutrophil leukocyte-dependent acute arthritis in rats. Eur J Pharmacol 622:58-64. doi:10.1016/j.ejphar.2009.09.012

Hashioka S et al. (2007) Phosphatidylserine and phosphatidylcholine-containing liposomes inhibit amyloid beta and interferon-gamma-induced microglial activation. Free Radic Biol Med 42:945-954. doi:10.1016/j.freeradbiomed.2006.12.003

Hatch GM (2004) Cell biology of cardiac mitochondrial phospholipids. Biochem Cell Biol 82:99-112. doi:10.1139/o03-074

He BP, Wen W, Strong MJ (2002) Activated microglia (BV-2) facilitation of TNF-alpha-mediated motor neuron death in vitro. J Neuroimmunol 128:31-38

Heese K, Hock C, Otten U (1998) Inflammatory signals induce neurotrophin expression in human microglial cells. J Neurochem 70:699-707

Heo DK, Lim HM, Nam JH, Lee MG, Kim JY (2015) Regulation of phagocytosis and cytokine secretion by store-operated calcium entry in primary isolated murine microglia. Cell Signal 27:177-186. doi:10.1016/j.cellsig.2014.11.003

Hermann AC, Millard PJ, Blake SL, Kim CH (2004) Development of a respiratory burst assay using zebrafish kidneys and embryos. J Immunol Methods 292:119-129. doi:10.1016/j.jim.2004.06.016

Hickman SE, Allison EK, El Khoury J (2008) Microglial dysfunction and defective beta-amyloid clearance pathways in aging Alzheimer's disease mice. J Neurosci 28:8354-8360. doi:10.1523/JNEUROSCI.0616-08.2008

Hickman SE, El Khoury J (2014) TREM2 and the neuroimmunology of Alzheimer's disease. Biochem Pharmacol 88:495-498. doi:10.1016/j.bcp.2013.11.021

Honda K, Casadesus G, Petersen RB, Perry G, Smith MA (2004) Oxidative stress and redox-active iron in Alzheimer's disease. Ann N Y Acad Sci 1012:179-182

Hong Y, Muenzner J, Grimm SK, Pletneva EV (2012) Origin of the conformational heterogeneity of cardiolipin-bound cytochrome C. J Am Chem Soc 134:18713-18723. doi:10.1021/ja307426k

Horvath RJ, Nutile-McMenemy N, Alkaitis MS, Deleo JA (2008) Differential migration, LPS-induced cytokine, chemokine, and NO expression in immortalized BV-2 and HAPI cell lines and primary microglial cultures. J Neurochem 107:557-569. doi:10.1111/j.1471-4159.2008.05633.x

Hsiao YH, Hung HC, Chen SH, Gean PW (2014) Social interaction rescues memory deficit in an animal model of Alzheimer's disease by increasing BDNF-dependent hippocampal neurogenesis. J Neurosci 34:16207-16219. doi:10.1523/JNEUROSCI.0747-14.2014

Hu LF, Wong PT, Moore PK, Bian JS (2007) Hydrogen sulfide attenuates lipopolysaccharide-induced inflammation by inhibition of p38 mitogen-activated protein kinase in microglia. J Neurochem 100:1121-1128. doi:10.1111/j.1471-4159.2006.04283.x

Huang DC, Strasser A (2000) BH3-Only proteins-essential initiators of apoptotic cell death. Cell 103:839-842

Huang EJ, Reichardt LF (2001) Neurotrophins: roles in neuronal development and function. Annu Rev Neurosci 24:677-736. doi:10.1146/annurev.neuro.24.1.677

Huang Y, Mucke L (2012) Alzheimer mechanisms and therapeutic strategies. Cell 148:1204-1222. doi:10.1016/j.cell.2012.02.040

Ibarguren M, Lopez DJ, Escriba PV (2014) The effect of natural and synthetic fatty acids on membrane structure, microdomain organization, cellular functions and human health. Biochim Biophys Acta 1838:1518-1528. doi:10.1016/j.bbamem.2013.12.021

Jacobson J, Duchen MR, Heales SJ (2002) Intracellular distribution of the fluorescent dye nonyl acridine orange responds to the mitochondrial membrane potential: implications for assays of cardiolipin and mitochondrial mass. J Neurochem 82:224-233

Jazvinscak Jembrek M, Hof PR, Simic G (2015) Ceramides in Alzheimer's disease: key mediators of neuronal apoptosis induced by oxidative stress and Abeta accumulation. Oxid Med Cell Longev 2015:346783. doi:10.1155/2015/346783

Jessen KR (2004) Glial cells. Int J Biochem Cell Biol 36:1861-1867. doi:10.1016/j.biocel.2004.02.023

Jonckheere AI, Smeitink JA, Rodenburg RJ (2012) Mitochondrial ATP synthase: architecture, function and pathology. J Inherit Metab Dis 35:211-225. doi:10.1007/s10545-011-9382-9

Jung YY et al. (2013) Protective effect of phosphatidylcholine on lipopolysaccharide-induced acute inflammation in multiple organ injury. Korean J Physiol Pharmacol 17:209-216. doi:10.4196/kjpp.2013.17.3.209

Kagan VE et al. (2005) Cytochrome c acts as a cardiolipin oxygenase required for release of proapoptotic factors. Nat Chem Biol 1:223-232. doi:10.1038/nchembio727

Karran E, Mercken M, De Strooper B (2011) The amyloid cascade hypothesis for Alzheimer's disease: an appraisal for the development of therapeutics. Nat Rev Drug Discov 10:698-712. doi:10.1038/nrd3505

Kaur G, Dufour JM (2012) Cell lines: valuable tools or useless artifacts. Spermatogenesis 2:1-5. doi:10.4161/spmg.19885

Keirstead HS, Blakemore WF (1999) The role of oligodendrocytes and oligodendrocyte progenitors in CNS remyelination. Adv Exp Med Biol 468:183-197

Keller I, Heckhausen H (1990) Readiness potentials preceding spontaneous motor acts: voluntary vs. involuntary control. Electroencephalogr Clin Neurophysiol 76:351-361

Kettenmann H, Verkhratsky A (2008) Neuroglia: the 150 years after. Trends Neurosci 31:653-659. doi:10.1016/j.tins.2008.09.003

Kiebish MA, Han X, Cheng H, Seyfried TN (2009) In vitro growth environment produces lipidomic and electron transport chain abnormalities in mitochondria from non-tumorigenic astrocytes and brain tumours. ASN Neuro 1. doi:10.1042/AN20090011

Kim TH et al. (2004) Bid-cardiolipin interaction at mitochondrial contact site contributes to mitochondrial cristae reorganization and cytochrome C release. Mol Biol Cell 15:3061-3072. doi:10.1091/mbc.E03-12-0864

Klegeris A, Bissonnette CJ, McGeer PL (2005) Modulation of human microglia and THP-1 cell toxicity by cytokines endogenous to the nervous system. Neurobiol Aging 26:673-682. doi:10.1016/j.neurobiolaging.2004.06.012

Klegeris A, McGeer PL (2000) Interaction of various intracellular signaling mechanisms involved in mononuclear phagocyte toxicity toward neuronal cells. J Leukoc Biol 67:127-133

Klegeris A, McGeer PL (2001) Inflammatory cytokine levels are influenced by interactions between THP-1 monocytic, U-373 MG astrocytic, and SH-SY5Y neuronal cell lines of human origin. Neurosci Lett 313:41-44

Klegeris A, McGeer PL (2003) Toxicity of human monocytic THP-1 cells and microglia toward SH-SY5Y neuroblastoma cells is reduced by inhibitors of 5-lipoxygenase and its activating protein FLAP. J Leukoc Biol 73:369-378

Klegeris A, Pelech S, Giasson BI, Maguire J, Zhang H, McGeer EG, McGeer PL (2008) Alpha-synuclein activates stress signaling protein kinases in THP-1 cells and microglia. Neurobiol Aging 29:739-752. doi:10.1016/j.neurobiolaging.2006.11.013

Koenigsknecht J, Landreth G (2004) Microglial phagocytosis of fibrillar beta-amyloid through a beta1 integrin-dependent mechanism. J Neurosci 24:9838-9846. doi:10.1523/JNEUROSCI.2557-04.2004

Kolomiytseva IK, Markevich LN, Ignat'ev DA, Bykova OV (2010) Lipids of nuclear fractions from neurons and glia of rat neocortex under conditions of artificial hypobiosis. Biochemistry (Mosc) 75:1132-1138

Kovalevich J, Langford D (2013) Considerations for the use of SH-SY5Y neuroblastoma cells in neurobiology. Methods Mol Biol 1078:9-21. doi:10.1007/978-1-62703-640-5_2

Kraft AD, Harry GJ (2011) Features of microglia and neuroinflammation relevant to environmental exposure and neurotoxicity. Int J Environ Res Public Health 8:2980-3018. doi:10.3390/ijerph8072980

Kulikov AV, Shilov ES, Mufazalov IA, Gogvadze V, Nedospasov SA, Zhivotovsky B (2012) Cytochrome c: the Achilles' heel in apoptosis. Cell Mol Life Sci 69:1787-1797. doi:10.1007/s00018-011-0895-z

Kuo YC, Liu YC (2014) Cardiolipin-incorporated liposomes with surface CRM197 for enhancing neuronal survival against neurotoxicity. Int J Pharm 473:334-344. doi:10.1016/j.ijpharm.2014.07.003

Lapuente-Brun E et al. (2013) Supercomplex assembly determines electron flux in the mitochondrial electron transport chain. Science 340:1567-1570. doi:10.1126/science.1230381

Lee JK, Tansey MG (2013) Microglia isolation from adult mouse brain. Methods Mol Biol 1041:17-23. doi:10.1007/978-1-62703-520-0_3

Leonard EJ, Skeel A, Yoshimura T, Rankin J (1993) Secretion of monocyte chemoattractant protein-1 (MCP-1) by human mononuclear phagocytes. Adv Exp Med Biol 351:55-64

Levy R, Rotrosen D, Nagauker O, Leto TL, Malech HL (1990) Induction of the respiratory burst in HL-60 cells. Correlation of function and protein expression. J Immunol 145:2595-2601

Li XX, Tsoi B, Li YF, Kurihara H, He RR (2015) Cardiolipin and its different properties in mitophagy and apoptosis. J Histochem Cytochem 63:301-311. doi:10.1369/0022155415574818

Liu X, Miller MJ, Joshi MS, Sadowska-Krowicka H, Clark DA, Lancaster JR, Jr. (1998) Diffusion-limited reaction of free nitric oxide with erythrocytes. J Biol Chem 273:18709-18713

Liu Y, Peterson DA, Kimura H, Schubert D (1997) Mechanism of cellular 3-(4,5-dimethylthiazol-2-yl)-2,5-diphenyltetrazolium bromide (MTT) reduction. J Neurochem 69:581-593

Lull ME, Block ML (2010) Microglial activation and chronic neurodegeneration. Neurotherapeutics 7:354-365. doi:10.1016/j.nurt.2010.05.014

Lutter M, Fang M, Luo X, Nishijima M, Xie X, Wang X (2000) Cardiolipin provides specificity for targeting of tBid to mitochondria. Nat Cell Biol 2:754-761. doi:10.1038/35036395

Lutter M, Perkins GA, Wang X (2001) The pro-apoptotic Bcl-2 family member tBid localizes to mitochondrial contact sites. BMC Cell Biol 2:22

Maderna P, Godson C (2003) Phagocytosis of apoptotic cells and the resolution of inflammation. Biochim Biophys Acta 1639:141-151

Maezawa I, Zimin PI, Wulff H, Jin LW (2011) Amyloid-beta protein oligomer at low nanomolar concentrations activates microglia and induces microglial neurotoxicity. J Biol Chem 286:3693-3706. doi:10.1074/jbc.M110.135244

Majerova P et al. (2014) Microglia display modest phagocytic capacity for extracellular tau oligomers. J Neuroinflammation 11:161. doi:10.1186/s12974-014-0161-z

Malawista SE, Gee JB, Bensch KG (1971) Cytochalasin B reversibly inhibits phagocytosis: functional, metabolic, and ultrastructural effects in human blood leukocytes and rabbit alveolar macrophages. Yale J Biol Med 44:286-300

Mancuso DJ et al. (2009) Genetic ablation of calcium-independent phospholipase A2{gamma} leads to alterations in hippocampal cardiolipin content and molecular species distribution, mitochondrial degeneration, autophagy, and cognitive dysfunction. J Biol Chem 284:35632-35644. doi:10.1074/jbc.M109.055194

Mandelkow EM, Mandelkow E (2012) Biochemistry and cell biology of tau protein in neurofibrillary degeneration. Cold Spring Harb Perspect Med 2:a006247. doi:10.1101/cshperspect.a006247

Mandrekar-Colucci S, Landreth GE (2010) Microglia and inflammation in Alzheimer's disease. CNS Neurol Disord Drug Targets 9:156-167

Maniti O, Lecompte MF, Marcillat O, Desbat B, Buchet R, Vial C, Granjon T (2009) Mitochondrial creatine kinase binding to phospholipid monolayers induces cardiolipin segregation. Biophys J 96:2428-2438. doi:10.1016/j.bpj.2008.12.3911

Mariani E, Polidori MC, Cherubini A, Mecocci P (2005) Oxidative stress in brain aging, neurodegenerative and vascular diseases: an overview. J Chromatogr B Analyt Technol Biomed Life Sci 827:65-75. doi:10.1016/j.jchromb.2005.04.023

Martin-Moreno AM, Reigada D, Ramirez BG, Mechoulam R, Innamorato N, Cuadrado A, de Ceballos ML (2011) Cannabidiol and other cannabinoids reduce microglial activation in vitro and in vivo: relevance to Alzheimer's disease. Mol Pharmacol 79:964-973. doi:10.1124/mol.111.071290

Masters JR (2000) Human cancer cell lines: fact and fantasy. Nat Rev Mol Cell Biol 1:233-236. doi:10.1038/35043102

Mayo L, Levy A, Jacob-Hirsch J, Amariglio N, Rechavi G, Stein R (2011) Bid regulates the immunological profile of murine microglia and macrophages. Glia 59:397-412. doi:10.1002/glia.21109

McCaulley ME, Grush KA (2015) Alzheimer's disease: exploring the role of inflammation and implications for treatment. Int J Alzheimers Dis 2015:515248. doi:10.1155/2015/515248

McCloy RA, Rogers S, Caldon CE, Lorca T, Castro A, Burgess A (2014) Partial inhibition of Cdk1 in G 2 phase overrides the SAC and decouples mitotic events. Cell Cycle 13:1400-1412. doi:10.4161/cc.28401

McMillin JB, Dowhan W (2002) Cardiolipin and apoptosis. Biochim Biophys Acta 1585:97-107

Mejia EM, Nguyen H, Hatch GM (2014) Mammalian cardiolipin biosynthesis. Chem Phys Lipids 179:11-16. doi:10.1016/j.chemphyslip.2013.10.001

Mennicken F, Maki R, de Souza EB, Quirion R (1999) Chemokines and chemokine receptors in the CNS: a possible role in neuroinflammation and patterning. Trends Pharmacol Sci 20:73-78

Meyer K, Kaspar BK (2016) Glia-neuron interactions in neurological diseases: testing non-cell autonomy in a dish. Brain Res 1656:27-39. doi:10.1016/j.brainres.2015.12.051

Miki Y, Ono K, Hata S, Suzuki T, Kumamoto H, Sasano H (2012) The advantages of co-culture over mono cell culture in simulating in vivo environment. J Steroid Biochem Mol Biol 131:68-75. doi:10.1016/j.jsbmb.2011.12.004

Miranda KM, Espey MG, Wink DA (2001) A rapid, simple spectrophotometric method for simultaneous detection of nitrate and nitrite. Nitric Oxide 5:62-71. doi:10.1006/niox.2000.0319

Mitchell DB, Santone, K.S. & Acosta, D. (1980) Evaluation of cytotoxicity in cultured cells by enzyme leakage. J Tissue Cult Methods 6. doi:10.1007/BF02082861

Mitra A, Mishra L, Li S (2013) Technologies for deriving primary tumor cells for use in personalized cancer therapy. Trends Biotechnol 31:347-354. doi:10.1016/j.tibtech.2013.03.006

Monteiro-Cardoso VF et al. (2015) Cardiolipin profile changes are associated to the early synaptic mitochondrial dysfunction in Alzheimer's disease. J Alzheimers Dis 43:1375-1392. doi:10.3233/JAD-141002

Morales I, Guzman-Martinez L, Cerda-Troncoso C, Farias GA, Maccioni RB (2014) Neuroinflammation in the pathogenesis of Alzheimer's disease. A rational framework for the search of novel therapeutic approaches. Front Cell Neurosci 8:112. doi:10.3389/fncel.2014.00112

Mrak RE, Griffin WS (2005) Glia and their cytokines in progression of neurodegeneration. Neurobiol Aging 26:349-354. doi:10.1016/j.neurobiolaging.2004.05.010

Multhaup G, Ruppert T, Schlicksupp A, Hesse L, Beher D, Masters CL, Beyreuther K (1997) Reactive oxygen species and Alzheimer's disease. Biochem Pharmacol 54:533-539

Murphy FC, Nimmo-Smith I, Lawrence AD (2003) Functional neuroanatomy of emotions: a meta-analysis. Cogn Affect Behav Neurosci 3:207-233

Nakajima A, Kurihara H, Yagita H, Okumura K, Nakano H (2008) Mitochondrial extrusion through the cytoplasmic vacuoles during cell death. J Biol Chem 283:24128-24135. doi:10.1074/jbc.M802996200

Nakajima K, Kohsaka S (2001) Microglia: activation and their significance in the central nervous system. J Biochem 130:169-175

Nedergaard M, Ransom B, Goldman SA (2003) New roles for astrocytes: redefining the functional architecture of the brain. Trends Neurosci 26:523-530. doi:10.1016/j.tins.2003.08.008

Neniskyte U, Neher JJ, Brown GC (2011) Neuronal death induced by nanomolar amyloid beta is mediated by primary phagocytosis of neurons by microglia. J Biol Chem 286:39904-39913. doi:10.1074/jbc.M111.267583

Nimmerjahn A, Kirchhoff F, Helmchen F (2005) Resting microglial cells are highly dynamic surveillants of brain parenchyma in vivo. Science 308:1314-1318. doi:10.1126/science.1110647

Nishiyama-Naruke A, Curi R (2000) Phosphatidylcholine participates in the interaction between macrophages and lymphocytes. Am J Physiol Cell Physiol 278:C554-560

Olson JK, Miller SD (2004) Microglia initiate central nervous system innate and adaptive immune responses through multiple TLRs. J Immunol 173:3916-3924

Ordonez-Gutierrez L et al. (2015) Repeated intraperitoneal injections of liposomes containing phosphatidic acid and cardiolipin reduce amyloid-beta levels in APP/PS1 transgenic mice. Nanomedicine 11:421-430. doi:10.1016/j.nano.2014.09.015

Orlando A et al. (2013) Effect of nanoparticles binding beta-amyloid peptide on nitric oxide production by cultured endothelial cells and macrophages. Int J Nanomedicine 8:1335-1347. doi:10.2147/IJN.S40297

Osborn LM, Kamphuis W, Wadman WJ, Hol EM (2016) Astrogliosis: an integral player in the pathogenesis of Alzheimer's disease. Prog Neurobiol. doi:10.1016/j.pneurobio.2016.01.001

Ott M, Gogvadze V, Orrenius S, Zhivotovsky B (2007) Mitochondria, oxidative stress and cell death. Apoptosis 12:913-922. doi:10.1007/s10495-007-0756-2

Pahlman S, Mamaeva S, Meyerson G, Mattsson ME, Bjelfman C, Ortoft E, Hammerling U (1990) Human neuroblastoma cells in culture: a model for neuronal cell differentiation and function. Acta Physiol Scand Suppl 592:25-37

Painter MM, Atagi Y, Liu CC, Rademakers R, Xu H, Fryer JD, Bu G (2015) TREM2 in CNS homeostasis and neurodegenerative disease. Mol Neurodegener 10:43. doi:10.1186/s13024-015-0040-9

Pan C, Kumar C, Bohl S, Klingmueller U, Mann M (2009) Comparative proteomic phenotyping of cell lines and primary cells to assess preservation of cell type-specific functions. Mol Cell Proteomics 8:443-450. doi:10.1074/mcp.M800258-MCP200

Pan XD, Zhu YG, Lin N, Zhang J, Ye QY, Huang HP, Chen XC (2011) Microglial phagocytosis induced by fibrillar beta-amyloid is attenuated by oligomeric beta-amyloid: implications for Alzheimer's disease. Mol Neurodegener 6:45. doi:10.1186/1750-1326-6-45

Pangborn MC (1942) Isolation and purification of a serologically active phospholipid from beef heart. J Biol Chem 143:247-256

Paradies G, Petrosillo G, Paradies V, Ruggiero FM (2009) Role of cardiolipin peroxidation and Ca2+ in mitochondrial dysfunction and disease. Cell Calcium 45:643-650. doi:10.1016/j.ceca.2009.03.012

Paradies G, Petrosillo G, Paradies V, Ruggiero FM (2011) Mitochondrial dysfunction in brain aging: role of oxidative stress and cardiolipin. Neurochem Int 58:447-457. doi:10.1016/j.neuint.2010.12.016

Paresce DM, Chung H, Maxfield FR (1997) Slow degradation of aggregates of the Alzheimer's disease amyloid beta-protein by microglial cells. J Biol Chem 272:29390-29397

Park JY et al. (2009) On the mechanism of internalization of alpha-synuclein into microglia: roles of ganglioside GM1 and lipid raft. J Neurochem 110:400-411. doi:10.1111/j.1471-4159.2009.06150.x

Parpura V et al. (2012) Glial cells in (patho)physiology. J Neurochem 121:4-27. doi:10.1111/j.1471-4159.2012.07664.x

Petrosillo G, Matera M, Casanova G, Ruggiero FM, Paradies G (2008) Mitochondrial dysfunction in rat brain with aging involvement of complex I, reactive oxygen species and cardiolipin. Neurochem Int 53:126-131. doi:10.1016/j.neuint.2008.07.001

Pfeiffer K, Gohil V, Stuart RA, Hunte C, Brandt U, Greenberg ML, Schagger H (2003) Cardiolipin stabilizes respiratory chain supercomplexes. J Biol Chem 278:52873-52880. doi:10.1074/jbc.M308366200

Pointer CB, Klegeris A (2016) Cardiolipin in central nervous system physiology and pathology. Cell Mol Neurobiol. doi:10.1007/s10571-016-0458-9

Pope S, Land JM, Heales SJ (2008) Oxidative stress and mitochondrial dysfunction in neurodegeneration; cardiolipin a critical target? Biochim Biophys Acta 1777:794-799. doi:10.1016/j.bbabio.2008.03.011

Porcellini E, Ianni M, Carbone I, Franceschi M, Licastro F (2013) Monocyte chemoattractant protein-1 promoter polymorphism and plasma levels in Alzheimer's disease. Immun Ageing 10:6. doi:10.1186/1742-4933-10-6

Prince M, Wimo A, Guerchet M, Ali G-C, Wu Y-T, Prina M (2015) World Alzheimer Report 2015. Alzheimer's Disease International

Prinz M, Priller J (2017) The role of peripheral immune cells in the CNS in steady state and disease. Nat Neurosci 20:136-144. doi:10.1038/nn.4475

Raemy E, Montessuit S, Pierredon S, van Kampen AH, Vaz FM, Martinou JC (2016) Cardiolipin or MTCH2 can serve as tBID receptors during apoptosis. Cell Death Differ. doi:10.1038/cdd.2015.166

Regier MC, Maccoux LJ, Weinberger EM, Regehr KJ, Berry SM, Beebe DJ, Alarid ET (2016) Transitions from mono- to co- to tri-culture uniquely affect gene expression in breast cancer, stromal, and immune compartments. Biomed Microdevices 18:70. doi:10.1007/s10544-016-0083-x

Reitz C (2012) Alzheimer's disease and the amyloid cascade hypothesis: a critical review. Int J Alzheimers Dis 2012:369808. doi:10.1155/2012/369808

Revilla S et al. (2014) Lenti-GDNF gene therapy protects against Alzheimer's disease-like neuropathology in 3xTg-AD mice and MC65 cells. CNS Neurosci Ther 20:961-972. doi:10.1111/cns.12312

Ribrault C, Sekimoto K, Triller A (2011) From the stochasticity of molecular processes to the variability of synaptic transmission. Nat Rev Neurosci 12:375-387. doi:10.1038/nrn3025

Richardson MP, Ayliffe MJ, Helbert M, Davies EG (1998) A simple flow cytometry assay using dihydrorhodamine for the measurement of the neutrophil respiratory burst in whole blood: comparison with the quantitative nitrobluetetrazolium test. J Immunol Methods 219:187-193

Rogers J, Lue LF (2001) Microglial chemotaxis, activation, and phagocytosis of amyloid beta-peptide as linked phenomena in Alzheimer's disease. Neurochem Int 39:333-340

Ruggiero FM, Cafagna F, Petruzzella V, Gadaleta MN, Quagliariello E (1992) Lipid composition in synaptic and nonsynaptic mitochondria from rat brains and effect of aging. J Neurochem 59:487-491

Saijo K, Glass CK (2011) Microglial cell origin and phenotypes in health and disease. Nat Rev Immunol 11:775-787. doi:10.1038/nri3086

Sathappa M, Alder NN (2016) The ionization properties of cardiolipin and its variants in model bilayers. Biochim Biophys Acta 1858:1362-1372. doi:10.1016/j.bbamem.2016.03.007

Schlame M (2013) Cardiolipin remodeling and the function of tafazzin. Biochim Biophys Acta 1831:582-588. doi:10.1016/j.bbalip.2012.11.007

Schlame M, Rua D, Greenberg ML (2000) The biosynthesis and functional role of cardiolipin. Prog Lipid Res 39:257-288

Schlattner U et al. (2009) Mitochondrial kinases and their molecular interaction with cardiolipin. Biochim Biophys Acta 1788:2032-2047. doi:10.1016/j.bbamem.2009.04.018

Segawa K, Nagata S (2015) An apoptotic 'eat me' signal: phosphatidylserine exposure. Trends Cell Biol 25:639-650. doi:10.1016/j.tcb.2015.08.003

Sen T, Sen N, Tripathi G, Chatterjee U, Chakrabarti S (2006) Lipid peroxidation associated cardiolipin loss and membrane depolarization in rat brain mitochondria. Neurochem Int 49:20-27. doi:10.1016/j.neuint.2005.12.018

Sergeant N et al. (2008) Biochemistry of tau in Alzheimer's disease and related neurological disorders. Expert Rev Proteomics 5:207-224. doi:10.1586/14789450.5.2.207

Sheng W et al. (2011) Pro-inflammatory cytokines and lipopolysaccharide induce changes in cell morphology, and upregulation of ERK1/2, iNOS and sPLA(2)-IIA expression in astrocytes and microglia. J Neuroinflammation 8:121. doi:10.1186/1742-2094-8-121

Sherwood CC et al. (2006) Evolution of increased glia-neuron ratios in the human frontal cortex. Proc Natl Acad Sci U S A 103:13606-13611. doi:10.1073/pnas.0605843103

Shin MK et al. (2014) Neuropep-1 ameliorates learning and memory deficits in an Alzheimer's disease mouse model, increases brain-derived neurotrophic factor expression in the brain, and causes reduction of amyloid beta plaques. Neurobiol Aging 35:990-1001. doi:10.1016/j.neurobiolaging.2013.10.091

Sierra A, Abiega O, Shahraz A, Neumann H (2013) Janus-faced microglia: beneficial and detrimental consequences of microglial phagocytosis. Front Cell Neurosci 7:6. doi:10.3389/fncel.2013.00006

Simon HU, Haj-Yehia A, Levi-Schaffer F (2000) Role of reactive oxygen species (ROS) in apoptosis induction. Apoptosis 5:415-418

Sincich LC, Horton JC, Sharpee TO (2009) Preserving information in neural transmission. J Neurosci 29:6207-6216. doi:10.1523/JNEUROSCI.3701-08.2009

Skaper SD (2012) The neurotrophin family of neurotrophic factors: an overview. Methods Mol Biol 846:1-12. doi:10.1007/978-1-61779-536-7_1

Solito E, Sastre M (2012) Microglia function in Alzheimer's disease. Front Pharmacol 3:14. doi:10.3389/fphar.2012.00014

Sorice M et al. (2004) Cardiolipin and its metabolites move from mitochondria to other cellular membranes during death receptor-mediated apoptosis. Cell Death Differ 11:1133-1145. doi:10.1038/sj.cdd.4401457

Sorice M et al. (2000) Cardiolipin on the surface of apoptotic cells as a possible trigger for antiphospholipids antibodies. Clin Exp Immunol 122:277-284

Sparvero LJ, Amoscato AA, Kochanek PM, Pitt BR, Kagan VE, Bayir H (2010) Mass-spectrometry based oxidative lipidomics and lipid imaging: applications in traumatic brain injury. J Neurochem 115:1322-1336. doi:10.1111/j.1471-4159.2010.07055.x

Speer O, Back N, Buerklen T, Brdiczka D, Koretsky A, Wallimann T, Eriksson O (2005) Octameric mitochondrial creatine kinase induces and stabilizes contact sites between the inner and outer membrane. Biochem J 385:445-450. doi:10.1042/BJ20040386

Spielman LJ, Bahniwal M, Little JP, Walker DG, Klegeris A (2015) Insulin modulates in vitro secretion of cytokines and cytotoxins by human glial cells. Curr Alzheimer Res 12:684-693

Stansley B, Post J, Hensley K (2012) A comparative review of cell culture systems for the study of microglial biology in Alzheimer's disease. J Neuroinflammation 9:115. doi:10.1186/1742-2094-9-115

Streit WJ, Walter SA, Pennell NA (1999) Reactive microgliosis. Prog Neurobiol 57:563-581

Terwel D, Dewachter I, Van Leuven F (2002) Axonal transport, tau protein, and neurodegeneration in Alzheimer's disease. Neuromolecular Med 2:151-165. doi:10.1385/NMM:2:2:151

Theriault P, ElAli A, Rivest S (2015) The dynamics of monocytes and microglia in Alzheimer's disease. Alzheimers Res Ther 7:41. doi:10.1186/s13195-015-0125-2

Tokes T et al. (2011) Protective effects of a phosphatidylcholine-enriched diet in lipopolysaccharide-induced experimental neuroinflammation in the rat. Shock 36:458-465. doi:10.1097/SHK.0b013e31822f36b0

Treede I et al. (2007) Anti-inflammatory effects of phosphatidylcholine. J Biol Chem 282:27155-27164. doi:10.1074/jbc.M704408200

Tsuchiya S, Yamabe M, Yamaguchi Y, Kobayashi Y, Konno T, Tada K (1980) Establishment and characterization of a human acute monocytic leukemia cell line (THP-1). Int J Cancer 26:171-176

Tyurin VA et al. (2008) Oxidative lipidomics of programmed cell death. Methods Enzymol 442:375-393. doi:10.1016/S0076-6879(08)01419-5

van Gurp M, Festjens N, van Loo G, Saelens X, Vandenabeele P (2003) Mitochondrial intermembrane proteins in cell death. Biochem Biophys Res Commun 304:487-497

Vance JE, Tasseva G (2013) Formation and function of phosphatidylserine and phosphatidylethanolamine in mammalian cells. Biochim Biophys Acta 1831:543-554. doi:10.1016/j.bbalip.2012.08.016

Venigalla M, Sonego S, Gyengesi E, Sharman MJ, Munch G (2015) Novel promising therapeutics against chronic neuroinflammation and neurodegeneration in Alzheimer's disease. Neurochem Int 95:63-74. doi:10.1016/j.neuint.2015.10.011

Vieira DB, Gamarra LF (2016) Getting into the brain: liposome-based strategies for effective drug delivery across the blood-brain barrier. Int J Nanomedicine 11:5381-5414. doi:10.2147/IJN.S117210

Vladimirov YA, Proskurnina EV, Alekseev AV (2013) Molecular mechanisms of apoptosis. structure of cytochrome c-cardiolipin complex. Biochemistry (Mosc) 78:1086-1097. doi:10.1134/S0006297913100027

von Bernhardi R, Cornejo F, Parada GE, Eugenin J (2015) Role of TGFbeta signaling in the pathogenesis of Alzheimer's disease. Front Cell Neurosci 9:426. doi:10.3389/fncel.2015.00426

Wakselman S, Bechade C, Roumier A, Bernard D, Triller A, Bessis A (2008) Developmental neuronal death in hippocampus requires the microglial CD11b integrin and DAP12 immunoreceptor. J Neurosci 28:8138-8143. doi:10.1523/JNEUROSCI.1006-08.2008

Wang WY, Tan MS, Yu JT, Tan L (2015) Role of pro-inflammatory cytokines released from microglia in Alzheimer's disease. Ann Transl Med 3:136. doi:10.3978/j.issn.2305-5839.2015.03.49

Wang Y, Mandelkow E (2016) Tau in physiology and pathology. Nat Rev Neurosci 17:5-21. doi:10.1038/nrn.2015.1

Watters JJ, Sommer JA, Pfeiffer ZA, Prabhu U, Guerra AN, Bertics PJ (2002) A differential role for the mitogen-activated protein kinases in lipopolysaccharide signaling: the MEK/ERK pathway is not essential for nitric oxide and interleukin 1beta production. J Biol Chem 277:9077-9087. doi:10.1074/jbc.M104385200

Weldon DT et al. (1998) Fibrillar beta-amyloid induces microglial phagocytosis, expression of inducible nitric oxide synthase, and loss of a select population of neurons in the rat CNS in vivo. J Neurosci 18:2161-2173

Witting A, Muller P, Herrmann A, Kettenmann H, Nolte C (2000) Phagocytic clearance of apoptotic neurons by microglia/brain macrophages in vitro: involvement of lectin-, integrin-, and phosphatidylserine-mediated recognition. J Neurochem 75:1060-1070

Wortmann M (2012) Dementia: a global health priority - highlights from an ADI and World Health Organization report. Alzheimers Res Ther 4:40. doi:10.1186/alzrt143

Wu Y, Tibrewal N, Birge RB (2006) Phosphatidylserine recognition by phagocytes: a view to a kill. Trends Cell Biol 16:189-197. doi:10.1016/j.tcb.2006.02.003

Wyss-Coray T, Rogers J (2012) Inflammation in Alzheimer disease-a brief review of the basic science and clinical literature. Cold Spring Harb Perspect Med 2:a006346. doi:10.1101/cshperspect.a006346

Xicoy H, Wieringa B, Martens GJ (2017) The SH-SY5Y cell line in Parkinson's disease research: a systematic review. Mol Neurodegener 12:10. doi:10.1186/s13024-017-0149-0

Xie HR, Hu LS, Li GY (2010) SH-SY5Y human neuroblastoma cell line: in vitro cell model of dopaminergic neurons in Parkinson's disease. Chin Med J (Engl) 123:1086-1092

Xu Y, Kelley RI, Blanck TJ, Schlame M (2003) Remodeling of cardiolipin by phospholipid transacylation. J Biol Chem 278:51380-51385. doi:10.1074/jbc.M307382200

Yabuuchi H, O'Brien JS (1968) Brain cardiolipin: isolation and fatty acid positions. J Neurochem 15:1383-1390

Yamamoto M, Kamatsuka Y, Ohishi A, Nishida K, Nagasawa K (2013) P2X7 receptors regulate engulfing activity of non-stimulated resting astrocytes. Biochem Biophys Res Commun 439:90-95. doi:S0006-291X(13)01348-X [pii] 10.1016/j.bbrc.2013.08.022

Yang I, Han SJ, Kaur G, Crane C, Parsa AT (2010) The role of microglia in central nervous system immunity and glioma immunology. J Clin Neurosci 17:6-10. doi:10.1016/j.jocn.2009.05.006

Ye C, Shen Z, Greenberg ML (2016) Cardiolipin remodeling: a regulatory hub for modulating cardiolipin metabolism and function. J Bioenerg Biomembr 48:113-123. doi:10.1007/s10863-014-9591-7

Zhang L, Bell RJ, Kiebish MA, Seyfried TN, Han X, Gross RW, Chuang JH (2011) A mathematical model for the determination of steady-state cardiolipin remodeling mechanisms using lipidomic data. PLoS One 6:e21170. doi:10.1371/journal.pone.0021170

Zhou C, Huang Y, Przedborski S (2008) Oxidative stress in Parkinson's disease: a mechanism of pathogenic and therapeutic significance. Ann N Y Acad Sci 1147:93-104. doi:10.1196/annals.1427.023

Zotova E, Nicoll JA, Kalaria R, Holmes C, Boche D (2010) Inflammation in Alzheimer's disease: relevance to pathogenesis and therapy. Alzheimers Res Ther 2:1. doi:10.1186/alzrt24

Zurier RB, Hoffstein S, Weissmann G (1973) Cytochalasin B: effect on lysosomal enzyme release from human leukocytes. Proc Natl Acad Sci USA 70:844-848

Appendices

Appendix A: Primary Murine Microglia Extraction Reagents

1. **F10 Medium with Glucose:** 0.45 mg/ml D-(+)-glucose was dissolved in F10 medium. The solution was stored at 4^{O}C in an airtight bottle.
2. **F0 Medium with Glucose:** 0.45 mg/ml D-(+)-glucose was dissolved in F0 medium. The solution was stored at 4^{O}C in an airtight bottle.
3. **Dissociation Medium:** 0.1% v/v DNase I, 1 mg/ml papain and 0.132 M D-(+)-trehalose dihydrate were dissolved in 14 ml of F10 medium with glucose. The solution was made just prior to conducting the extraction and was not stored.
4. **30% SIP Solution:** 30% v/v percoll was dissolved in 1x HBSS. The solution was stored at 4^{O}C in an airtight bottle.
5. **37% SIP Solution:** 37% v/v percoll was dissolved in 1x HBSS. The solution was stored at 4^{O}C in an airtight bottle.
6. **70% SIP Solution:** 70% v/v percoll was dissolved in 1x HBSS. The solution was stored at 4^{O}C in an airtight bottle.

Appendix B: Enzyme-Linked Immunosorbent Assay (ELISA) Reagents

1. **Phosphate Stock (200 mM):** 3.7 g of monobasic sodium phosphate and 40.3 g of dibasic sodium phosphate were dissolved in 500 ml milli-Q water, pH = 7.3. The solution was stored at room temperature in an airtight bottle.
2. **PBS-Tween:** 9 g of sodium chloride was dissolved in 950 ml milli-Q water. Subsequently, 50 ml phosphate stock and 0.5 ml Tween (0.05% v/v) were added, pH = 7.4. The solution was stored at room temperature in an airtight bottle.
3. **Blocking Solution:** 1% w/v skim milk powder and 1% w/v BSA were dissolved in PBS. The solution was stored at $4^{O}C$ for up to one week.
4. **Coating Buffer (0.1 M Sodium Bicarbonate Buffer):** 0.159 g of sodium bicarbonate and 0.293 g of sodium carbonate were dissolved in 100 ml of milli-Q water. The pH was corrected to 9.6. The solution was stored at room temperature in an airtight bottle.
5. **Substrate Buffer:** 101 mg of $MgCl_2x5H_2O$ was dissolved in 800 ml milli-Q water. Subsequently, 97 ml of diethanolamine was added. The pH was corrected to 9.8, and milli-Q water was added to a final volume of 1 L. The solution was stored in the dark at $4^{O}C$ in an airtight bottle.
6. **Alkaline Phosphatase Substrate Solution:** 1mg/ml of phosphatase substrate was dissolved in substrate buffer in the dark. The solution was made just prior to use and was not stored.